

EUROPEAN ORGANISATION FOR NUCLEAR RESEARCH (CERN)



Submitted to: JHEP

CERN-EP-2017-161
11th May 2018

Angular analysis of $B_d^0 \rightarrow K^* \mu^+ \mu^-$ decays in pp collisions at $\sqrt{s} = 8$ TeV with the ATLAS detector

The ATLAS Collaboration

An angular analysis of the decay $B_d^0 \rightarrow K^* \mu^+ \mu^-$ is presented, based on proton–proton collision data recorded by the ATLAS experiment at the LHC. The study is using 20.3 fb^{-1} of integrated luminosity collected during 2012 at centre-of-mass energy of $\sqrt{s} = 8$ TeV. Measurements of the K^* longitudinal polarisation fraction and a set of angular parameters obtained for this decay are presented. The results are compatible with the Standard Model predictions.

1 Introduction

Flavour-changing neutral currents (FCNC) have played a significant role in the construction of the Standard Model of particle physics (SM). These processes are forbidden at tree level and can proceed only via loops, hence are rare. An important set of FCNC processes involve the transition of a b -quark to an $s\mu^+\mu^-$ final state mediated by electroweak box and penguin diagrams. If heavy new particles exist, they may contribute to FCNC decay amplitudes, affecting the measurement of observables related to the decay under study. Hence FCNC processes allow searches for contributions from sources of physics beyond the SM (hereafter referred to as new physics). This analysis focuses on the decay $B_d^0 \rightarrow K^{*0}(892)\mu^+\mu^-$, where $K^{*0}(892) \rightarrow K^+\pi^-$. Hereafter, the $K^{*0}(892)$ is referred to as K^* and charge conjugation is implied throughout, unless stated otherwise. In addition to angular observables such as the forward-backward asymmetry A_{FB}^1 , there is considerable interest in measurements of the charge asymmetry, differential branching fraction, isospin asymmetry, and ratio of rates of decay into dimuon and dielectron final states, all as a function of the invariant mass squared of the dilepton system q^2 . All of these observable sets can be sensitive to different types of new physics that allow for FCNCs at tree or loop level. The BaBar, Belle, CDF, CMS, and LHCb collaborations have published the results of studies of the angular distributions for $B_d^0 \rightarrow K^*\mu^+\mu^-$ [1–8]. The LHCb Collaboration has reported a potential hint, at the level of 3.4 standard deviations, of a deviation from SM calculations [3, 4] in this decay mode when using a parameterization of the angular distribution designed to minimise uncertainties from hadronic form factors. Measurements using this approach were also reported by the Belle Collaboration [8] and they are consistent with the LHCb experiment’s results and with the SM calculations. This paper presents results following the methodology outlined in Ref. [3] and the convention adopted by the LHCb Collaboration for the definition of angular observables described in Ref. [9]. The results obtained here are compared with theoretical predictions that use the form factors computed in Ref. [10].

This article presents the results of an angular analysis of the decay $B_d^0 \rightarrow K^*\mu^+\mu^-$ with the ATLAS detector, using 20.3 fb^{-1} of pp collision data at a centre-of-mass energy $\sqrt{s} = 8 \text{ TeV}$ delivered by the Large Hadron Collider (LHC) [11] during 2012. Results are presented in six different bins of q^2 in the range 0.04 to 6.0 GeV^2 , where three of these bins overlap. Backgrounds, including a radiative tail from $B_d^0 \rightarrow K^*J/\psi$ events, increase for q^2 above 6.0 GeV^2 , and for this reason, data above this value are not studied.

The operator product expansion used to describe the decay $B_d^0 \rightarrow K^*\mu^+\mu^-$ encodes short-distance contributions in terms of Wilson coefficients and long-distance contributions in terms of operators [12]. Global fits for Wilson coefficients have been performed using measurements of $B_d^0 \rightarrow K^*\mu^+\mu^-$ and other rare processes. Such studies aim to connect deviations from the SM predictions in several processes to identify a consistent pattern hinting at the structure of a potential underlying new-physics Lagrangian, see Refs. [13–15]. The parameters presented in this article can be used as inputs to these global fits.

2 Analysis method

Three angular variables describing the decay are defined according to convention described by the LHCb Collaboration in Ref. [9]: the angle between the K^+ and the direction opposite to the B_d^0 in the K^*

¹ The forward-backward asymmetry is given by the normalised difference between the number of positive muons going in the forward and backward directions with respect to the direction opposite to B_d^0 momentum in the dimuon rest frame.

centre-of-mass frame (θ_K); the angle between the μ^+ and the direction opposite to the B_d^0 in the dimuon centre-of-mass frame (θ_L); and the angle between the two decay planes formed by the $K\pi$ and the dimuon systems in the B_d^0 rest frame (ϕ). For \bar{B}_d^0 mesons the definitions are given with respect to the negatively charged particles. Figure 1 illustrates the angles used.

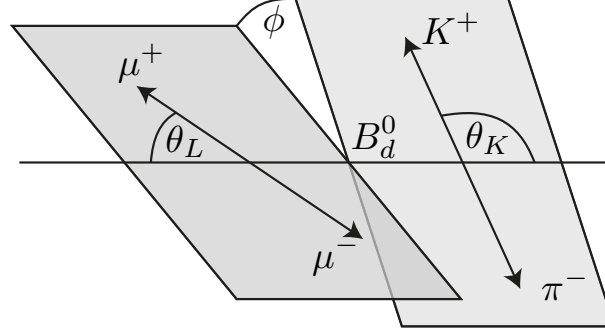


Figure 1: An illustration of the $B_d^0 \rightarrow K^* \mu^+ \mu^-$ decay showing the angles θ_K , θ_L and ϕ defined in the text. Angles are computed in the rest frame of the K^* , dimuon system and B_d^0 meson, respectively.

The angular differential decay rate for $B_d^0 \rightarrow K^* \mu^+ \mu^-$ is a function of q^2 , $\cos \theta_K$, $\cos \theta_L$ and ϕ , and can be written in several ways [16]. The form to express the differential decay amplitude as a function of the angular parameters uses coefficients that may be represented by the helicity or transversity amplitudes [17] and is written as²

$$\begin{aligned} \frac{1}{d\Gamma/dq^2 d\cos\theta_L d\cos\theta_K d\phi dq^2} &= \frac{9}{32\pi} \left[\frac{3(1-F_L)}{4} \sin^2 \theta_K + F_L \cos^2 \theta_K + \frac{1-F_L}{4} \sin^2 \theta_K \cos 2\theta_L \right. \\ &\quad - F_L \cos^2 \theta_K \cos 2\theta_L + S_3 \sin^2 \theta_K \sin^2 \theta_L \cos 2\phi \\ &\quad + S_4 \sin 2\theta_K \sin 2\theta_L \cos \phi + S_5 \sin 2\theta_K \sin \theta_L \cos \phi \\ &\quad + S_6 \sin^2 \theta_K \cos \theta_L + S_7 \sin 2\theta_K \sin \theta_L \sin \phi \\ &\quad \left. + S_8 \sin 2\theta_K \sin 2\theta_L \sin \phi + S_9 \sin^2 \theta_K \sin^2 \theta_L \sin 2\phi \right]. \end{aligned} \quad (1)$$

Here F_L is the fraction of longitudinally polarised K^* mesons and the S_i are angular coefficients. These angular parameters are functions of the real and imaginary parts of the transversity amplitudes of B_d^0 decays into $K^* \mu^+ \mu^-$. The forward-backward asymmetry is given by $A_{FB} = 3S_6/4$. The predictions for the S parameters depend on hadronic form factors which have significant uncertainties at leading order. It is possible to reduce the theoretical uncertainty in these predictions by transforming the S_i using ratios constructed to cancel form factor uncertainties at leading order. These ratios are given by Refs. [17, 18]

² This equation neglects possible $K\pi$ S -wave contributions. The effect of an S -wave contribution is considered following the method used by LHCb in Ref. [3].

as

$$P_1 = \frac{2S_3}{1 - F_L} \quad (2)$$

$$P_2 = \frac{2}{3} \frac{A_{\text{FB}}}{1 - F_L} \quad (3)$$

$$P_3 = -\frac{S_9}{1 - F_L} \quad (4)$$

$$P'_{j=4,5,6,8} = \frac{S_{i=4,5,7,8}}{\sqrt{F_L(1 - F_L)}}. \quad (5)$$

All of the parameters introduced, F_L , S_i and $P_j^{(\prime)}$, may vary with q^2 and the data are analysed in q^2 bins to obtain an average value for a given parameter in that bin.

3 The ATLAS detector, data, and Monte Carlo samples

The ATLAS experiment at the LHC is a general-purpose detector with a cylindrical geometry and nearly 4π coverage in solid angle [19]. It consists of an inner detector (ID) for tracking, a calorimeter system and a muon spectrometer (MS). The ID consists of silicon pixel and strip detectors, with a straw-tube transition radiation tracker providing additional information for tracks passing through the central region of the detector.³ The ID has a coverage of $|\eta| < 2.5$, and is immersed in a 2T axial magnetic field generated by a superconducting solenoid. The calorimeter system, consisting of liquid argon and scintillator-tile sampling calorimeter subsystems, surrounds the ID. The outermost part of the detector is the MS, which employs several detector technologies in order to provide muon identification and a muon trigger. A toroidal magnet system is embedded in the MS. The ID, calorimeter system and MS have full azimuthal coverage.

The data analysed here were recorded in 2012 during Run 1 of the LHC. The centre-of-mass energy of the pp system was $\sqrt{s} = 8$ TeV. After applying data-quality criteria, the data sample analysed corresponds to an integrated luminosity of 20.3 fb^{-1} . A number of Monte Carlo (MC) signal and background event samples were generated, with b -hadron production in pp collisions simulated with PYTHIA 8.186 [20, 21]. The AU2 set of tuned parameters [22] is used together with the CTEQ6L1 PDF set [23]. The EvtGen 1.2.0 program [24] is used for the properties of b - and c -hadron decays. The simulation included modelling of multiple interactions per pp bunch crossing in the LHC with PYTHIA soft QCD processes. The simulated events were then passed through the full ATLAS detector simulation program based on GEANT 4 [25, 26] and reconstructed in the same way as data. The samples of MC generated events are described further in Section 5.

³ ATLAS uses a right-handed coordinate system with its origin at the nominal interaction point (IP) in the centre of the detector and the z -axis along the beam pipe. The x -axis points from the IP to the centre of the LHC ring, and the y -axis points upward. Cylindrical coordinates (r, Φ) are used in the transverse plane, Φ being the azimuthal angle around the z -axis. The pseudorapidity is defined in terms of the polar angle θ as $\eta = -\ln \tan(\theta/2)$.

4 Event selection

Several trigger signatures constructed from the MS and ID inputs are selected based on availability during the data-taking period, prescale factor and efficiency for signal identification. Data are combined from 19 trigger chains where 21%, 89% or 5% of selected events pass at least one trigger with one, two, or at least three muons identified online in the MS, respectively. Of the events passing the requirement of at least two muons, the largest contribution comes from the chain requiring one muon with a transverse momentum $p_T > 4$ GeV and the other muon with $p_T > 6$ GeV. This combination of triggers ensures that the analysis remains sensitive to events down to the kinematic threshold of $q^2 = 4m_\mu^2$, where m_μ is the muon mass. The effective average trigger efficiency for selected signal events is about 29%, determined from signal MC simulation.

Muon track candidates are formed offline by combining information from both the ID and MS [27]. Tracks are required to satisfy $|\eta| < 2.5$. Candidate muon (kaon and pion) tracks in the ID are required to satisfy $p_T > 3.5$ (0.5) GeV. Pairs of oppositely charged muons are required to originate from a common vertex with a fit quality $\chi^2/\text{NDF} < 10$.

Candidate K^* mesons are formed using pairs of oppositely charged kaon and pion candidates reconstructed from hits in the ID. Candidates are required to satisfy $p_T(K^*) > 3.0$ GeV. As the ATLAS detector does not have a dedicated charged-particle identification system, candidates are reconstructed with both possible $K\pi$ mass hypotheses. The selection implicitly relies on the kinematics of the reconstructed K^* meson to determine which of the two tracks corresponds to the kaon. If both candidates in an event satisfy selection criteria, they are retained and one of them is selected in the next step following a procedure described below. The $K\pi$ invariant mass is required to lie in a window of twice the natural width around the nominal mass of 896 MeV, i.e. in the range [846, 946] MeV. The charge of the kaon candidate is used to assign the flavour of the reconstructed B_d^0 candidate.

The B_d^0 candidates are reconstructed from a K^* candidate and a pair of oppositely charged muons. The four-track vertex is fitted and required to satisfy $\chi^2/\text{NDF} < 2$ to suppress background. A significant amount of combinatorial, B_d^0 , B^+ , B_s^0 and Λ_b background contamination remains at this stage. Combinatorial background is suppressed by requiring a B_d^0 candidate lifetime significance $\tau/\sigma_\tau > 12.5$, where the decay time uncertainty σ_τ is calculated from the covariance matrices associated with the four-track vertex fit and with the primary vertex fit. Background from final states partially reconstructed as $B \rightarrow \mu^+\mu^-X$ accumulates at invariant mass below the B_d^0 mass and contributes to the signal region. It is suppressed by imposing an asymmetric mass cut around the nominal B_d^0 mass, $5150 \text{ MeV} < m_{K\pi\mu\mu} < 5700 \text{ MeV}$. The high-mass sideband is retained, as the parameter values for the combinatorial background shapes are extracted from the fit to data described in Section 5. To further suppress background, it is required that the angle Θ , defined between the vector from the primary vertex to the B_d^0 candidate decay vertex and the B_d^0 candidate momentum, satisfies $\cos \Theta > 0.999$. Resolution effects on $\cos \theta_K$, $\cos \theta_L$ and ϕ were found to have a negligible effect on the ATLAS $B_s^0 \rightarrow J/\psi\phi$ analysis [28]. It is assumed to also be the case for $B_d^0 \rightarrow K^*\mu^+\mu^-$.

On average 12% of selected events in the data have more than one reconstructed B_d^0 candidate. The fraction is 17% for signal MC samples and 2–10% for exclusive background MC samples. A two-step selection process is used for such events. For 4% of these events it is possible to select a candidate with the smallest value of the B_d^0 vertex χ^2/NDF . However, the majority, about 96%, of multiple candidates arise from four-track combinations where the kaon and pion assignments are ambiguous. As these candidates have degenerate values for the B_d^0 candidate vertex χ^2/NDF , a second selection step is required. The B_d^0

candidate reconstructed with the smallest value of $|m_{K\pi} - m_{K^*}|/\sigma(m_{K\pi})$ is retained for analysis, where $m_{K\pi}$ is the K^* candidate mass, $\sigma(m_{K\pi})$ is the uncertainty in this quantity, and m_{K^*} is the world average value of the K^* mass.

The selection procedure results in an incorrect flavour tag (mistag) for some signal events. The mistag probability of a B_d^0 (\bar{B}_d^0) meson is denoted by ω ($\bar{\omega}$) and is determined from MC simulated events to be 0.1088 ± 0.0005 (0.1086 ± 0.0005). The mistag probability varies slightly with q^2 such that the difference $\omega - \bar{\omega}$ remains consistent with zero. Hence the average mistag rate $\langle\omega\rangle$ in a given q^2 bin is used to account for this effect. If a candidate is mistagged, the values of $\cos\theta_L$, $\cos\theta_K$ and ϕ change sign, while the latter two are also slightly shaped by the swapped hadron track mass hypothesis. Sign changes in these angles affect the overall sign of the terms multiplied by the coefficients S_5 , S_6 , S_8 and S_9 (similarly for the corresponding $P^{(\prime)}$ parameters) in Equation (1). The corollary is that mistagged events result in a dilution factor of $(1 - 2\langle\omega\rangle)$ for the affected coefficients.

The region $q^2 \in [0.98, 1.1]$ GeV² is vetoed to remove any potential contamination from the $\phi(1020)$ resonance. The remaining data with $q^2 \in [0.04, 6.0]$ GeV² are analysed in order to extract the signal parameters of interest. Two $K^*c\bar{c}$ control regions are defined for B_d^0 decays into K^*J/ψ and $K^*\psi(2S)$, respectively as $q^2 \in [8, 11]$ and $[12, 15]$ GeV². The control samples are used to extract values for nuisance parameters describing the signal probability density function (pdf) from data as discussed in Section 5.3.

For $q^2 < 6$ GeV² the selected data sample consists of 787 events and is composed of signal $B_d^0 \rightarrow K^*\mu^+\mu^-$ decay events as well as background that is dominated by a combinatorial component that does not peak in $m_{K\pi\mu\mu}$ and does not exhibit a resonant structure in q^2 . Other background contributions are considered when estimating systematic uncertainties. Above 6 GeV² the background contribution increases significantly, including events coming from $B_d^0 \rightarrow K^*J/\psi$ with a radiative $J/\psi \rightarrow \mu^+\mu^-\gamma$ decay. Scalar $K\pi$ contributions are neglected in the nominal fit and considered only when addressing systematic uncertainties. The data are analysed in the q^2 bins $[0.04, 2.0]$, $[2.0, 4.0]$ and $[4.0, 6.0]$ GeV², where the bin width is chosen to provide a sample of signal events sufficient to perform an angular analysis. The width is much larger than the q^2 resolution obtained from MC simulated signal events and observed in data for B_d^0 decays into K^*J/ψ and $K^*\psi(2S)$. Additional overlapping bins $[0.04, 4.0]$, $[1.1, 6.0]$ and $[0.04, 6.0]$ GeV² are analysed in order to facilitate comparison with results of other experiments and with theoretical predictions.

5 Maximum-likelihood fit

Extended unbinned maximum-likelihood fits of the angular distributions of the signal decay are performed on the data for each q^2 bin. The discriminating variables used in the fit are $m_{K\pi\mu\mu}$, the cosines of the helicity angles ($\cos\theta_K$ and $\cos\theta_L$), and ϕ . The likelihood \mathcal{L} for a given q^2 bin is

$$\mathcal{L} = \frac{e^{-n}}{N!} \prod_{k=1}^N \sum_l n_l P_{kl}(m_{K\pi\mu\mu}, \cos\theta_K, \cos\theta_L, \phi; \hat{p}, \hat{\theta}), \quad (6)$$

where N is the total number of events, the sum runs over signal and background components, n_l is the fitted yield for the l^{th} component, n is the sum over n_l , and P_{kl} is the pdf evaluated for event k and component l . In the nominal fit, l iterates only over one signal and one background component. The \hat{p} are parameters of interest (F_L , S_i) and $\hat{\theta}$ are nuisance parameters. The remainder of this section discusses the signal model

(Section 5.1), treatment of background (Section 5.2), use of $K^*c\bar{c}$ decay control samples (Section 5.3), fitting procedure and validation (Section 5.4).

5.1 Signal model

The signal mass distribution is modelled by a Gaussian distribution with the width given by the per-event uncertainty in the $K\pi\mu\mu$ mass, $\sigma(m_{K\pi\mu\mu})$, as estimated from the track fit, multiplied by a unit-less scale factor ξ , i.e. the width given by $\xi \cdot \sigma(m_{K\pi\mu\mu})$. The mean values of the B_d^0 candidate mass (m_0) and ξ of the signal Gaussian pdf are determined from fits to data in the control regions as described in Section 5.3. The simultaneous extraction of all coefficients using the full angular distribution of Equation (1) requires a certain minimum signal yield and signal purity to avoid a pathological fit behaviour. A significant fraction of fits to ensembles of simulated pseudo-experiments do not converge using the full distribution. This is mitigated using trigonometric transformations to fold certain angular distributions and thereby simplify Equation (1) such that only three parameters are extracted in one fit: F_L , S_3 and one of the other S parameters. Following Ref. [3], the transformations listed below are used:

$$F_L, S_3, S_4, P'_4 : \begin{cases} \phi \rightarrow -\phi & \text{for } \phi < 0 \\ \phi \rightarrow \pi - \phi & \text{for } \theta_L > \frac{\pi}{2} \\ \theta_L \rightarrow \pi - \theta_L & \text{for } \theta_L > \frac{\pi}{2}, \end{cases} \quad (7)$$

$$F_L, S_3, S_5, P'_5 : \begin{cases} \phi \rightarrow -\phi & \text{for } \phi < 0 \\ \theta_L \rightarrow \pi - \theta_L & \text{for } \theta_L > \frac{\pi}{2}, \end{cases} \quad (8)$$

$$F_L, S_3, S_7, P'_6 : \begin{cases} \phi \rightarrow \pi - \phi & \text{for } \phi > \frac{\pi}{2} \\ \phi \rightarrow -\pi - \phi & \text{for } \phi < -\frac{\pi}{2} \\ \theta_L \rightarrow \pi - \theta_L & \text{for } \theta_L > \frac{\pi}{2}, \end{cases} \quad (9)$$

$$F_L, S_3, S_8, P'_8 : \begin{cases} \phi \rightarrow \pi - \phi & \text{for } \phi > \frac{\pi}{2} \\ \phi \rightarrow -\pi - \phi & \text{for } \phi < -\frac{\pi}{2} \\ \theta_L \rightarrow \pi - \theta_L & \text{for } \theta_L > \frac{\pi}{2} \\ \theta_K \rightarrow \pi - \theta_K & \text{for } \theta_L > \frac{\pi}{2}. \end{cases} \quad (10)$$

On applying transformation (7), (8), (9), and (10), the angular variable ranges become

$$\begin{aligned} \cos \theta_L &\in [0, 1], \cos \theta_K \in [-1, 1] \text{ and } \phi \in [0, \pi], \\ \cos \theta_L &\in [0, 1], \cos \theta_K \in [-1, 1] \text{ and } \phi \in [0, \pi], \\ \cos \theta_L &\in [0, 1], \cos \theta_K \in [-1, 1] \text{ and } \phi \in [-\pi/2, \pi/2], \\ \cos \theta_L &\in [0, 1], \cos \theta_K \in [-1, 1] \text{ and } \phi \in [-\pi/2, \pi/2], \end{aligned}$$

respectively. A consequence of using the folding schemes is that S_6 (A_{FB}) and S_9 cannot be extracted from the data. For these schemes the angular parameters of interest, denoted by \hat{p} in Equation (6), are (F_L, S_3, S_i) where $i = 4, 5, 7, 8$. These translate into (F_L, P_1, P'_j) , where $j = 4, 5, 6, 8$, using Equation (5).

The values and uncertainties of F_L and S_3 obtained from the four fits are consistent with each other and the results reported are those found to have the smallest systematic uncertainty.

Three MC samples are used to study the signal reconstruction and acceptance. Two of them follow the SM prediction for the decay angle distributions taken from Ref. [29], with separate samples generated for B_d^0 and \bar{B}_d^0 decays. The third MC sample has $F_L = 1/3$ and the angular distributions are generated uniformly in $\cos \theta_K$, $\cos \theta_L$ and ϕ . The samples are used to study the effect of potential mistagging and reconstruction differences between particle and antiparticle decays and for determination of the acceptance. The acceptance function is defined as the ratio of reconstructed and generated distributions of $\cos \theta_K$, $\cos \theta_L$, ϕ , i.e. it is compensating for the bias in the angular distributions resulting from triggering, reconstruction and selection of events. It is described by sixth-order (second-order) polynomial distributions for $\cos \theta_K$ and $\cos \theta_L$ (ϕ) and is assumed to factorise for each angular distribution, i.e. using $\varepsilon(\cos \theta_K, \cos \theta_L, \phi) = \varepsilon(\cos \theta_K)\varepsilon(\cos \theta_L)\varepsilon(\phi)$. A systematic uncertainty is assessed in order to account for this assumption. The acceptance function multiplies the angular distribution in the fit, i.e. the signal pdf is

$$P_{kl} = \varepsilon(\cos \theta_K)\varepsilon(\cos \theta_L)\varepsilon(\phi)g(\cos \theta_K, \cos \theta_L, \phi) \cdot G(m_{K\pi\mu\mu}),$$

where $g(\cos \theta_K, \cos \theta_L, \phi)$ is an angular differential decay rate resulting from one of the four folding schemes applied to Equation (1) and $G(m_{K\pi\mu\mu})$ is the signal mass distribution. The MC sample generated with uniform $\cos \theta_K$, $\cos \theta_L$ and ϕ distributions is used to determine the nominal acceptance functions for each of the transformed variables defined in Equations (7)–(10). The other samples are used to estimate the related systematic uncertainty. Among the angular variables the $\cos \theta_L$ distribution is the most affected by the acceptance. This is a result of the minimum transverse momentum requirements on the muons in the trigger and the larger inefficiency to reconstruct low-momentum muons, such that large values of $|\cos \theta_L|$ are inaccessible at low q^2 . As q^2 increases, the acceptance effects become less severe. The $\cos \theta_K$ distribution is affected by the ability to reconstruct the $K\pi$ system, but that effect shows no significant variation with q^2 . There is no significant acceptance effect for ϕ . Figure 2 shows the acceptance functions used for $\cos \theta_K$ and $\cos \theta_L$ for two different q^2 ranges for the nominal angular distribution given in Equation (1).

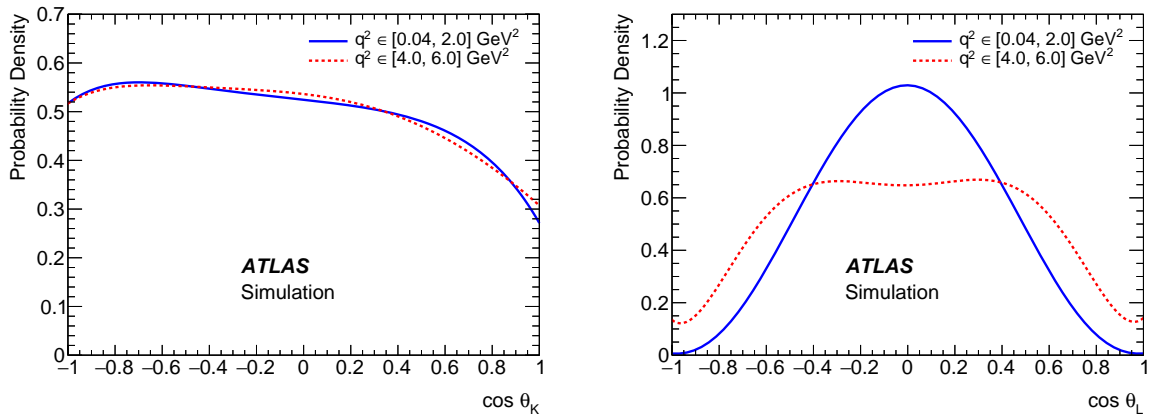


Figure 2: The acceptance functions for (left) $\cos \theta_K$ and (right) $\cos \theta_L$ for (solid) $q^2 \in [0.04, 2.0] \text{ GeV}^2$ and (dashed) $q^2 \in [4.0, 6.0] \text{ GeV}^2$, that shape the angular decay rate of Equation (1).

5.2 Background modes

The fit to data includes a combinatorial background component that does not peak in the $m_{K\pi\mu\mu}$ distribution. It is assumed that the background pdf factorises into a product of one-dimensional terms. The mass distribution of this component is described by an exponential function and second-order Chebychev polynomials are used to model the $\cos\theta_K$, $\cos\theta_L$ and ϕ distributions. The values of the nuisance parameters describing these shapes are obtained from fits to the data independently for each q^2 bin.

Inclusive samples of $b\bar{b} \rightarrow \mu^+\mu^-X$ and $c\bar{c} \rightarrow \mu^+\mu^-X$ decays and eleven exclusive B_d^0 , B_s^0 , B^+ and Λ_b background samples are studied in order to identify contributions of interest to be included in the fit model, or to be considered when estimating systematic uncertainties. The relevant exclusive modes found to be of interest are discussed below. Events with B_c decays are suppressed by excluding the q^2 range containing the J/ψ and $\psi(2S)$, and by charm meson vetoes discussed in Section 7. The exclusive background decays considered for the signal mode are $\Lambda_b \rightarrow \Lambda(1520)\mu^+\mu^-$, $\Lambda_b \rightarrow pK^-\mu^+\mu^-$, $B^+ \rightarrow K^{(*)+}\mu^+\mu^-$ and $B_s^0 \rightarrow \phi\mu^+\mu^-$. These background contributions are accounted for as systematic uncertainties estimated as described in Section 7.

Two distinct background contributions not considered above are observed in the $\cos\theta_K$ and $\cos\theta_L$ distributions. They are not accounted for in the nominal fit to data, and are treated as systematic effects. A peak is found in the $\cos\theta_K$ distribution near 1.0 and appears to have contributions from at least two distinct sources. One of these arises from misreconstructed B^+ decays, such as $B^+ \rightarrow K^+\mu\mu$ and $B^+ \rightarrow \pi^+\mu\mu$. These decays can be reconstructed as signal if another track is combined with the hadron to form a K^* candidate in such a way that the event passes the reconstruction and selection. The second contribution comes from combinations of two charged tracks that pass the selection and are reconstructed as a K^* candidate. These fake K^* candidates accumulate around $\cos\theta_K$ of 1.0 and are observed in the $K\pi$ mass sidebands away from the K^* meson. They are distinct from the structure of expected S -, P - and D -wave $K\pi$ decays resulting from a signal $B_d^0 \rightarrow K\pi\mu\mu$ transition. The origin of this source of background is not fully understood. The observed excess may arise from a statistical fluctuation, an unknown background process, or a combination of both. Systematic uncertainties are assigned to evaluate the effect of these two background contributions, as described in Section 7.

Another peak is found in the $\cos\theta_L$ distribution near values of ± 0.7 . It is associated with partially reconstructed B decays into final states with a charm meson. This is studied using Monte Carlo simulated events for the decays $D^0 \rightarrow K^-\pi^+$, $D^+ \rightarrow K^-\pi^+\pi^+$ and $D_s^+ \rightarrow K^+K^-\pi^+$. Events with a B meson decaying via an intermediate charm meson D^0 , D^+ or D_s^+ are found to pass the selection and are reconstructed in such a way that they accumulate around 0.7 in $|\cos\theta_L|$. These are removed from the data sample when estimating systematic uncertainties, as described in Section 7.

5.3 $K^*c\bar{c}$ control sample fits

The mass distribution obtained from the simulated samples for $K^*c\bar{c}$ decays and the signal mode, in different bins of q^2 , are found to be consistent with each other. Values of m_0 and ξ for $B_d^0 \rightarrow K^*J/\psi$ and $B_d^0 \rightarrow K^*\psi(2S)$ events are used for the signal pdf and extracted from fits to the data. An extended unbinned maximum-likelihood fit is performed in the two $K^*c\bar{c}$ control region samples. There are three exclusive backgrounds included: $\Lambda_b \rightarrow \Lambda c\bar{c}$, $B^+ \rightarrow K^+c\bar{c}$ and $B_s^0 \rightarrow K^*c\bar{c}$. The $K^*c\bar{c}$ pdf has the same form as the signal model, combinatorial background is described by an exponential distribution, and double and triple Gaussian pdfs determined from MC simulated events are used to describe the

exclusive background contributions. A systematic uncertainty is evaluated by allowing for 0, 1, 2 and 3 exclusive background components. The control sample fit projections for the variant of the fit including all three exclusive backgrounds can be found in Figure 3. The peak position and scale factor of the signal pdf are not sensitive to the exclusive background model used. From these fits the statistical and systematic uncertainties in the values of m_0 and ξ are extracted for the B_d^0 component in order to be used in the $B_d^0 \rightarrow K^* \mu^+ \mu^-$ fits. From the J/ψ control data it is determined that the values for the nuisance parameters describing the signal model pdf in the $K\pi\mu\mu$ mass are $m_0 = 5276.6 \pm 0.3 \pm 0.4$ MeV and $\xi = 1.210 \pm 0.004 \pm 0.002$, where the uncertainties are statistical and systematic, respectively. The $\psi(2S)$ sample yields compatible results albeit with larger uncertainties. These results are similar to those obtained from the MC simulated samples, and the numbers derived from the $K^* J/\psi$ data are used for the signal region fits.

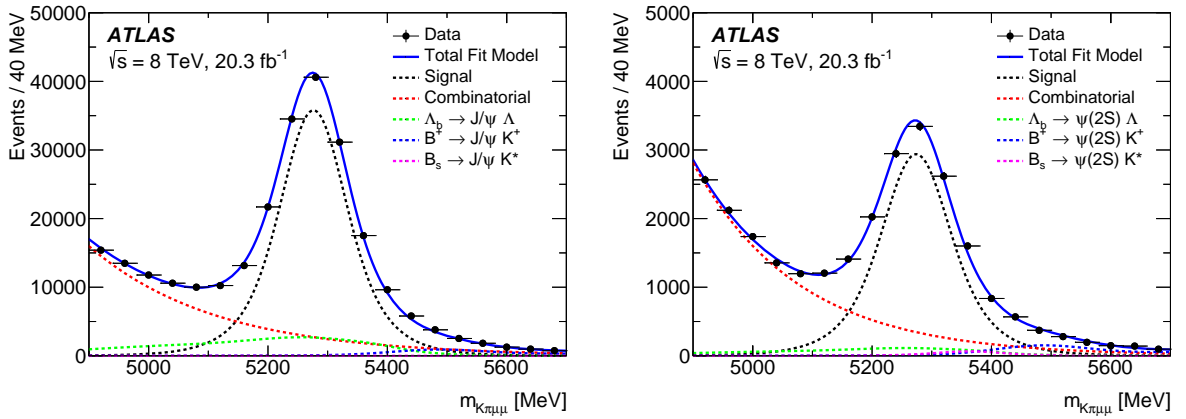


Figure 3: Fits to the $K\pi\mu\mu$ invariant mass distributions for the (left) $K^* J/\psi$ and (right) $K^* \psi(2S)$ control region samples. The data are shown as points and the total fit model as the solid lines. The dashed lines represent (black) signal, (red) combinatorial background, (green) Λ_b background, (blue) B^+ background and (magenta) B_s^0 background components.

5.4 Fitting procedure and validation

A two-step fit process is performed for the different signal bins in q^2 . The first step is a fit to the $K\pi\mu^+\mu^-$ invariant mass distribution, using the event-by-event uncertainty in the reconstructed mass as a conditional variable. For this fit, the parameters m_0 and ξ are fixed to the values obtained from fits to data control samples as described in Section 5.3. A second step adds the (transformed) $\cos\theta_K$, $\cos\theta_L$ and ϕ variables to the likelihood in order to extract F_L and the S parameters along with the values for the nuisance parameters related to the combinatorial background shapes. Some nuisance parameters, namely m_0 , ξ , signal and background yields, and the exponential shape parameter for the background mass pdf, are fixed to the results obtained from the first step.

The fit procedure is validated using ensembles of simulated pseudo-experiments generated with the F_L and S parameters corresponding to those obtained from the data. The purpose of these experiments is to measure the intrinsic fit bias resulting from the likelihood estimator used to extract signal parameters. These ensembles are also used to check that the uncertainties extracted from the fit are consistent with expectations. Ensembles of simulated pseudo-experiments are performed in which signal MC events are

injected into samples of background events generated from the likelihood. The signal yield determined from the first step in the fit process is found to be unbiased. The angular parameters extracted from the nominal fits have biases with magnitudes ranging between 0.01 and 0.04, depending on the fit variation and q^2 bin. A similar procedure is used to estimate the effect of neglecting S -wave contamination in the data sample. Neglecting the S -wave component in the fit model results in a bias between 0.00 and 0.02 in the angular parameters. Similarly, neglecting exclusive background contributions from Λ_b , B^+ and B_s^0 decays that peak in $m_{K\pi\mu\mu}$ near the B_d^0 mass results in a bias of less than 0.01 on the angular parameters. All these effects are included in the systematic uncertainties described in section 7. The $P^{(\prime)}$ parameters are obtained using the fit results and covariance matrices from the second fit along with Equations (2)–(5).

6 Results

The event yields obtained from the fits are summarised in Table 1 where only statistical uncertainties are reported. Figures 4 through 9 show for the different q^2 bins the distributions of the variables used in the fit for the S_5 folding scheme (corresponding to the transformation of Equation (8)) with the total, signal and background fitted pdfs superimposed. Similar sets of distributions are obtained for the three other folding schemes: S_4 , S_7 and S_8 . The results of the angular fits to the data in terms of the S_i and $P_j^{(\prime)}$ can be found in Tables 2 and 3. Statistical and systematic uncertainties are quoted in the tables. The distributions of F_L and the S_i parameters as a function of q^2 are shown in Figure 10 and those for $P_j^{(\prime)}$ are shown in Figure 11. The correlations between F_L and the S_i parameters and between F_L and the $P_j^{(\prime)}$ are given in Appendix A.

Table 1: The values of fitted signal, n_{signal} , and background, $n_{\text{background}}$, yields obtained for different bins in q^2 . The uncertainties indicated are statistical.

q^2 [GeV ²]	n_{signal}	$n_{\text{background}}$
[0.04, 2.0]	128 ± 22	122 ± 22
[2.0, 4.0]	106 ± 23	113 ± 23
[4.0, 6.0]	114 ± 24	204 ± 26
[0.04, 4.0]	236 ± 31	233 ± 32
[1.1, 6.0]	275 ± 35	363 ± 36
[0.04, 6.0]	342 ± 39	445 ± 40

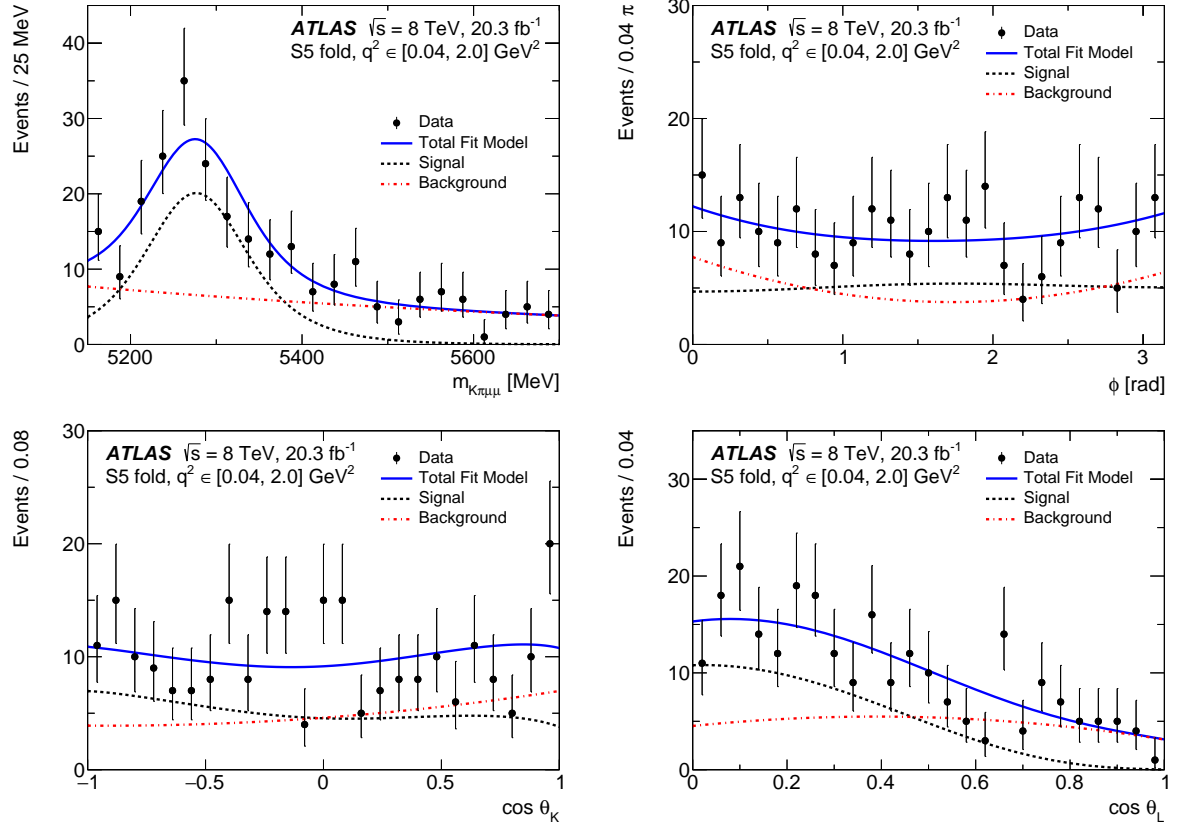


Figure 4: The distributions of (top left) $m_{K\pi\mu\mu}$, (top right) ϕ , (bottom left) $\cos \theta_K$, and (bottom right) $\cos \theta_L$ obtained for $q^2 \in [0.04, 2.0] \text{ GeV}^2$. The (blue) solid line is a projection of the total pdf, the (red) dot-dashed line represents the background, and the (black) dashed line represents the signal component. These plots are obtained from a fit using the S_5 folding scheme.

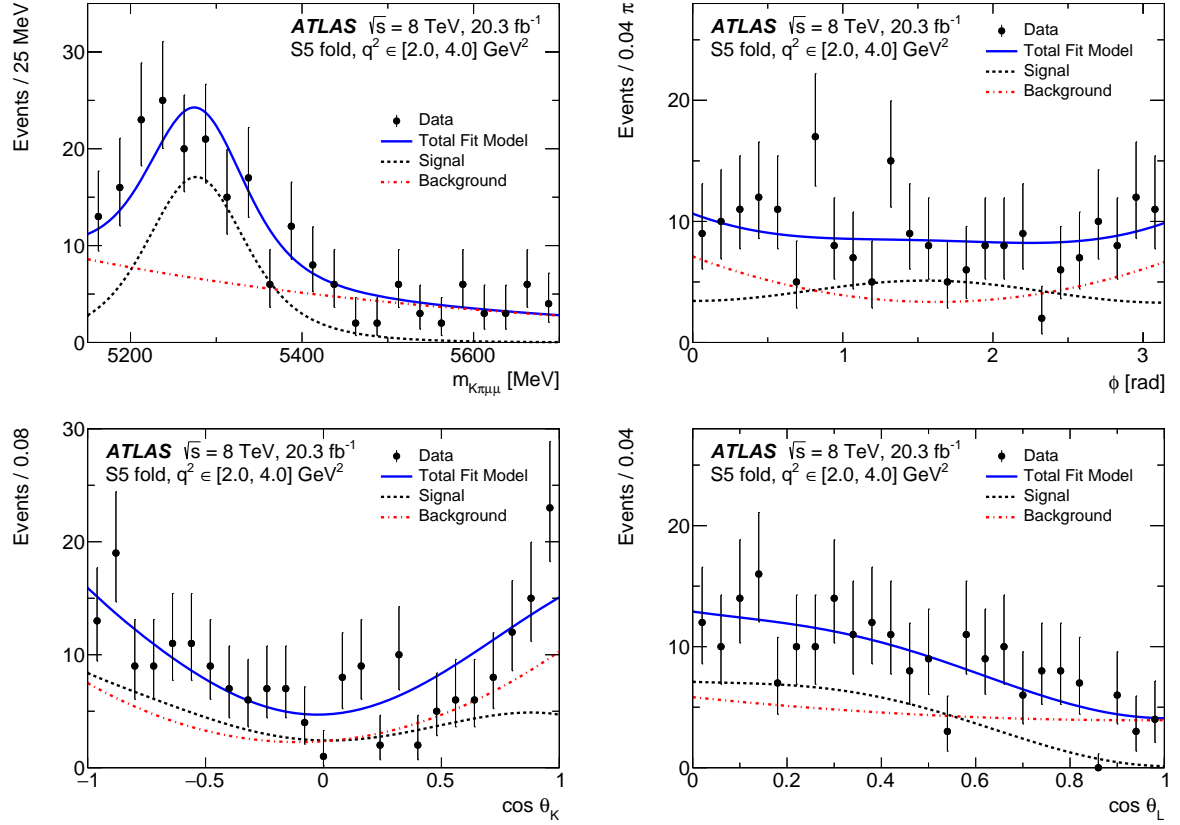


Figure 5: The distributions of (top left) $m_{K\pi\mu\mu}$, (top right) ϕ , (bottom left) $\cos \theta_K$, and (bottom right) $\cos \theta_L$ obtained for $q^2 \in [2.0, 4.0] \text{ GeV}^2$. The (blue) solid line is a projection of the total pdf, the (red) dot-dashed line represents the background, and the (black) dashed line represents the signal component. These plots are obtained from a fit using the S_5 folding scheme.

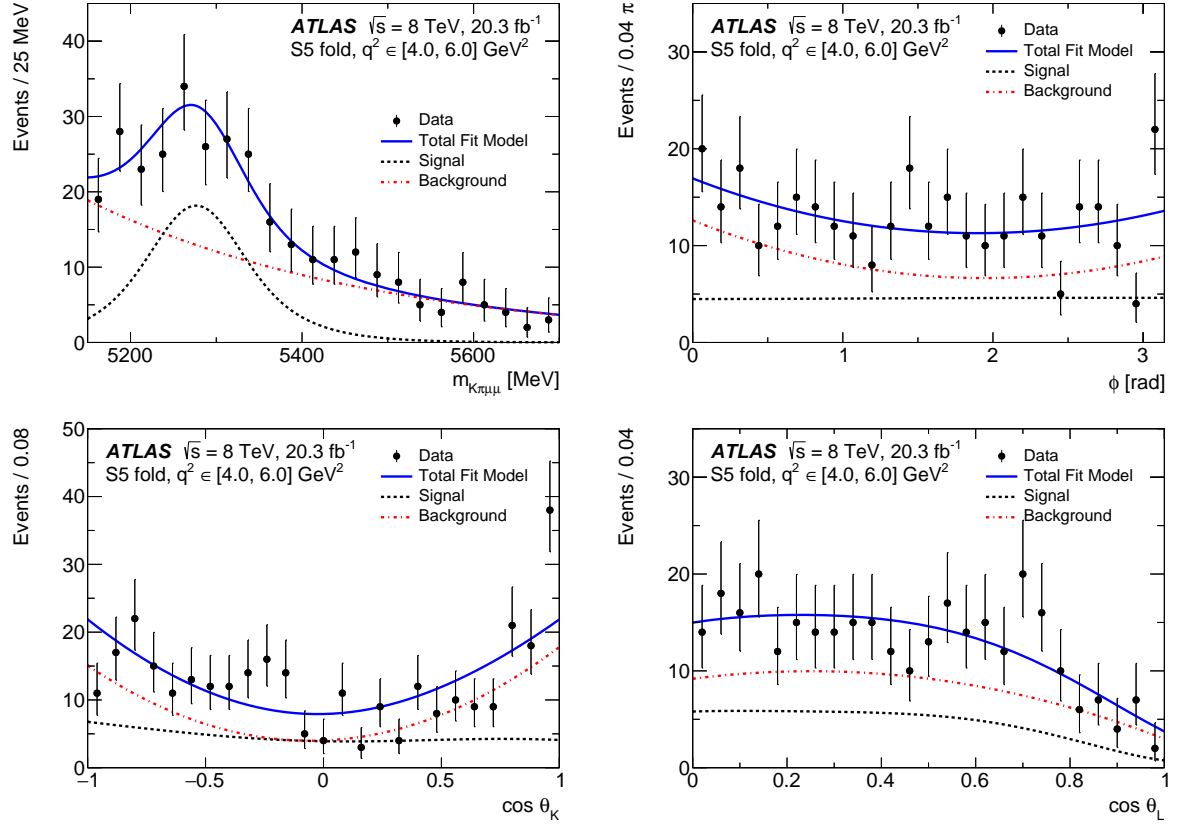


Figure 6: The distributions of (top left) $m_{K\pi\mu\mu}$, (top right) ϕ , (bottom left) $\cos \theta_K$, and (bottom right) $\cos \theta_L$ obtained for $q^2 \in [4.0, 6.0]$ GeV 2 . The (blue) solid line is a projection of the total pdf, the (red) dot-dashed line represents the background, and the (black) dashed line represents the signal component. These plots are obtained from a fit using the S_5 folding scheme.

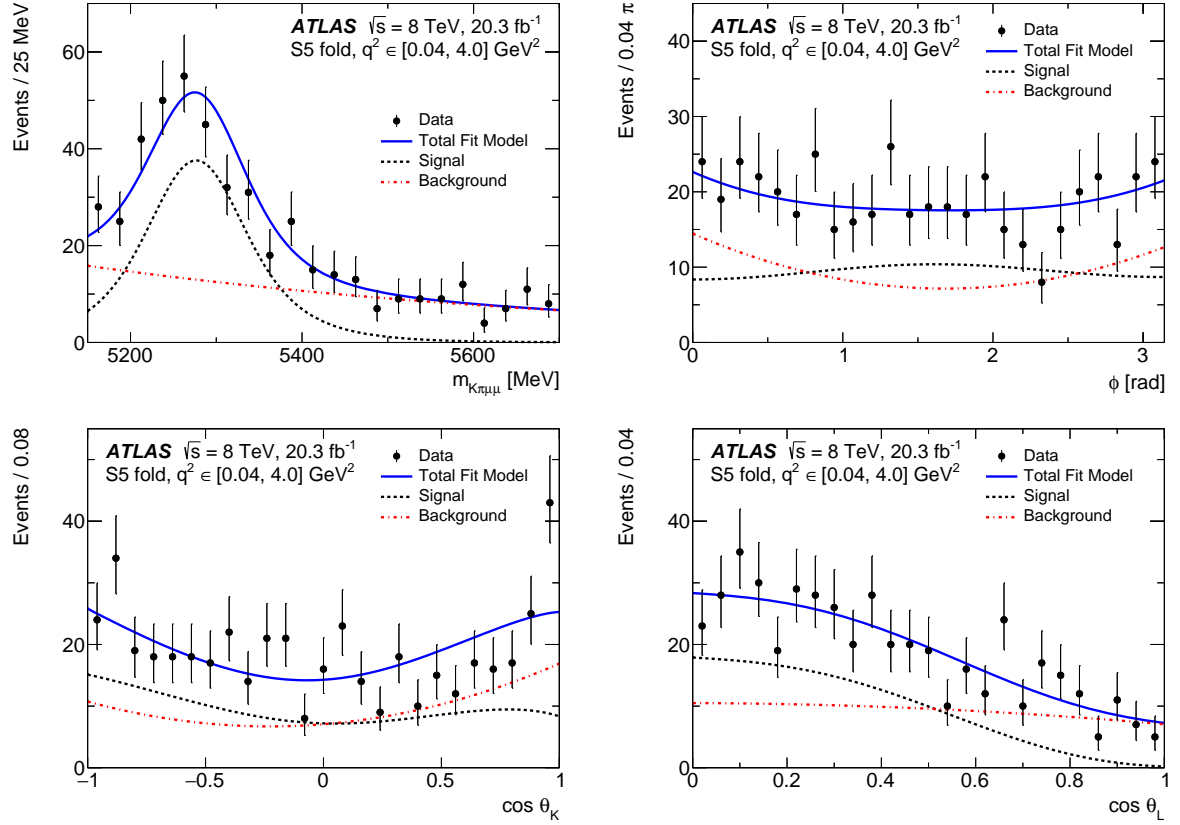


Figure 7: The distributions of (top left) $m_{K\pi\mu\mu}$, (top right) ϕ , (bottom left) $\cos \theta_K$, and (bottom right) $\cos \theta_L$ obtained for $q^2 \in [0.04, 4.0] \text{ GeV}^2$. The (blue) solid line is a projection of the total pdf, the (red) dot-dashed line represents the background, and the (black) dashed line represents the signal component. These plots are obtained from a fit using the S_5 folding scheme.

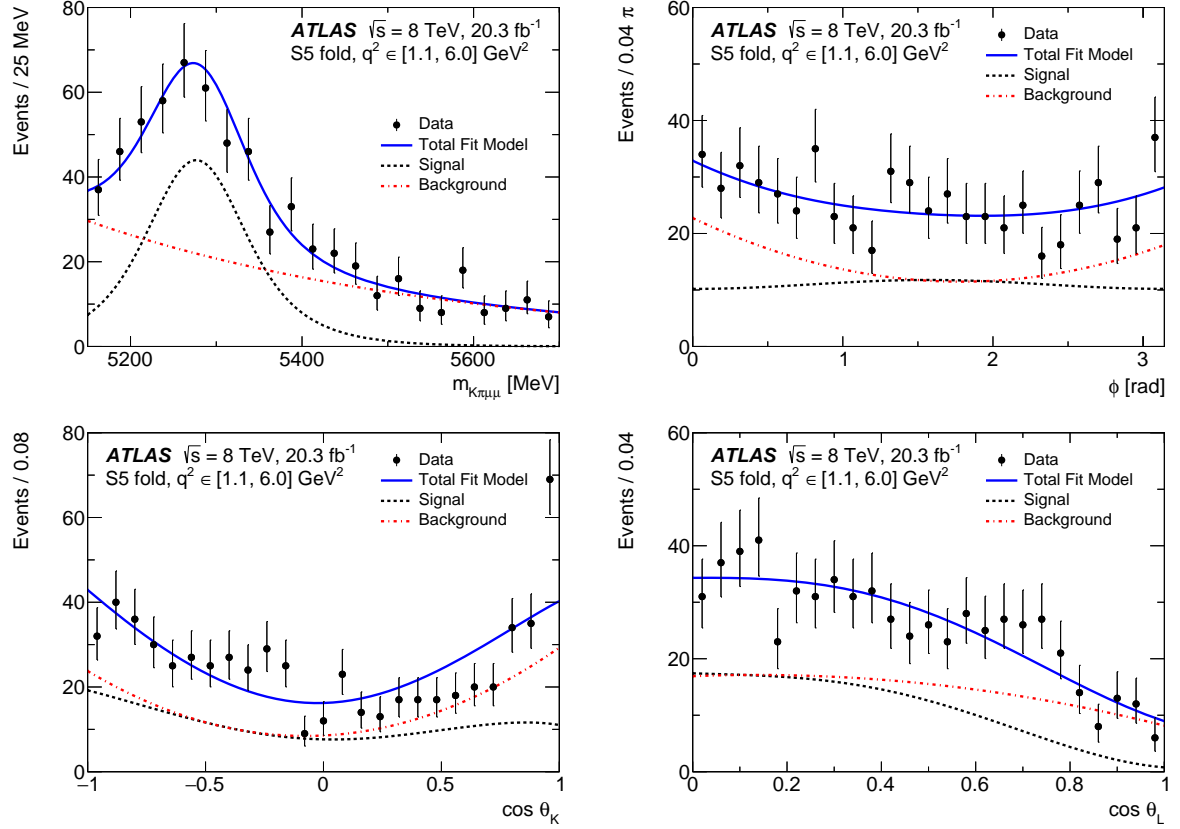


Figure 8: The distributions of (top left) $m_{K\pi\mu\mu}$, (top right) ϕ , (bottom left) $\cos \theta_K$, and (bottom right) $\cos \theta_L$ obtained for $q^2 \in [1.1, 6.0] \text{ GeV}^2$. The (blue) solid line is a projection of the total pdf, the (red) dot-dashed line represents the background, and the (black) dashed line represents the signal component. These plots are obtained from a fit using the S_5 folding scheme.

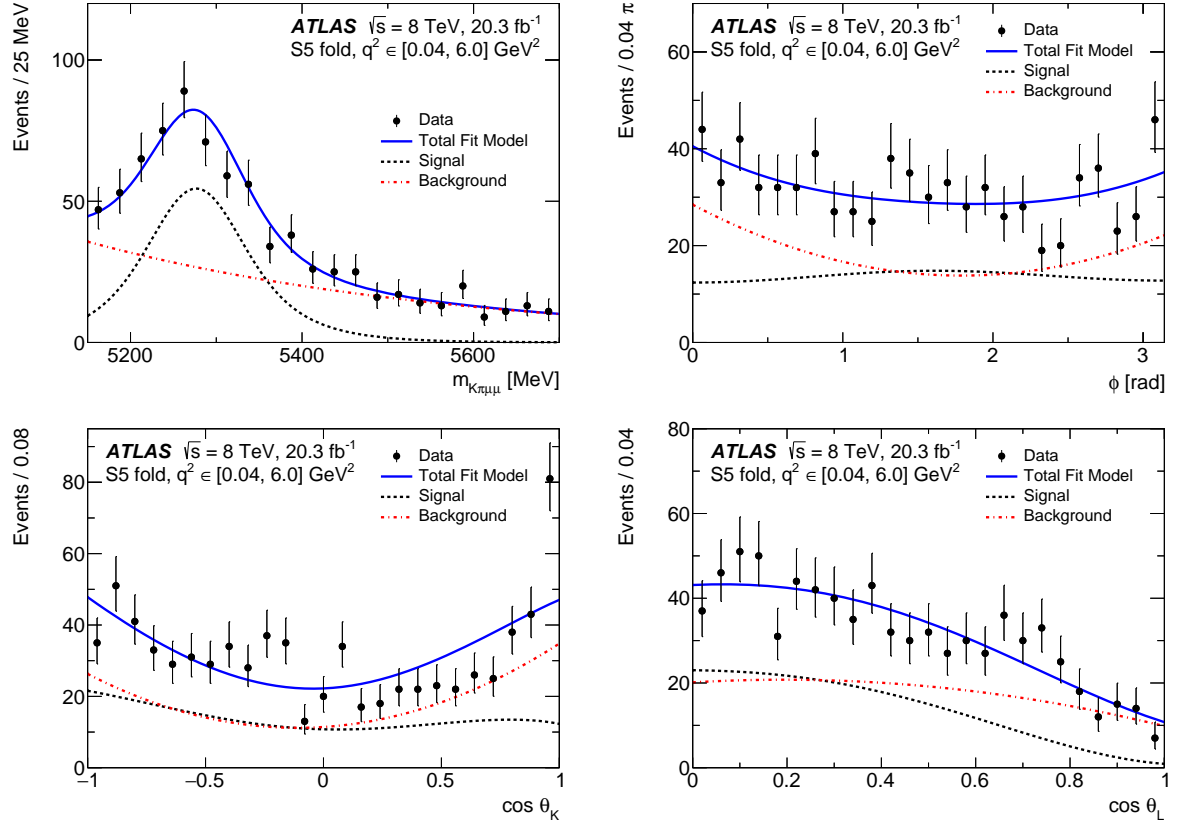


Figure 9: The distributions of (top left) $m_{K\pi\mu\mu}$, (top right) ϕ , (bottom left) $\cos \theta_K$, and (bottom right) $\cos \theta_L$ obtained for $q^2 \in [0.04, 6.0]$ GeV 2 . The (blue) solid line is a projection of the total pdf, the (red) dot-dashed line represents the background, and the (black) dashed line represents the signal component. These plots are obtained from a fit using the S_5 folding scheme.

Table 2: The values of F_L , and S_3 , S_4 , S_5 , S_7 and S_8 parameters obtained for different bins in q^2 . The uncertainties indicated are statistical and systematic, respectively.

q^2 [GeV ²]	F_L	S_3	S_4	S_5	S_7	S_8
[0.04, 2.0]	$0.44 \pm 0.08 \pm 0.07$	$-0.02 \pm 0.09 \pm 0.02$	$0.15 \pm 0.20 \pm 0.10$	$0.33 \pm 0.13 \pm 0.08$	$-0.09 \pm 0.10 \pm 0.02$	$-0.14 \pm 0.24 \pm 0.09$
[2.0, 4.0]	$0.64 \pm 0.11 \pm 0.05$	$-0.15 \pm 0.10 \pm 0.07$	$-0.37 \pm 0.15 \pm 0.10$	$-0.16 \pm 0.15 \pm 0.06$	$0.15 \pm 0.14 \pm 0.09$	$0.52 \pm 0.20 \pm 0.19$
[4.0, 6.0]	$0.42 \pm 0.13 \pm 0.12$	$0.00 \pm 0.12 \pm 0.07$	$0.32 \pm 0.16 \pm 0.09$	$0.13 \pm 0.18 \pm 0.09$	$0.03 \pm 0.13 \pm 0.07$	$-0.12 \pm 0.21 \pm 0.05$
[0.04, 4.0]	$0.52 \pm 0.07 \pm 0.06$	$-0.05 \pm 0.06 \pm 0.04$	$-0.15 \pm 0.12 \pm 0.09$	$0.16 \pm 0.10 \pm 0.05$	$0.01 \pm 0.08 \pm 0.05$	$0.19 \pm 0.16 \pm 0.12$
[1.1, 6.0]	$0.56 \pm 0.07 \pm 0.06$	$-0.04 \pm 0.07 \pm 0.03$	$0.03 \pm 0.11 \pm 0.07$	$0.00 \pm 0.10 \pm 0.04$	$0.02 \pm 0.08 \pm 0.06$	$0.11 \pm 0.14 \pm 0.10$
[0.04, 6.0]	$0.50 \pm 0.06 \pm 0.04$	$-0.04 \pm 0.06 \pm 0.03$	$0.03 \pm 0.10 \pm 0.07$	$0.14 \pm 0.09 \pm 0.03$	$0.02 \pm 0.07 \pm 0.05$	$0.07 \pm 0.13 \pm 0.09$

Table 3: The values of P_1 , P'_4 , P'_5 , P'_6 and P'_8 parameters obtained for different bins in q^2 . The uncertainties indicated are statistical and systematic, respectively.

q^2 [GeV ²]	P_1	P'_4	P'_5	P'_6	P'_8
[0.04, 2.0]	$-0.05 \pm 0.30 \pm 0.08$	$0.31 \pm 0.40 \pm 0.20$	$0.67 \pm 0.26 \pm 0.16$	$-0.18 \pm 0.21 \pm 0.04$	$-0.29 \pm 0.48 \pm 0.18$
[2.0, 4.0]	$-0.78 \pm 0.51 \pm 0.34$	$-0.76 \pm 0.31 \pm 0.21$	$-0.33 \pm 0.31 \pm 0.13$	$0.31 \pm 0.28 \pm 0.19$	$1.07 \pm 0.41 \pm 0.39$
[4.0, 6.0]	$0.14 \pm 0.43 \pm 0.26$	$0.64 \pm 0.33 \pm 0.18$	$0.26 \pm 0.35 \pm 0.18$	$0.06 \pm 0.27 \pm 0.13$	$-0.24 \pm 0.42 \pm 0.09$
[0.04, 4.0]	$-0.22 \pm 0.26 \pm 0.16$	$-0.30 \pm 0.24 \pm 0.17$	$0.32 \pm 0.21 \pm 0.11$	$0.01 \pm 0.17 \pm 0.10$	$0.38 \pm 0.33 \pm 0.24$
[1.1, 6.0]	$-0.17 \pm 0.31 \pm 0.13$	$0.05 \pm 0.22 \pm 0.14$	$0.01 \pm 0.21 \pm 0.08$	$0.03 \pm 0.17 \pm 0.12$	$0.23 \pm 0.28 \pm 0.20$
[0.04, 6.0]	$-0.15 \pm 0.23 \pm 0.10$	$0.05 \pm 0.20 \pm 0.14$	$0.27 \pm 0.19 \pm 0.06$	$0.03 \pm 0.15 \pm 0.10$	$0.14 \pm 0.27 \pm 0.17$

7 Systematic uncertainties

Systematic uncertainties in the parameter values obtained from the angular analysis come from several sources. The methods for determining these uncertainties are based either on a comparison of nominal and modified fit results, or on observed fit biases in modified pseudo-experiments. The systematic uncertainties are symmetrised. The most significant ones are described in the following, in decreasing order of importance.

- A systematic uncertainty is assigned for the combinatorial $K\pi$ (fake K^*) background peaking at $\cos \theta_K$ values around 1.0 obtained by comparing results of the nominal fit to that where data above $\cos \theta_K = 0.9$ are excluded from the fit.
- A systematic uncertainty is derived to account for background arising from partially reconstructed $B \rightarrow D^0/D^+/D_s^+ X$ decays, that manifest in an accumulation of events at $|\cos \theta_L|$ values around 0.7. Two-track or three-track combinations are formed from the signal candidate tracks, and are reconstructed assuming the pion or kaon mass hypothesis. A veto is then applied for events in which a track combination has a mass in a window of 30 MeV around the D^0 , D^+ or D_s^+ meson mass. Similarly, a veto is implemented to reject $B^+ \rightarrow K^+ \mu^+ \mu^-$ and $B^+ \rightarrow \pi^+ \mu^+ \mu^-$ events that pass the event selection. Here B^+ candidates are reconstructed from one of the hadrons from the K^* candidate and the muons in the signal candidate. Signal candidates that have a three-track mass within 50 MeV of the B^+ mass are excluded from the fit. A few percent of signal events are removed when applying these vetoes, with a corresponding effect on the acceptance distributions. The fit results obtained from the data samples with vetoes applied are compared to those obtained from the nominal fit and the change in each result is taken as the systematic uncertainty from these backgrounds. This systematic uncertainty dominates the measurement of F_L at higher values of q^2 .
- The background pdf shape has an uncertainty arising from the choice of model. For the mass distribution it is assumed that an exponential function model is adequate; however, for the angular variables the data are re-fitted using third-order Chebychev polynomials. The change from the nominal result is taken as the uncertainty from this source.
- The acceptance function is assumed to factorise into three separate components, one each for $\cos \theta_K$, $\cos \theta_L$ and ϕ . To validate this assumption, the signal MC data are fitted with the acceptance function obtained from that sample. Differences in the fit results from expectation are small and taken as the uncertainty resulting from this assumption.
- A systematic uncertainty is assigned for the angular background pdf model by comparing the nominal result to that with a reduced fit range of $m_{K\pi\mu\mu} \in [5200, 5700]$ MeV, in particular to account for possible residues of the partially reconstructed B -decays.
- A correction is applied to the data by shifting the track p_T according to the uncertainties arising from biases in rapidity and momentum scale. The change in results obtained is ascribed to the uncertainty in the ID alignment and knowledge of the magnetic field.
- The maximum-likelihood estimator used is intrinsically biased. Ensembles of MC simulated events are used in order to ascertain the bias in the extracted values of the parameters of interest. The bias is assigned as a systematic uncertainty.

- The p_T spectrum of B_d^0 candidates observed in data is not accurately reproduced by the MC simulation. This difference in the kinematics results in a slight modification of the acceptance functions. This is accounted for by reweighting signal MC simulated events to resemble the p_T spectrum found in data. The change in fitted parameter values obtained due to the reweighting is taken as the systematic uncertainty resulting from this difference.
- The signal decay mode is resonant $K^* \rightarrow K\pi$ decay, but scalar contributions from non-resonant $K\pi$ transitions may also exist. The LHCb Collaboration reported an S -wave contribution at the level of 5% of the signal [4, 30]. Ensembles of MC simulated events are fitted with 5% of the signal being drawn from an S -wave sample of events and the remaining 95% from signal. The observed change in fit bias is assigned as the systematic uncertainty from this source. Any variation in S -wave content as a function of q^2 would not significantly affect the results reported here.
- The values of the nuisance parameters of the fit model obtained from MC control samples and fits to the data mass distribution have associated uncertainties. These parameters include m_0 , ξ , the signal and background yields, the shape parameter of the combinatorial background mass distribution, and the parameters of the signal acceptance functions. The uncertainty in the value of each of these parameters is varied independently in order to assess the effect on parameters of interest. This source of uncertainty has a small effect on the measurements reported here.
- Background from exclusive modes peaking in $m_{K\pi\mu\mu}$ is neglected in the nominal fit. This may affect the fitted results and is accounted for by computing the fit bias obtained when embedding MC simulated samples of $\Lambda_b \rightarrow \Lambda(1520)\mu^+\mu^-$, $\Lambda_b \rightarrow pK^-\mu^+\mu^-$, $B^+ \rightarrow K^{(*)+}\mu^+\mu^-$ and $B_s^0 \rightarrow \phi\mu^+\mu^-$ into ensembles of pseudo-data generated from the fit model containing only combinatorial background and signal components. The change in fit bias observed when adding exclusive backgrounds is taken as the systematic error arising from neglecting those modes in the fit.
- The difference from nominal results obtained when fitting the B_d^0 signal MC events with the acceptance function for \bar{B}_d^0 is taken as an upper limit of the systematic error resulting from event migration due to mistagging the B_d^0 flavour.
- The parameters S_5 and S_8 , as well as the respective $P_j^{(\prime)}$ parameters are affected by dilution and thus have a multiplicative scaling applied to them. This dilution factor depends on the kinematics of the K^* decay and has a systematic uncertainty associated with it. The effect of data/MC differences in the p_T spectrum of B_d^0 candidates on the mistag probability was studied and found to be negligible. The uncertainty due to the limited number of MC events is used to compute the statistical uncertainty of ω and $\bar{\omega}$. Studies of MC simulated events indicate that there is no significant difference between the mistag probability for B_d^0 and \bar{B}_d^0 events and the analysis assumes that the average mistag probability provides an adequate description of this effect. The magnitude of the mistag probability difference, $|\omega - \bar{\omega}|$, is included as a systematic uncertainty resulting from this assumption.

The total systematic uncertainties of the fitted S_i and $P_j^{(\prime)}$ parameter values are presented in Tables 2 and 3, where the dominant contributions for F_L come from the modelling of the angular distributions of the combinatorial background and the partially reconstructed decays peaking in $\cos\theta_K$ and $\cos\theta_L$. These contributions and in addition also ID alignment and magnetic field calibration affect S_3 (P_1). The largest systematic uncertainty contribution to S_3 (P_1) comes from partially reconstructed decays entering the signal region. This also affects the measurement of S_5 (P_5') and S_7 (P_6'). The partially reconstructed decays peaking in $\cos\theta_L$ affect the measurement of S_4 (P_4') and S_8 (P_8'), whereas the fake K^* background in $\cos\theta_K$ affects S_4 (P_4'), S_5 (P_5'), and S_8 (P_8'). The parameterization of the signal acceptance is another

significant systematic uncertainty source for S_4 (P'_4). The systematic uncertainties are smaller than the statistical uncertainties for all parameters measured.

8 Comparison with theoretical computations

The results of theoretical approaches of Ciuchini et al. (CFFMPSV) [31], Descotes-Genon et al. (DHMV) [32], and Jäger and Camalich (JC) [33, 34] are shown in Figure 10 for the S parameters, and in Figure 11 for the $P^{(\prime)}$ parameters, along with the results presented here.⁴

QCD factorisation is used by DHMV and JC, where the latter focus on the impact of long-distance corrections using a helicity amplitude approach. The CFFMPSV group takes a different approach, using the QCD factorisation framework to perform compatibility checks of the LHCb data with theoretical predictions. This approach also allows information from a given experimentally measured parameter of interest to be excluded in order to make a fit-based prediction of the expected value of that parameter from the rest of the data.

With the exception of the P'_4 and P'_5 measurements in $q^2 \in [4.0, 6.0] \text{ GeV}^2$ and P'_8 in $q^2 \in [2.0, 4.0] \text{ GeV}^2$ there is good agreement between theory and measurement. The P'_4 and P'_5 parameters have statistical correlation of 0.37 in the $q^2 \in [4.0, 6.0] \text{ GeV}^2$ bin. The observed deviation from the SM prediction of P'_4 and P'_5 is for both parameters approximately 2.7 standard deviations (local) away from the calculation of DHMV for this bin. The deviations are less significant for the other calculation and the fit approach. All measurements are found to be within three standard deviations of the range covered by the different predictions. Hence, including experimental and theoretical uncertainties, the measurements presented here are found to agree with the predicted SM contributions to this decay.

⁴ This result uses the experimental convention of Equations (2)–(5) following the LHCb Collaboration’s notation in Ref. [3]. In the DHMV calculation, a different convention is used as explained by Equation (16) in Ref. [15].

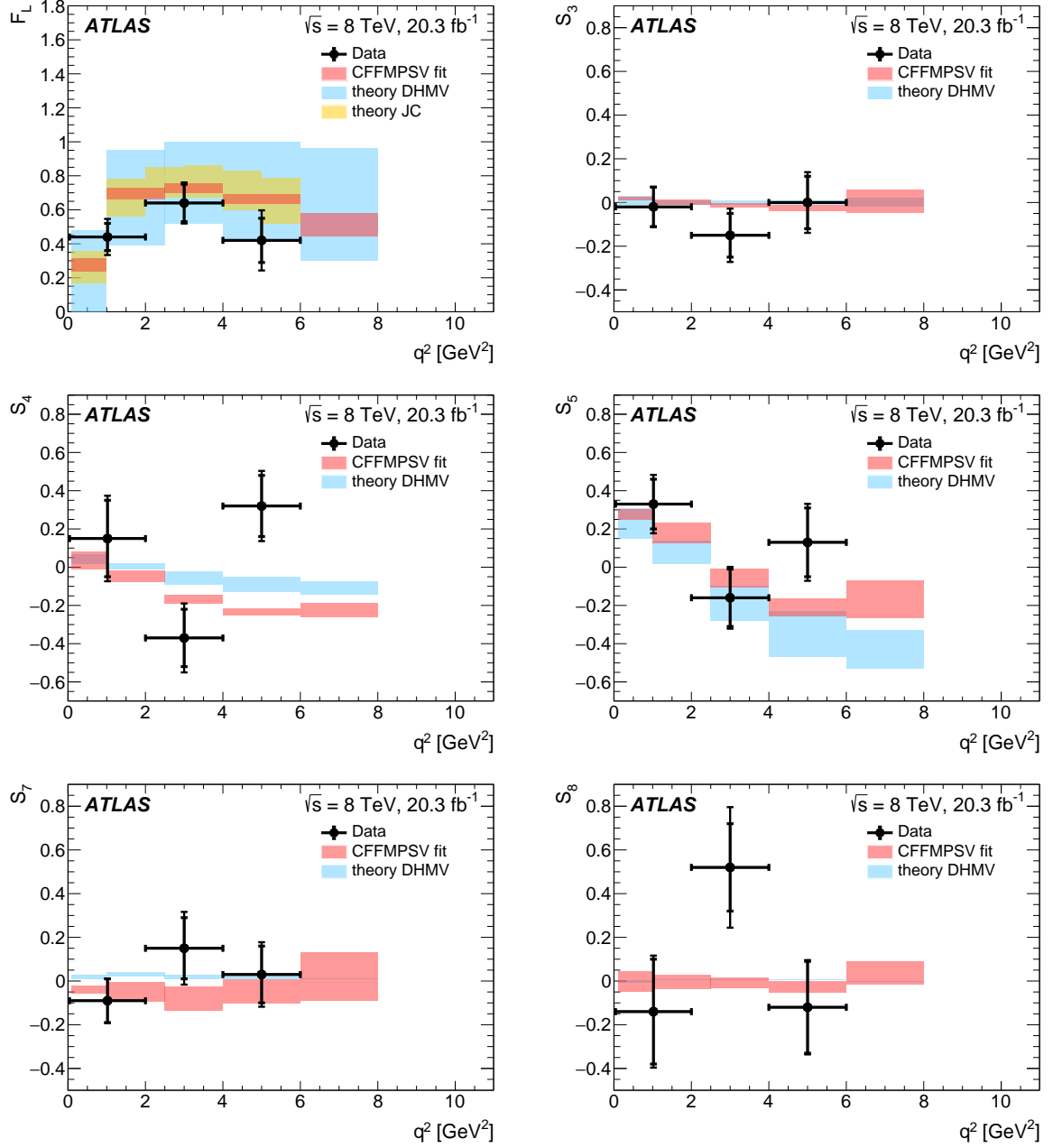


Figure 10: The measured values of F_L , S_3 , S_4 , S_5 , S_7 , S_8 compared with predictions from the theoretical calculations discussed in the text (Section 8). Statistical and total uncertainties are shown for the data, i.e. the inner mark indicates the statistical uncertainty and the total error bar the total uncertainty.

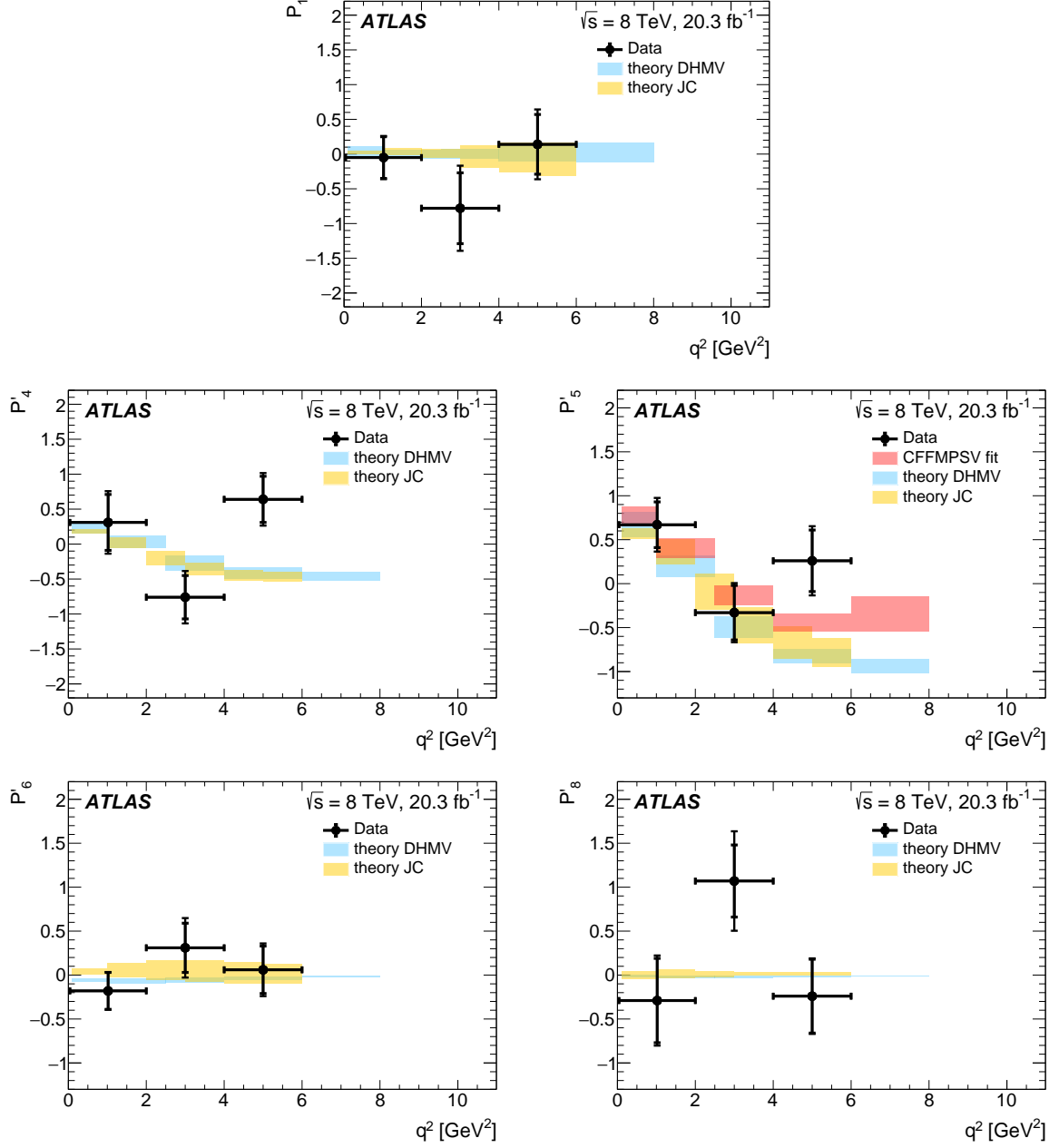


Figure 11: The measured values of P_1 , P_4' , P_5' , P_6' , P_8' compared with predictions from the theoretical calculations discussed in the text (Section 8). Statistical and total uncertainties are shown for the data, i.e. the inner mark indicates the statistical uncertainty and the total error bar the total uncertainty.

9 Conclusion

The results of an angular analysis of the rare decay $B_d^0 \rightarrow K^* \mu^+ \mu^-$ are presented. This flavour-changing neutral current process is sensitive to potential new-physics contributions. The $B_d^0 \rightarrow K^* \mu^+ \mu^-$ analysis presented here uses a total of 20.3 fb^{-1} of $\sqrt{s} = 8 \text{ TeV}$ pp collision data collected by the ATLAS experiment at the LHC in 2012. An extended unbinned maximum-likelihood fit of the angular distribution of the signal decay is performed in order to extract the parameters F_L , S_i and $P_j^{(\prime)}$ in six bins of q^2 . Three of these bins overlap in order to report results in ranges compatible with other experiments and phenomenology studies. All measurements are found to be within three standard deviation of the range covered by the different predictions. The results are also compatible with the results of the LHCb, CMS and Belle collaborations.

Acknowledgements

We thank CERN for the very successful operation of the LHC, as well as the support staff from our institutions without whom ATLAS could not be operated efficiently.

We acknowledge the support of ANPCyT, Argentina; YerPhI, Armenia; ARC, Australia; BMWFW and FWF, Austria; ANAS, Azerbaijan; SSTC, Belarus; CNPq and FAPESP, Brazil; NSERC, NRC and CFI, Canada; CERN; CONICYT, Chile; CAS, MOST and NSFC, China; COLCIENCIAS, Colombia; MSMT CR, MPO CR and VSC CR, Czech Republic; DNRF and DNSRC, Denmark; IN2P3-CNRS, CEA-DRF/IRFU, France; SRNSFG, Georgia; BMBF, HGF, and MPG, Germany; GSRT, Greece; RGC, Hong Kong SAR, China; ISF, I-CORE and Benoziyo Center, Israel; INFN, Italy; MEXT and JSPS, Japan; CNRST, Morocco; NWO, Netherlands; RCN, Norway; MNiSW and NCN, Poland; FCT, Portugal; MNE/IFA, Romania; MES of Russia and NRC KI, Russian Federation; JINR; MESTD, Serbia; MSSR, Slovakia; ARRS and MIZŠ, Slovenia; DST/NRF, South Africa; MINECO, Spain; SRC and Wallenberg Foundation, Sweden; SERI, SNSF and Cantons of Bern and Geneva, Switzerland; MOST, Taiwan; TAEK, Turkey; STFC, United Kingdom; DOE and NSF, United States of America. In addition, individual groups and members have received support from BCKDF, the Canada Council, CANARIE, CRC, Compute Canada, FQRNT, and the Ontario Innovation Trust, Canada; EPLANET, ERC, ERDF, FP7, Horizon 2020 and Marie Skłodowska-Curie Actions, European Union; Investissements d’Avenir Labex and Idex, ANR, Région Auvergne and Fondation Partager le Savoir, France; DFG and AvH Foundation, Germany; Herakleitos, Thales and Aristeia programmes co-financed by EU-ESF and the Greek NSRF; BSF, GIF and Minerva, Israel; BRF, Norway; CERCA Programme Generalitat de Catalunya, Generalitat Valenciana, Spain; the Royal Society and Leverhulme Trust, United Kingdom.

The crucial computing support from all WLCG partners is acknowledged gratefully, in particular from CERN, the ATLAS Tier-1 facilities at TRIUMF (Canada), NDGF (Denmark, Norway, Sweden), CC-IN2P3 (France), KIT/GridKA (Germany), INFN-CNAF (Italy), NL-T1 (Netherlands), PIC (Spain), ASGC (Taiwan), RAL (UK) and BNL (USA), the Tier-2 facilities worldwide and large non-WLCG resource providers. Major contributors of computing resources are listed in Ref. [35].

Appendix

A Correlation Matrices

Four folding schemes are applied to the data in order to extract F_L , S_3 , S_4 , S_5 , S_7 and S_8 from four separate fits. The $P^{(\prime)}$ parameters are subsequently derived from the fit results using Equations (2)–(5). It is not possible to extract a full correlation matrix between fitted parameters obtained from different fits. In order to reconstruct the correlation matrix, ensembles of pseudo-experiments are simulated using the pdf corresponding to the nominal angular distributions. Each simulated ensemble has the four folding schemes applied to it and four fits are performed on the resulting samples. The distributions obtained for pairs of parameters obtained from fits to these ensembles are used to compute Pearson correlation coefficients for those pairs. Correlation matrices for F_L and the S parameters are reconstructed from all possible pairings for a given q^2 bin. A similar method is used to extract the correlation matrices for the $P^{(\prime)}$ parameters. This procedure is repeated for each q^2 bin studied in order to obtain correlation matrices given in the remainder of this appendix. The correlation matrices are statistical only. Contributions from systematic uncertainties are not included, since the measurement precision is statistically limited.

- Table 4 (5) shows the statistical correlation matrix for F_L and S ($P^{(\prime)}$) parameters for the q^2 bin $[0.04, 2.0]$ GeV^2 .
- Table 6 (7) shows the statistical correlation matrix for F_L and S ($P^{(\prime)}$) parameters for the q^2 bin $[2.0, 4.0]$ GeV^2 .
- Table 8 (9) shows the statistical correlation matrix for F_L and S ($P^{(\prime)}$) parameters for the q^2 bin $[4.0, 6.0]$ GeV^2 .
- Table 10 (11) shows the statistical correlation matrix for F_L and S ($P^{(\prime)}$) parameters for the q^2 bin $[0.04, 4.0]$ GeV^2 .
- Table 12 (13) shows the statistical correlation matrix for F_L and S ($P^{(\prime)}$) parameters for the q^2 bin $[1.1, 6.0]$ GeV^2 .
- Table 14 (15) shows the statistical correlation matrix for F_L and S ($P^{(\prime)}$) parameters for the q^2 bin $[0.04, 6.0]$ GeV^2 .

Table 4: Statistical correlation matrix for the F_L and S parameters obtained for $q^2 \in [0.04, 2.0]$ GeV^2 .

	F_L	S_3	S_4	S_5	S_7	S_8
F_L	1.00	0.11	−0.13	0.03	0.16	0.24
S_3		1.00	0.31	0.28	0.73	0.45
S_4			1.00	0.58	0.19	0.22
S_5				1.00	0.14	0.28
S_7					1.00	0.59
S_8						1.00

Table 5: Statistical correlation matrix for the $P^{(\prime)}$ parameters obtained for $q^2 \in [0.04, 2.0]$ GeV².

	P_1	P'_4	P'_5	P'_6	P'_8
P_1	1.00	0.04	0.05	0.62	0.32
P'_4		1.00	0.53	-0.08	-0.06
P'_5			1.00	0.00	0.22
P'_6				1.00	0.55
P'_8					1.00

Table 6: Statistical correlation matrix for the F_L and S parameters obtained for $q^2 \in [2.0, 4.0]$ GeV².

	F_L	S_3	S_4	S_5	S_7	S_8
F_L	1.00	0.27	0.35	-0.04	-0.15	-0.37
S_3		1.00	-0.08	-0.44	-0.09	-0.20
S_4			1.00	0.60	-0.02	-0.12
S_5				1.00	-0.11	-0.20
S_7					1.00	0.63
S_8						1.00

Table 7: Statistical correlation matrix for the $P^{(\prime)}$ parameters obtained for $q^2 \in [2.0, 4.0]$ GeV².

	P_1	P'_4	P'_5	P'_6	P'_8
P_1	1.00	-0.12	-0.21	0.05	0.05
P'_4		1.00	0.51	0.08	0.03
P'_5			1.00	-0.23	0.22
P'_6				1.00	0.66
P'_8					1.00

Table 8: Statistical correlation matrix for the F_L and S parameters obtained for $q^2 \in [4.0, 6.0]$ GeV².

	F_L	S_3	S_4	S_5	S_7	S_8
F_L	1.00	0.33	-0.18	0.04	0.22	0.28
S_3		1.00	0.15	0.23	0.60	0.05
S_4			1.00	0.52	0.03	0.01
S_5				1.00	0.28	0.27
S_7					1.00	0.60
S_8						1.00

Table 9: Statistical correlation matrix for the $P^{(\prime)}$ parameters obtained for $q^2 \in [4.0, 6.0]$ GeV².

	P_1	P'_4	P'_5	P'_6	P'_8
P_1	1.00	0.11	0.34	0.41	0.16
P'_4		1.00	0.37	0.06	0.04
P'_5			1.00	0.39	0.33
P'_6				1.00	0.62
P'_8					1.00

Table 10: Statistical correlation matrix for the F_L and S parameters obtained for $q^2 \in [0.04, 4.0]$ GeV².

	F_L	S_3	S_4	S_5	S_7	S_8
F_L	1.00	0.08	0.05	0.01	0.18	0.14
S_3		1.00	-0.04	0.03	0.29	-0.16
S_4			1.00	0.79	0.08	0.03
S_5				1.00	0.03	-0.02
S_7					1.00	0.60
S_8						1.00

Table 11: Statistical correlation matrix for the $P^{(\prime)}$ parameters obtained for $q^2 \in [0.04, 4.0]$ GeV².

	P_1	P'_4	P'_5	P'_6	P'_8
P_1	1.00	-0.07	0.00	0.21	0.12
P'_4		1.00	0.78	0.08	0.02
P'_5			1.00	0.03	-0.04
P'_6				1.00	0.59
P'_8					1.00

Table 12: Statistical correlation matrix for the F_L and S parameters obtained for $q^2 \in [1.1, 6.0]$ GeV².

	F_L	S_3	S_4	S_5	S_7	S_8
F_L	1.00	0.05	0.00	0.07	0.18	-0.03
S_3		1.00	0.41	0.46	0.32	-0.01
S_4			1.00	0.60	0.09	0.03
S_5				1.00	0.17	0.24
S_7					1.00	0.67
S_8						1.00

Table 13: Statistical correlation matrix for the $P^{(\prime)}$ parameters obtained for $q^2 \in [1.1, 6.0]$ GeV².

	P_1	P'_4	P'_5	P'_6	P'_8
P_1	1.00	0.23	-0.09	0.08	-0.07
P'_4		1.00	0.53	0.15	0.08
P'_5			1.00	0.28	0.24
P'_6				1.00	0.67
P'_8					1.00

Table 14: Statistical correlation matrix for the F_L and S parameters obtained for $q^2 \in [0.04, 6.0]$ GeV².

	F_L	S_3	S_4	S_5	S_7	S_8
F_L	1.00	0.03	0.01	-0.10	0.13	0.06
S_3		1.00	-0.02	-0.09	0.32	-0.01
S_4			1.00	0.68	0.00	0.04
S_5				1.00	-0.05	0.03
S_7					1.00	0.65
S_8						1.00

Table 15: Statistical correlation matrix for the $P^{(\prime)}$ parameters obtained for $q^2 \in [0.04, 6.0]$ GeV².

	P_1	P'_4	P'_5	P'_6	P'_8
P_1	1.00	-0.02	-0.14	0.17	0.04
P'_4		1.00	0.65	0.00	0.05
P'_5			1.00	-0.06	0.09
P'_6				1.00	0.61
P'_8					1.00

References

- [1] Belle Collaboration, *Measurement of the Differential Branching Fraction and Forward-Backward Asymmetry for $B \rightarrow K^{(*)}l^+l^-$* , *Phys. Rev. Lett.* **103** (2009) 171801, arXiv: [0904.0770 \[hep-ex\]](#).
- [2] CDF Collaboration, *Measurements of the Angular Distributions in the Decays $B \rightarrow K^{(*)}\mu^+\mu^-$ at CDF*, *Phys. Rev. Lett.* **108** (2012) 081807, arXiv: [1108.0695 \[hep-ex\]](#).
- [3] LHCb Collaboration, *Measurement of Form-Factor Independent Observables in the Decay $B^0 \rightarrow K^{*0}\mu^+\mu^-$* , *Phys. Rev. Lett.* **111** (2013) 191801, arXiv: [1308.1707 \[hep-ex\]](#).
- [4] LHCb Collaboration, *Angular analysis of the $B^0 \rightarrow K^{*0}\mu^+\mu^-$ decay using 3 fb^{-1} of integrated luminosity*, *JHEP* **02** (2016) 104, arXiv: [1512.04442 \[hep-ex\]](#).
- [5] CMS Collaboration, *Angular analysis of the decay $B^0 \rightarrow K^{*0}\mu^+\mu^-$ from pp collisions at $\sqrt{s} = 8\text{ TeV}$* , *Phys. Lett. B* **753** (2016) 424, arXiv: [1507.08126 \[hep-ex\]](#).
- [6] CMS Collaboration, *Measurement of angular parameters from the decay $B^0 \rightarrow K^{*0}\mu^+\mu^-$ in proton-proton collisions at $\sqrt{s} = 8\text{ TeV}$* , (2017), arXiv: [1710.02846 \[hep-ex\]](#).
- [7] BaBar Collaboration, *Measurement of angular asymmetries in the decays $B \rightarrow K^*\ell^+\ell^-$* , *Phys. Rev. D* **93** (2016) 052015, arXiv: [1508.07960 \[hep-ex\]](#).
- [8] Belle Collaboration, *Lepton-Flavor-Dependent Angular Analysis of $B \rightarrow K^*\ell^+\ell^-$* , *Phys. Rev. Lett.* **118** (2017) 111801, arXiv: [1612.05014 \[hep-ex\]](#).
- [9] LHCb Collaboration, *Differential branching fraction and angular analysis of the decay $B^0 \rightarrow K^{*0}\mu^+\mu^-$* , *JHEP* **08** (2013) 131, arXiv: [1304.6325 \[hep-ex\]](#).
- [10] A. Bharucha, D. M. Straub and R. Zwicky, *$B \rightarrow V\ell^+\ell^-$ in the Standard Model from light-cone sum rules*, *JHEP* **08** (2016) 098, arXiv: [1503.05534 \[hep-ph\]](#).
- [11] L. Evans and P. Bryant, *LHC Machine*, *JINST* **3** (2008) S08001.
- [12] K. G. Wilson and W. Zimmermann, *Operator product expansions and composite field operators in the general framework of quantum field theory*, *Commun. Math. Phys.* **24** (1972) 87.
- [13] W. Altmannshofer and D. M. Straub, *New physics in $B \rightarrow K^*\mu\mu$* ?, *Eur. Phys. J. C* **73** (2013) 2646, arXiv: [1308.1501 \[hep-ph\]](#).
- [14] T. Hurth, F. Mahmoudi and S. Neshatpour, *Global fits to $b \rightarrow s\ell\ell$ data and signs for lepton non-universality*, *JHEP* **12** (2014) 053, arXiv: [1410.4545 \[hep-ph\]](#).
- [15] S. Descotes-Genon, L. Hofer, J. Matias and J. Virto, *Global analysis of $b \rightarrow s\ell\ell$ anomalies*, *JHEP* **06** (2016) 092, arXiv: [1510.04239 \[hep-ph\]](#).
- [16] I. Dunietz, H. R. Quinn, A. Snyder, W. Toki and H. J. Lipkin, *How to extract CP violating asymmetries from angular correlations*, *Phys. Rev. D* **43** (1991) 2193.
- [17] S. Descotes-Genon, T. Hurth, J. Matias and J. Virto, *Optimizing the basis of $B \rightarrow K^*\ell^+\ell^-$ observables in the full kinematic range*, *JHEP* **05** (2013) 137, arXiv: [1303.5794 \[hep-ph\]](#).
- [18] S. Descotes-Genon, J. Matias, M. Ramon and J. Virto, *Implications from clean observables for the binned analysis of $B \rightarrow K^*\mu^+\mu^-$ at large recoil*, *JHEP* **01** (2013) 048, arXiv: [1207.2753 \[hep-ph\]](#).
- [19] ATLAS Collaboration, *The ATLAS Experiment at the CERN Large Hadron Collider*, *JINST* **3** (2008) S08003.

- [20] T. Sjostrand, S. Mrenna and P. Z. Skands, *PYTHIA 6.4 Physics and Manual*, **JHEP** **05** (2006) 026, arXiv: [hep-ph/0603175](#) [[hep-ph](#)].
- [21] T. Sjostrand, S. Mrenna and P. Z. Skands, *A brief Introduction to PYTHIA 8.1*, **Comput. Phys. Commun.** **178** (2008) 852, arXiv: [0710.3820](#) [[hep-ph](#)].
- [22] ATLAS Collaboration, *Summary of ATLAS Pythia 8 tunes*, ATL-PHYS-PUB-2012-003, 2012, URL: <https://cds.cern.ch/record/1474107>.
- [23] J. Pumplin et al., *New generation of parton distributions with uncertainties from global QCD analysis*, **JHEP** **07** (2002) 012, arXiv: [hep-ph/0201195](#) [[hep-ph](#)].
- [24] D. J. Lange, *The EvtGen particle decay simulation package*, **Nucl. Instrum. Meth. A** **462** (2001) 152.
- [25] S. Agostinelli et al., *GEANT4: A Simulation toolkit*, **Nucl. Instrum. Meth. A** **506** (2003) 250.
- [26] ATLAS Collaboration, *The ATLAS Simulation Infrastructure*, **Eur. Phys. J. C** **70** (2010) 823, arXiv: [1005.4568](#) [[physics.ins-det](#)].
- [27] ATLAS Collaboration, *Measurement of the muon reconstruction performance of the ATLAS detector using 2011 and 2012 LHC proton–proton collision data*, **Eur. Phys. J. C** **74** (2014) 3130, arXiv: [1407.3935](#) [[hep-ex](#)].
- [28] ATLAS Collaboration, *Measurement of the CP-violating phase ϕ_s and the B_s^0 meson decay width difference with $B_s^0 \rightarrow J/\psi\phi$ decays in ATLAS*, **JHEP** **08** (2016) 147, arXiv: [1601.03297](#) [[hep-ex](#)].
- [29] A. Ali, P. Ball, L. T. Handoko and G. Hiller, *A comparative study of the decays $B \rightarrow (K, K^*)\ell^+\ell^-$ in standard model and supersymmetric theories*, **Phys. Rev. D** **61** (2000) 074024, arXiv: [hep-ph/9910221](#).
- [30] LHCb Collaboration, *Measurements of the S-wave fraction in $B^0 \rightarrow K^+\pi^-\mu^+\mu^-$ decays and the $B^0 \rightarrow K^*(892)^0\mu^+\mu^-$ differential branching fraction*, **JHEP** **11** (2016) 047, arXiv: [1606.04731](#) [[hep-ex](#)].
- [31] M. Ciuchini et al., *$B \rightarrow K^*\ell^+\ell^-$ decays at large recoil in the Standard Model: a theoretical reappraisal*, **JHEP** **06** (2016) 116, arXiv: [1512.07157](#) [[hep-ph](#)].
- [32] S. Descotes-Genon, L. Hofer, J. Matias and J. Virto, *On the impact of power corrections in the prediction of $B \rightarrow K^*\mu^+\mu^-$ observables*, **JHEP** **12** (2014) 125, arXiv: [1407.8526](#) [[hep-ph](#)].
- [33] S. Jäger and J. Martin Camalich, *On $B \rightarrow V\ell\ell$ at small dilepton invariant mass, power corrections, and new physics*, **JHEP** **05** (2013) 043, arXiv: [1212.2263](#) [[hep-ph](#)].
- [34] S. Jäger and J. Martin Camalich, *Reassessing the discovery potential of the $B \rightarrow K^*\ell^+\ell^-$ decays in the large-recoil region: SM challenges and BSM opportunities*, **Phys. Rev. D** **93** (2016) 014028, arXiv: [1412.3183](#) [[hep-ph](#)].
- [35] ATLAS Collaboration, *ATLAS Computing Acknowledgements*, ATL-GEN-PUB-2016-002, URL: <https://cds.cern.ch/record/2202407>.

The ATLAS Collaboration

M. Aaboud^{137d}, G. Aad⁸⁸, B. Abbott¹¹⁵, O. Abidinov^{12,*}, B. Abeloos¹¹⁹, S.H. Abidi¹⁶¹, O.S. AbouZeid¹³⁹, N.L. Abraham¹⁵¹, H. Abramowicz¹⁵⁵, H. Abreu¹⁵⁴, R. Abreu¹¹⁸, Y. Abulaiti^{148a,148b}, B.S. Acharya^{167a,167b,a}, S. Adachi¹⁵⁷, L. Adamczyk^{41a}, J. Adelman¹¹⁰, M. Adersberger¹⁰², T. Adye¹³³, A.A. Affolder¹³⁹, T. Agatonovic-Jovin¹⁴, C. Agheorghiesei^{28c}, J.A. Aguilar-Saavedra^{128a,128f}, S.P. Ahlen²⁴, F. Ahmadov^{68,b}, G. Aielli^{135a,135b}, S. Akatsuka⁷¹, H. Akerstedt^{148a,148b}, T.P.A. Åkesson⁸⁴, E. Akilli⁵², A.V. Akimov⁹⁸, G.L. Alberghi^{22a,22b}, J. Albert¹⁷², P. Albicocco⁵⁰, M.J. Alconada Verzini⁷⁴, S.C. Alderweireldt¹⁰⁸, M. Aleksa³², I.N. Aleksandrov⁶⁸, C. Alexa^{28b}, G. Alexander¹⁵⁵, T. Alexopoulos¹⁰, M. Alhroob¹¹⁵, B. Ali¹³⁰, M. Aliev^{76a,76b}, G. Alimonti^{94a}, J. Alison³³, S.P. Alkire³⁸, B.M.M. Allbrooke¹⁵¹, B.W. Allen¹¹⁸, P.P. Allport¹⁹, A. Aloisio^{106a,106b}, A. Alonso³⁹, F. Alonso⁷⁴, C. Alpigiani¹⁴⁰, A.A. Alshehri⁵⁶, M.I. Alstady⁸⁸, B. Alvarez Gonzalez³², D. Álvarez Piqueras¹⁷⁰, M.G. Alvigi^{106a,106b}, B.T. Amadio¹⁶, Y. Amaral Coutinho^{26a}, C. Amelung²⁵, D. Amidei⁹², S.P. Amor Dos Santos^{128a,128c}, A. Amorim^{128a,128b}, S. Amoroso³², G. Amundsen²⁵, C. Anastopoulos¹⁴¹, L.S. Ancu⁵², N. Andari¹⁹, T. Andeen¹¹, C.F. Anders^{60b}, J.K. Anders⁷⁷, K.J. Anderson³³, A. Andreazza^{94a,94b}, V. Andrei^{60a}, S. Angelidakis⁹, I. Angelozzi¹⁰⁹, A. Angerami³⁸, A.V. Anisenkov^{111,c}, N. Anjos¹³, A. Annovi^{126a,126b}, C. Antel^{60a}, M. Antonelli⁵⁰, A. Antonov^{100,*}, D.J. Antrim¹⁶⁶, F. Anulli^{134a}, M. Aoki⁶⁹, L. Aperio Bella³², G. Arabidze⁹³, Y. Arai⁶⁹, J.P. Araque^{128a}, V. Araujo Ferraz^{26a}, A.T.H. Arce⁴⁸, R.E. Ardell⁸⁰, F.A. Arduh⁷⁴, J-F. Arguin⁹⁷, S. Argyropoulos⁶⁶, M. Arik^{20a}, A.J. Armbruster³², L.J. Armitage⁷⁹, O. Arnaez¹⁶¹, H. Arnold⁵¹, M. Arratia³⁰, O. Arslan²³, A. Artamonov⁹⁹, G. Artoni¹²², S. Artz⁸⁶, S. Asai¹⁵⁷, N. Asbah⁴⁵, A. Ashkenazi¹⁵⁵, L. Asquith¹⁵¹, K. Assamagan²⁷, R. Astalos^{146a}, M. Atkinson¹⁶⁹, N.B. Atlay¹⁴³, K. Augsten¹³⁰, G. Avolio³², B. Axen¹⁶, M.K. Ayoub¹¹⁹, G. Azuelos^{97,d}, A.E. Baas^{60a}, M.J. Baca¹⁹, H. Bachacou¹³⁸, K. Bachas^{76a,76b}, M. Backes¹²², M. Backhaus³², P. Bagnaia^{134a,134b}, M. Bahmani⁴², H. Bahrasemani¹⁴⁴, J.T. Baines¹³³, M. Bajic³⁹, O.K. Baker¹⁷⁹, E.M. Baldin^{111,c}, P. Balek¹⁷⁵, F. Balli¹³⁸, W.K. Balunas¹²⁴, E. Banas⁴², A. Bandyopadhyay²³, Sw. Banerjee^{176,e}, A.A.E. Bannoura¹⁷⁸, L. Barak³², E.L. Barberio⁹¹, D. Barberis^{53a,53b}, M. Barbero⁸⁸, T. Barillari¹⁰³, M-S Barisits³², J.T. Barkeloo¹¹⁸, T. Barklow¹⁴⁵, N. Barlow³⁰, S.L. Barnes^{36c}, B.M. Barnett¹³³, R.M. Barnett¹⁶, Z. Barnovska-Blenessy^{36a}, A. Baroncelli^{136a}, G. Barone²⁵, A.J. Barr¹²², L. Barranco Navarro¹⁷⁰, F. Barreiro⁸⁵, J. Barreiro Guimarães da Costa^{35a}, R. Bartoldus¹⁴⁵, A.E. Barton⁷⁵, P. Bartos^{146a}, A. Basalae¹²⁵, A. Bassalat^{119,f}, R.L. Bates⁵⁶, S.J. Batista¹⁶¹, J.R. Batley³⁰, M. Battaglia¹³⁹, M. Bauce^{134a,134b}, F. Bauer¹³⁸, H.S. Bawa^{145,g}, J.B. Beacham¹¹³, M.D. Beattie⁷⁵, T. Beau⁸³, P.H. Beauchemin¹⁶⁵, P. Bechtle²³, H.P. Beck^{18,h}, H.C. Beck⁵⁷, K. Becker¹²², M. Becker⁸⁶, M. Beckingham¹⁷³, C. Becot¹¹², A.J. Beddall^{20e}, A. Beddall^{20b}, V.A. Bednyakov⁶⁸, M. Bedognetti¹⁰⁹, C.P. Bee¹⁵⁰, T.A. Beermann³², M. Begalli^{26a}, M. Begel²⁷, J.K. Behr⁴⁵, A.S. Bell⁸¹, G. Bella¹⁵⁵, L. Bellagamba^{22a}, A. Bellerive³¹, M. Bellomo¹⁵⁴, K. Belotskiy¹⁰⁰, O. Beltramello³², N.L. Belyaev¹⁰⁰, O. Benary^{155,*}, D. Benčekroun^{137a}, M. Bender¹⁰², K. Bendtz^{148a,148b}, N. Benekos¹⁰, Y. Benhammou¹⁵⁵, E. Benhar Noccioli¹⁷⁹, J. Benitez⁶⁶, D.P. Benjamin⁴⁸, M. Benoit⁵², J.R. Bensinger²⁵, S. Bentvelsen¹⁰⁹, L. Beresford¹²², M. Beretta⁵⁰, D. Berge¹⁰⁹, E. Bergeas Kuutmann¹⁶⁸, N. Berger⁵, J. Beringer¹⁶, S. Berlendis⁵⁸, N.R. Bernard⁸⁹, G. Bernardi⁸³, C. Bernius¹⁴⁵, F.U. Bernlochner²³, T. Berry⁸⁰, P. Berta¹³¹, C. Bertella^{35a}, G. Bertoli^{148a,148b}, F. Bertolucci^{126a,126b}, I.A. Bertram⁷⁵, C. Bertsche⁴⁵, D. Bertsche¹¹⁵, G.J. Besjes³⁹, O. Bessidskaia Bylund^{148a,148b}, M. Bessner⁴⁵, N. Besson¹³⁸, C. Betancourt⁵¹, A. Bethani⁸⁷, S. Bethke¹⁰³, A.J. Bevan⁷⁹, J. Beyer¹⁰³, R.M. Bianchi¹²⁷, O. Biebel¹⁰², D. Biedermann¹⁷, R. Bielski⁸⁷, K. Bierwagen⁸⁶, N.V. Biesuz^{126a,126b}, M. Biglietti^{136a}, T.R.V. Billoud⁹⁷, H. Bilokon⁵⁰, M. Bindi⁵⁷, A. Bingul^{20b}, C. Bini^{134a,134b}, S. Biondi^{22a,22b}, T. Bisanz⁵⁷, C. Bittrich⁴⁷, D.M. Bjergaard⁴⁸, C.W. Black¹⁵², J.E. Black¹⁴⁵, K.M. Black²⁴, R.E. Blair⁶, T. Blazek^{146a}, I. Bloch⁴⁵, C. Blocker²⁵,

A. Blue⁵⁶, W. Blum^{86,*}, U. Blumenschein⁷⁹, S. Blunier^{34a}, G.J. Bobbink¹⁰⁹, V.S. Bobrovnikov^{111,c},
 S.S. Bocchetta⁸⁴, A. Bocci⁴⁸, C. Bock¹⁰², M. Boehler⁵¹, D. Boerner¹⁷⁸, D. Bogavac¹⁰²,
 A.G. Bogdanchikov¹¹¹, C. Bohm^{148a}, V. Boisvert⁸⁰, P. Bokan^{168,i}, T. Bold^{41a}, A.S. Boldyrev¹⁰¹,
 A.E. Bolz^{60b}, M. Bomben⁸³, M. Bona⁷⁹, M. Boonekamp¹³⁸, A. Borisov¹³², G. Borissov⁷⁵, J. Bortfeldt³²,
 D. Bortoletto¹²², V. Bortolotto^{62a}, D. Boscherini^{22a}, M. Bosman¹³, J.D. Bossio Sola²⁹, J. Boudreau¹²⁷,
 J. Bouffard², E.V. Bouhova-Thacker⁷⁵, D. Boumediene³⁷, C. Bourdarios¹¹⁹, S.K. Boutle⁵⁶, A. Boveia¹¹³,
 J. Boyd³², I.R. Boyko⁶⁸, J. Bracinik¹⁹, A. Brandt⁸, G. Brandt⁵⁷, O. Brandt^{60a}, U. Bratzler¹⁵⁸, B. Brau⁸⁹,
 J.E. Brau¹¹⁸, W.D. Breaden Madden⁵⁶, K. Brendlinger⁴⁵, A.J. Brennan⁹¹, L. Brenner¹⁰⁹, R. Brenner¹⁶⁸,
 S. Bressler¹⁷⁵, D.L. Briglin¹⁹, T.M. Bristow⁴⁹, D. Britton⁵⁶, D. Britzger⁴⁵, F.M. Brochu³⁰, I. Brock²³,
 R. Brock⁹³, G. Brooijmans³⁸, T. Brooks⁸⁰, W.K. Brooks^{34b}, J. Brosamer¹⁶, E. Brost¹¹⁰, J.H. Broughton¹⁹,
 P.A. Bruckman de Renstrom⁴², D. Bruncko^{146b}, A. Bruni^{22a}, G. Bruni^{22a}, L.S. Bruni¹⁰⁹, B.H. Brunt³⁰,
 M. Bruschi^{22a}, N. Bruscino²³, P. Bryant³³, L. Bryngemark⁴⁵, T. Buanes¹⁵, Q. Buat¹⁴⁴, P. Buchholz¹⁴³,
 A.G. Buckley⁵⁶, I.A. Budagov⁶⁸, F. Buehrer⁵¹, M.K. Bugge¹²¹, O. Bulekov¹⁰⁰, D. Bullock⁸,
 T.J. Burch¹¹⁰, S. Burdin⁷⁷, C.D. Burgard⁵¹, A.M. Burger⁵, B. Burghgrave¹¹⁰, K. Burka⁴², S. Burke¹³³,
 I. Burmeister⁴⁶, J.T.P. Burr¹²², E. Busato³⁷, D. Büscher⁵¹, V. Büscher⁸⁶, P. Bussey⁵⁶, J.M. Butler²⁴,
 C.M. Buttar⁵⁶, J.M. Butterworth⁸¹, P. Butti³², W. Buttinger²⁷, A. Buzatu^{35c}, A.R. Buzykaev^{111,c},
 S. Cabrera Urbán¹⁷⁰, D. Caforio¹³⁰, V.M. Cairo^{40a,40b}, O. Cakir^{4a}, N. Calace⁵², P. Calafiura¹⁶,
 A. Calandri⁸⁸, G. Calderini⁸³, P. Calfayan⁶⁴, G. Callea^{40a,40b}, L.P. Caloba^{26a}, S. Calvente Lopez⁸⁵,
 D. Calvet³⁷, S. Calvet³⁷, T.P. Calvet⁸⁸, R. Camacho Toro³³, S. Camarda³², P. Camarri^{135a,135b},
 D. Cameron¹²¹, R. Caminal Armadans¹⁶⁹, C. Camincher⁵⁸, S. Campana³², M. Campanelli⁸¹,
 A. Camplani^{94a,94b}, A. Campoverde¹⁴³, V. Canale^{106a,106b}, M. Cano Bret^{36c}, J. Cantero¹¹⁶, T. Cao¹⁵⁵,
 M.D.M. Capeans Garrido³², I. Caprini^{28b}, M. Caprini^{28b}, M. Capua^{40a,40b}, R.M. Carbone³⁸,
 R. Cardarelli^{135a}, F. Cardillo⁵¹, I. Carli¹³¹, T. Carli³², G. Carlino^{106a}, B.T. Carlson¹²⁷, L. Carminati^{94a,94b},
 R.M.D. Carney^{148a,148b}, S. Caron¹⁰⁸, E. Carquin^{34b}, S. Carrá^{94a,94b}, G.D. Carrillo-Montoya³²,
 J. Carvalho^{128a,128c}, D. Casadei¹⁹, M.P. Casado^{13,j}, M. Casolino¹³, D.W. Casper¹⁶⁶, R. Castelijns¹⁰⁹,
 V. Castillo Gimenez¹⁷⁰, N.F. Castro^{128a,k}, A. Catinaccio³², J.R. Catmore¹²¹, A. Cattai³², J. Caudron²³,
 V. Cavaliere¹⁶⁹, E. Cavallaro¹³, D. Cavalli^{94a}, M. Cavalli-Sforza¹³, V. Cavasinni^{126a,126b}, E. Celebi^{20d},
 F. Ceradini^{136a,136b}, L. Cerda Alberich¹⁷⁰, A.S. Cerqueira^{26b}, A. Cerri¹⁵¹, L. Cerrito^{135a,135b}, F. Cerutti¹⁶,
 A. Cervelli¹⁸, S.A. Cetin^{20d}, A. Chafaq^{137a}, D. Chakraborty¹¹⁰, S.K. Chan⁵⁹, W.S. Chan¹⁰⁹,
 Y.L. Chan^{62a}, P. Chang¹⁶⁹, J.D. Chapman³⁰, D.G. Charlton¹⁹, C.C. Chau¹⁶¹, C.A. Chavez Barajas¹⁵¹,
 S. Che¹¹³, S. Cheatham^{167a,167c}, A. Chegwidan⁹³, S. Chekanov⁶, S.V. Chekulaev^{163a}, G.A. Chelkov^{68,l},
 M.A. Chelstowska³², C. Chen⁶⁷, H. Chen²⁷, J. Chen^{36a}, S. Chen^{35b}, S. Chen¹⁵⁷, X. Chen^{35c,m},
 Y. Chen⁷⁰, H.C. Cheng⁹², H.J. Cheng^{35a}, A. Cheplakov⁶⁸, E. Cheremushkina¹³²,
 R. Cherkaoui El Moursli^{137e}, E. Cheu⁷, K. Cheung⁶³, L. Chevalier¹³⁸, V. Chiarella⁵⁰,
 G. Chiarelli^{126a,126b}, G. Chiodini^{76a}, A.S. Chisholm³², A. Chitan^{28b}, Y.H. Chiu¹⁷², M.V. Chizhov⁶⁸,
 K. Choi⁶⁴, A.R. Chomont³⁷, S. Chouridou¹⁵⁶, V. Christodoulou⁸¹, D. Chromek-Burckhart³²,
 M.C. Chu^{62a}, J. Chudoba¹²⁹, A.J. Chuinard⁹⁰, J.J. Chwastowski⁴², L. Chytka¹¹⁷, A.K. Ciftci^{4a},
 D. Cinca⁴⁶, V. Cindro⁷⁸, I.A. Cioara²³, C. Ciocca^{22a,22b}, A. Ciochio¹⁶, F. Ciotto^{106a,106b}, Z.H. Citron¹⁷⁵,
 M. Citterio^{94a}, M. Ciubancan^{28b}, A. Clark⁵², B.L. Clark⁵⁹, M.R. Clark³⁸, P.J. Clark⁴⁹, R.N. Clarke¹⁶,
 C. Clement^{148a,148b}, Y. Coadou⁸⁸, M. Cobal^{167a,167c}, A. Coccaro⁵², J. Cochran⁶⁷, L. Colasurdo¹⁰⁸,
 B. Cole³⁸, A.P. Colijn¹⁰⁹, J. Collot⁵⁸, T. Colombo¹⁶⁶, P. Conde Muiño^{128a,128b}, E. Coniavitis⁵¹,
 S.H. Connell^{147b}, I.A. Connelly⁸⁷, S. Constantinescu^{28b}, G. Conti³², F. Conventi^{106a,n}, M. Cooke¹⁶,
 A.M. Cooper-Sarkar¹²², F. Cormier¹⁷¹, K.J.R. Cormier¹⁶¹, M. Corradi^{134a,134b}, F. Corriveau^{90,o},
 A. Cortes-Gonzalez³², G. Cortiana¹⁰³, G. Costa^{94a}, M.J. Costa¹⁷⁰, D. Costanzo¹⁴¹, G. Cottin³⁰,
 G. Cowan⁸⁰, B.E. Cox⁸⁷, K. Cranmer¹¹², S.J. Crawley⁵⁶, R.A. Creager¹²⁴, G. Cree³¹,
 S. Crépe-Renaudin⁵⁸, F. Crescioli⁸³, W.A. Cribbs^{148a,148b}, M. Cristinziani²³, V. Croft¹⁰⁸,
 G. Crosetti^{40a,40b}, A. Cueto⁸⁵, T. Cuhadar Donszelmann¹⁴¹, A.R. Cukierman¹⁴⁵, J. Cummings¹⁷⁹,

M. Curatolo⁵⁰, J. Cúth⁸⁶, P. Czodrowski³², G. D'amen^{22a,22b}, S. D'Auria⁵⁶, L. D'eraimo⁸³, M. D'Onofrio⁷⁷, M.J. Da Cunha Sargedas De Sousa^{128a,128b}, C. Da Via⁸⁷, W. Dabrowski^{41a}, T. Dado^{146a}, T. Dai⁹², O. Dale¹⁵, F. Dallaire⁹⁷, C. Dallapiccola⁸⁹, M. Dam³⁹, J.R. Dandoy¹²⁴, M.F. Daneri²⁹, N.P. Dang¹⁷⁶, A.C. Daniells¹⁹, N.S. Dann⁸⁷, M. Danninger¹⁷¹, M. Dano Hoffmann¹³⁸, V. Dao¹⁵⁰, G. Darbo^{53a}, S. Darmora⁸, J. Dassoulas³, A. Dattagupta¹¹⁸, T. Daubney⁴⁵, W. Davey²³, C. David⁴⁵, T. Davidek¹³¹, D.R. Davis⁴⁸, P. Davison⁸¹, E. Dawe⁹¹, I. Dawson¹⁴¹, K. De⁸, R. de Asmundis^{106a}, A. De Benedetti¹¹⁵, S. De Castro^{22a,22b}, S. De Cecco⁸³, N. De Groot¹⁰⁸, P. de Jong¹⁰⁹, H. De la Torre⁹³, F. De Lorenzi⁶⁷, A. De Maria⁵⁷, D. De Pedis^{134a}, A. De Salvo^{134a}, U. De Sanctis^{135a,135b}, A. De Santo¹⁵¹, K. De Vasconcelos Corga⁸⁸, J.B. De Vivie De Regie¹¹⁹, W.J. Dearnaley⁷⁵, R. Debbe²⁷, C. Debenedetti¹³⁹, D.V. Dedovich⁶⁸, N. Dehghanian³, I. Deigaard¹⁰⁹, M. Del Gaudio^{40a,40b}, J. Del Peso⁸⁵, D. Delgove¹¹⁹, F. Deliot¹³⁸, C.M. Delitzsch⁵², A. Dell'Acqua³², L. Dell'Asta²⁴, M. Dell'Orso^{126a,126b}, M. Della Pietra^{106a,106b}, D. della Volpe⁵², M. Delmastro⁵, C. Delporte¹¹⁹, P.A. Delsart⁵⁸, D.A. DeMarco¹⁶¹, S. Demers¹⁷⁹, M. Demichev⁶⁸, A. Demilly⁸³, S.P. Denisov¹³², D. Denysiuk¹³⁸, D. Derendarz⁴², J.E. Derkaoui^{137d}, F. Derue⁸³, P. Dervan⁷⁷, K. Desch²³, C. Deterre⁴⁵, K. Dette⁴⁶, M.R. Devesa²⁹, P.O. Deviveiros³², A. Dewhurst¹³³, S. Dhaliwal²⁵, F.A. Di Bello⁵², A. Di Ciaccio^{135a,135b}, L. Di Ciaccio⁵, W.K. Di Clemente¹²⁴, C. Di Donato^{106a,106b}, A. Di Girolamo³², B. Di Girolamo³², B. Di Micco^{136a,136b}, R. Di Nardo³², K.F. Di Petrillo⁵⁹, A. Di Simone⁵¹, R. Di Sipio¹⁶¹, D. Di Valentino³¹, C. Diaconu⁸⁸, M. Diamond¹⁶¹, F.A. Dias³⁹, M.A. Diaz^{34a}, E.B. Diehl⁹², J. Dietrich¹⁷, S. Díez Cornell⁴⁵, A. Dimitrievska¹⁴, J. Dingfelder²³, P. Dita^{28b}, S. Dita^{28b}, F. Dittus³², F. Djama⁸⁸, T. Djobava^{54b}, J.I. Djuvsland^{160a}, M.A.B. do Vale^{26c}, D. Dobos³², M. Dobre^{28b}, C. Doglioni⁸⁴, J. Dolejsi¹³¹, Z. Dolezal¹³¹, M. Donadelli^{26d}, S. Donati^{126a,126b}, P. Dondero^{123a,123b}, J. Donini³⁷, J. Dopke¹³³, A. Doria^{106a}, M.T. Dova⁷⁴, A.T. Doyle⁵⁶, E. Drechsler⁵⁷, M. Dris¹⁰, Y. Du^{36b}, J. Duarte-Campderros¹⁵⁵, A. Dubreuil⁵², E. Duchovni¹⁷⁵, G. Duckeck¹⁰², A. Ducourthial⁸³, O.A. Ducu^{97,p}, D. Duda¹⁰⁹, A. Dudarev³², A.Ch. Dudder⁸⁶, E.M. Duffield¹⁶, L. Duflo¹¹⁹, M. Dührssen³², M. Dumancic¹⁷⁵, A.E. Dumitriu^{28b}, A.K. Duncan⁵⁶, M. Dunford^{160a}, H. Duran Yildiz^{4a}, M. Düren⁵⁵, A. Durglishvili^{54b}, D. Duschinger⁴⁷, B. Dutta⁴⁵, D. Duvnjak¹, M. Dyndal⁴⁵, B.S. Dziedzic⁴², C. Eckardt⁴⁵, K.M. Ecker¹⁰³, R.C. Edgar⁹², T. Eifert³², G. Eigen¹⁵, K. Einsweiler¹⁶, T. Ekelof¹⁶⁸, M. El Kacimi^{137c}, R. El Kosseifi⁸⁸, V. Ellajosyula⁸⁸, M. Ellert¹⁶⁸, S. Elles⁵, F. Ellinghaus¹⁷⁸, A.A. Elliot¹⁷², N. Ellis³², J. Elmsheuser²⁷, M. Elsing³², D. Emelianov¹³³, Y. Enari¹⁵⁷, O.C. Endner⁸⁶, J.S. Ennis¹⁷³, J. Erdmann⁴⁶, A. Ereditato¹⁸, M. Ernst²⁷, S. Errede¹⁶⁹, M. Escalier¹¹⁹, C. Escobar¹⁷⁰, B. Esposito⁵⁰, O. Estrada Pastor¹⁷⁰, A.I. Etienvre¹³⁸, E. Etzion¹⁵⁵, H. Evans⁶⁴, A. Ezhilov¹²⁵, M. Ezzi^{137e}, F. Fabbri^{22a,22b}, L. Fabbri^{22a,22b}, V. Fabiani¹⁰⁸, G. Facini⁸¹, R.M. Fakhrtudinov¹³², S. Falciano^{134a}, R.J. Falla⁸¹, J. Faltova³², Y. Fang^{35a}, M. Fanti^{94a,94b}, A. Farbin⁸, A. Farilla^{136a}, C. Farina¹²⁷, E.M. Farina^{123a,123b}, T. Farooque⁹³, S. Farrell¹⁶, S.M. Farrington¹⁷³, P. Farthouat³², F. Fassi^{137e}, P. Fassnacht³², D. Fassouliotis⁹, M. Faucci Giannelli⁸⁰, A. Favareto^{53a,53b}, W.J. Fawcett¹²², L. Fayard¹¹⁹, O.L. Fedin^{125,q}, W. Fedorko¹⁷¹, S. Feigl¹²¹, L. Feligioni⁸⁸, C. Feng^{36b}, E.J. Feng³², H. Feng⁹², M.J. Fenton⁵⁶, A.B. Fenyuk¹³², L. Feremenga⁸, P. Fernandez Martinez¹⁷⁰, S. Fernandez Perez¹³, J. Ferrando⁴⁵, A. Ferrari¹⁶⁸, P. Ferrari¹⁰⁹, R. Ferrari^{123a}, D.E. Ferreira de Lima^{60b}, A. Ferrer¹⁷⁰, D. Ferrere⁵², C. Ferretti⁹², F. Fiedler⁸⁶, A. Filipčič⁷⁸, M. Filipuzzi⁴⁵, F. Filthaut¹⁰⁸, M. Fincke-Keeler¹⁷², K.D. Finelli¹⁵², M.C.N. Fiolhais^{128a,128c,r}, L. Fiorini¹⁷⁰, A. Fischer², C. Fischer¹³, J. Fischer¹⁷⁸, W.C. Fisher⁹³, N. Flaschel⁴⁵, I. Fleck¹⁴³, P. Fleischmann⁹², R.R.M. Fletcher¹²⁴, T. Flick¹⁷⁸, B.M. Flierl¹⁰², L.R. Flores Castillo^{62a}, M.J. Flowerdew¹⁰³, G.T. Forcolin⁸⁷, A. Formica¹³⁸, F.A. Förster¹³, A. Forti⁸⁷, A.G. Foster¹⁹, D. Fournier¹¹⁹, H. Fox⁷⁵, S. Fracchia¹⁴¹, P. Francavilla⁸³, M. Franchini^{22a,22b}, S. Franchino^{60a}, D. Francis³², L. Franconi¹²¹, M. Franklin⁵⁹, M. Frate¹⁶⁶, M. Fraternali^{123a,123b}, D. Freeborn⁸¹, S.M. Fressard-Batraneanu³², B. Freund⁹⁷, D. Froidevaux³², J.A. Frost¹²², C. Fukunaga¹⁵⁸, T. Fusayasu¹⁰⁴, J. Fuster¹⁷⁰, C. Gabaldon⁵⁸, O. Gabizon¹⁵⁴, A. Gabrielli^{22a,22b}, A. Gabrielli¹⁶, G.P. Gach^{41a}, S. Gadatsch³², S. Gadomski⁸⁰, G. Gagliardi^{53a,53b},

L.G. Gagnon⁹⁷, C. Galea¹⁰⁸, B. Galhardo^{128a,128c}, E.J. Gallas¹²², B.J. Gallop¹³³, P. Gallus¹³⁰, G. Galster³⁹, K.K. Gan¹¹³, S. Ganguly³⁷, Y. Gao⁷⁷, Y.S. Gao^{145,g}, F.M. Garay Walls⁴⁹, C. García¹⁷⁰, J.E. García Navarro¹⁷⁰, J.A. García Pascual^{135a}, M. Garcia-Sciveres¹⁶, R.W. Gardner³³, N. Garelli¹⁴⁵, V. Garonne¹²¹, A. Gascon Bravo⁴⁵, K. Gasnikova⁴⁵, C. Gatti⁵⁰, A. Gaudiello^{53a,53b}, G. Gaudio^{123a}, I.L. Gavrilenko⁹⁸, C. Gay¹⁷¹, G. Gaycken²³, E.N. Gazis¹⁰, C.N.P. Gee¹³³, J. Geisen⁵⁷, M. Geisen⁸⁶, M.P. Geisler^{60a}, K. Gellerstedt^{148a,148b}, C. Gemme^{53a}, M.H. Genest⁵⁸, C. Geng⁹², S. Gentile^{134a,134b}, C. Gentsos¹⁵⁶, S. George⁸⁰, D. Gerbaudo¹³, A. Gershon¹⁵⁵, G. Geßner⁴⁶, S. Ghasemi¹⁴³, M. Ghneimat²³, B. Giacobbe^{22a}, S. Giagu^{134a,134b}, N. Giangiacomi^{22a,22b}, P. Giannetti^{126a,126b}, S.M. Gibson⁸⁰, M. Gignac¹⁷¹, M. Gilchriese¹⁶, D. Gillberg³¹, G. Gilles¹⁷⁸, D.M. Gingrich^{3,d}, N. Giokaris^{9,*}, M.P. Giordani^{167a,167c}, F.M. Giorgi^{22a}, P.F. Giraud¹³⁸, P. Giromini⁵⁹, D. Giugni^{94a}, F. Giuli¹²², C. Giuliani¹⁰³, M. Giulini^{60b}, B.K. Gjølsten¹²¹, S. Gkaitatzis¹⁵⁶, I. Gkialas^{9,s}, E.L. Gkoukousis¹³⁹, P. Gkoutoumis¹⁰, L.K. Gladilin¹⁰¹, C. Glasman⁸⁵, J. Glatzer¹³, P.C.F. Glaysheer⁴⁵, A. Glazov⁴⁵, M. Goblirsch-Kolb²⁵, J. Godlewski⁴², S. Goldfarb⁹¹, T. Golling⁵², D. Golubkov¹³², A. Gomes^{128a,128b,128d}, R. Gonçalo^{128a}, R. Goncalves Gama^{26a}, J. Goncalves Pinto Firmino Da Costa¹³⁸, G. Gonella⁵¹, L. Gonella¹⁹, A. Gongadze⁶⁸, S. González de la Hoz¹⁷⁰, S. Gonzalez-Sevilla⁵², L. Goossens³², P.A. Gorbounov⁹⁹, H.A. Gordon²⁷, I. Gorelov¹⁰⁷, B. Gorini³², E. Gorini^{76a,76b}, A. Gorišek⁷⁸, A.T. Goshaw⁴⁸, C. Gössling⁴⁶, M.I. Gostkin⁶⁸, C.A. Gottardo²³, C.R. Goudet¹¹⁹, D. Goujdami^{137c}, A.G. Goussiou¹⁴⁰, N. Govender^{147b,t}, E. Gozani¹⁵⁴, L. Graber⁵⁷, I. Grabowska-Bold^{41a}, P.O.J. Gradin¹⁶⁸, J. Gramling¹⁶⁶, E. Gramstad¹²¹, S. Grancagnolo¹⁷, V. Gratchev¹²⁵, P.M. Gravila^{28f}, C. Gray⁵⁶, H.M. Gray¹⁶, Z.D. Greenwood^{82,u}, C. Grefe²³, K. Gregersen⁸¹, I.M. Gregor⁴⁵, P. Grenier¹⁴⁵, K. Grevtsov⁵, J. Griffiths⁸, A.A. Grillo¹³⁹, K. Grimm⁷⁵, S. Grinstein^{13,v}, Ph. Gris³⁷, J.-F. Grivaz¹¹⁹, S. Groh⁸⁶, E. Gross¹⁷⁵, J. Grosse-Knetter⁵⁷, G.C. Grossi⁸², Z.J. Grout⁸¹, A. Grummer¹⁰⁷, L. Guan⁹², W. Guan¹⁷⁶, J. Guenther⁶⁵, F. Guescini^{163a}, D. Guest¹⁶⁶, O. Gueta¹⁵⁵, B. Gui¹¹³, E. Guido^{53a,53b}, T. Guillemin⁵, S. Guindon², U. Gul⁵⁶, C. Gumpert³², J. Guo^{36c}, W. Guo⁹², Y. Guo^{36a,w}, R. Gupta⁴³, S. Gupta¹²², G. Gustavino^{134a,134b}, P. Gutierrez¹¹⁵, N.G. Gutierrez Ortiz⁸¹, C. Gutsche⁸¹, C. Guyot¹³⁸, M.P. Guzik^{41a}, C. Gwenlan¹²², C.B. Gwilliam⁷⁷, A. Haas¹¹², C. Haber¹⁶, H.K. Hadavand⁸, N. Haddad^{137e}, A. Hadeef⁸⁸, S. Hageböck²³, M. Hagihara¹⁶⁴, H. Hakobyan^{180,*}, M. Haleem⁴⁵, J. Haley¹¹⁶, G. Halladjian⁹³, G.D. Hallewell⁸⁸, K. Hamacher¹⁷⁸, P. Hamal¹¹⁷, K. Hamano¹⁷², A. Hamilton^{147a}, G.N. Hamity¹⁴¹, P.G. Hamnett⁴⁵, L. Han^{36a}, S. Han^{35a}, K. Hanagaki^{69,x}, K. Hanawa¹⁵⁷, M. Hance¹³⁹, B. Haney¹²⁴, P. Hanke^{60a}, J.B. Hansen³⁹, J.D. Hansen³⁹, M.C. Hansen²³, P.H. Hansen³⁹, K. Hara¹⁶⁴, A.S. Hard¹⁷⁶, T. Harenberg¹⁷⁸, F. Hariri¹¹⁹, S. Harkusha⁹⁵, R.D. Harrington⁴⁹, P.F. Harrison¹⁷³, N.M. Hartmann¹⁰², M. Hasegawa⁷⁰, Y. Hasegawa¹⁴², A. Hasib⁴⁹, S. Hassani¹³⁸, S. Haug¹⁸, R. Hauser⁹³, L. Hauswald⁴⁷, L.B. Havener³⁸, M. Havranek¹³⁰, C.M. Hawkes¹⁹, R.J. Hawkins³², D. Hayakawa¹⁵⁹, D. Hayden⁹³, C.P. Hays¹²², J.M. Hays⁷⁹, H.S. Hayward⁷⁷, S.J. Haywood¹³³, S.J. Head¹⁹, T. Heck⁸⁶, V. Hedberg⁸⁴, L. Heelan⁸, S. Heer²³, K.K. Heidegger⁵¹, S. Heim⁴⁵, T. Heim¹⁶, B. Heinemann^{45,y}, J.J. Heinrich¹⁰², L. Heinrich¹¹², C. Heinz⁵⁵, J. Hejbal¹²⁹, L. Helary³², A. Held¹⁷¹, S. Hellman^{148a,148b}, C. Helsen³², R.C.W. Henderson⁷⁵, Y. Heng¹⁷⁶, S. Henkelmann¹⁷¹, A.M. Henriques Correia³², S. Henrot-Versille¹¹⁹, G.H. Herbert¹⁷, H. Herde²⁵, V. Herget¹⁷⁷, Y. Hernández Jiménez^{147c}, H. Herr⁸⁶, G. Herten⁵¹, R. Hertenberger¹⁰², L. Hervas³², T.C. Herwig¹²⁴, G.G. Hesketh⁸¹, N.P. Hessey^{163a}, J.W. Hetherly⁴³, S. Higashino⁶⁹, E. Higón-Rodríguez¹⁷⁰, K. Hildebrand³³, E. Hill¹⁷², J.C. Hill³⁰, K.H. Hiller⁴⁵, S.J. Hillier¹⁹, M. Hils⁴⁷, I. Hinchliffe¹⁶, M. Hirose⁵¹, D. Hirschbuehl¹⁷⁸, B. Hiti⁷⁸, O. Hladik¹²⁹, X. Hoad⁴⁹, J. Hobbs¹⁵⁰, N. Hod^{163a}, M.C. Hodgkinson¹⁴¹, P. Hodgson¹⁴¹, A. Hoecker³², M.R. Hoferkamp¹⁰⁷, F. Hoenig¹⁰², D. Hohn²³, T.R. Holmes³³, M. Homann⁴⁶, S. Honda¹⁶⁴, T. Honda⁶⁹, T.M. Hong¹²⁷, B.H. Hooberman¹⁶⁹, W.H. Hopkins¹¹⁸, Y. Horii¹⁰⁵, A.J. Horton¹⁴⁴, J.-Y. Hostachy⁵⁸, S. Hou¹⁵³, A. Hoummada^{137a}, J. Howarth⁸⁷, J. Hoya⁷⁴, M. Hrabovsky¹¹⁷, J. Hrdinka³², I. Hristova¹⁷, J. Hrivnac¹¹⁹, T. Hryn'ova⁵, A. Hrynevich⁹⁶, P.J. Hsu⁶³, S.-C. Hsu¹⁴⁰, Q. Hu^{36a}, S. Hu^{36c}, Y. Huang^{35a}, Z. Hubacek¹³⁰, F. Hubaut⁸⁸, F. Huegging²³, T.B. Huffman¹²², E.W. Hughes³⁸, G. Hughes⁷⁵,

M. Huhtinen³², P. Huo¹⁵⁰, N. Huseynov^{68,b}, J. Huston⁹³, J. Huth⁵⁹, G. Iacobucci⁵², G. Iakovidis²⁷,
I. Ibragimov¹⁴³, L. Iconomidou-Fayard¹¹⁹, Z. Idrissi^{137e}, P. Iengo³², O. Igonkina^{109,z}, T. Iizawa¹⁷⁴,
Y. Ikegami⁶⁹, M. Ikeno⁶⁹, Y. Ilchenko^{11,aa}, D. Iliadis¹⁵⁶, N. Ilic¹⁴⁵, G. Introzzi^{123a,123b}, P. Ioannou^{9,*},
M. Iodice^{136a}, K. Iordanidou³⁸, V. Ippolito⁵⁹, M.F. Isacson¹⁶⁸, N. Ishijima¹²⁰, M. Ishino¹⁵⁷,
M. Ishitsuka¹⁵⁹, C. Issever¹²², S. Istin^{20a}, F. Ito¹⁶⁴, J.M. Iturbe Ponce^{62a}, R. Iuppa^{162a,162b}, H. Iwasaki⁶⁹,
J.M. Izen⁴⁴, V. Izzo^{106a}, S. Jabbar³, P. Jackson¹, R.M. Jacobs²³, V. Jain², K.B. Jakobi⁸⁶, K. Jakobs⁵¹,
S. Jakobsen⁶⁵, T. Jakoubek¹²⁹, D.O. Jamin¹¹⁶, D.K. Jana⁸², R. Jansky⁵², J. Janssen²³, M. Janus⁵⁷,
P.A. Janus^{41a}, G. Jarlskog⁸⁴, N. Javadov^{68,b}, T. Javůrek⁵¹, M. Javurkova⁵¹, F. Jeanneau¹³⁸, L. Jeanty¹⁶,
J. Jejelava^{54a,ab}, A. Jelinskas¹⁷³, P. Jenni^{51,ac}, C. Jeske¹⁷³, S. Jézéquel⁵, H. Ji¹⁷⁶, J. Jia¹⁵⁰, H. Jiang⁶⁷,
Y. Jiang^{36a}, Z. Jiang¹⁴⁵, S. Jiggins⁸¹, J. Jimenez Pena¹⁷⁰, S. Jin^{35a}, A. Jinaru^{28b}, O. Jinnouchi¹⁵⁹,
H. Jivan^{147c}, P. Johansson¹⁴¹, K.A. Johns⁷, C.A. Johnson⁶⁴, W.J. Johnson¹⁴⁰, K. Jon-And^{148a,148b},
R.W.L. Jones⁷⁵, S.D. Jones¹⁵¹, S. Jones⁷, T.J. Jones⁷⁷, J. Jongmanns^{60a}, P.M. Jorge^{128a,128b},
J. Jovicevic^{163a}, X. Ju¹⁷⁶, A. Juste Rozas^{13,v}, M.K. Köhler¹⁷⁵, A. Kaczmaraska⁴², M. Kado¹¹⁹,
H. Kagan¹¹³, M. Kagan¹⁴⁵, S.J. Kahn⁸⁸, T. Kaji¹⁷⁴, E. Kajomovitz⁴⁸, C.W. Kalderon⁸⁴, A. Kaluza⁸⁶,
S. Kama⁴³, A. Kamenshchikov¹³², N. Kanaya¹⁵⁷, L. Kanjir⁷⁸, V.A. Kantserov¹⁰⁰, J. Kanzaki⁶⁹,
B. Kaplan¹¹², L.S. Kaplan¹⁷⁶, D. Kar^{147c}, K. Karakostas¹⁰, N. Karastathis¹⁰, M.J. Kareem⁵⁷,
E. Karentzos¹⁰, S.N. Karpov⁶⁸, Z.M. Karpova⁶⁸, K. Karthik¹¹², V. Kartvelishvili⁷⁵, A.N. Karyukhin¹³²,
K. Kasahara¹⁶⁴, L. Kashif¹⁷⁶, R.D. Kass¹¹³, A. Kastanas¹⁴⁹, Y. Kataoka¹⁵⁷, C. Kato¹⁵⁷, A. Katre⁵²,
J. Katzy⁴⁵, K. Kawade⁷⁰, K. Kawagoe⁷³, T. Kawamoto¹⁵⁷, G. Kawamura⁵⁷, E.F. Kay⁷⁷,
V.F. Kazanin^{111,c}, R. Keeler¹⁷², R. Kehoe⁴³, J.S. Keller³¹, J.J. Kempster⁸⁰, J. Kendrick¹⁹,
H. Keoshkerian¹⁶¹, O. Kepka¹²⁹, B.P. Kerševan⁷⁸, S. Kersten¹⁷⁸, R.A. Keyes⁹⁰, M. Khader¹⁶⁹,
F. Khalil-zada¹², A. Khanov¹¹⁶, A.G. Kharlamov^{111,c}, T. Kharlamova^{111,c}, A. Khodinov¹⁶⁰, T.J. Khoo⁵²,
V. Khovanskij^{99,*}, E. Khramov⁶⁸, J. Khubua^{54b,ad}, S. Kido⁷⁰, C.R. Kilby⁸⁰, H.Y. Kim⁸, S.H. Kim¹⁶⁴,
Y.K. Kim³³, N. Kimura¹⁵⁶, O.M. Kind¹⁷, B.T. King⁷⁷, D. Kirchmeier⁴⁷, J. Kirk¹³³, A.E. Kiryunin¹⁰³,
T. Kishimoto¹⁵⁷, D. Kisielewska^{41a}, V. Kitali⁴⁵, K. Kiuchi¹⁶⁴, O. Kivernyk⁵, E. Kladiva^{146b},
T. Klapdor-Kleingrothaus⁵¹, M.H. Klein⁹², M. Klein⁷⁷, U. Klein⁷⁷, K. Kleinknecht⁸⁶, P. Klimek¹¹⁰,
A. Klimentov²⁷, R. Klingenberg⁴⁶, T. Klingl²³, T. Klioutchnikova³², E.-E. Kluge^{60a}, P. Kluit¹⁰⁹,
S. Kluth¹⁰³, E. Kneringer⁶⁵, E.B.F.G. Knoops⁸⁸, A. Knue¹⁰³, A. Kobayashi¹⁵⁷, D. Kobayashi¹⁵⁹,
T. Kobayashi¹⁵⁷, M. Kobel⁴⁷, M. Kocian¹⁴⁵, P. Kodys¹³¹, T. Koffas³¹, E. Koffeman¹⁰⁹, N.M. Köhler¹⁰³,
T. Koi¹⁴⁵, M. Kolb^{60b}, I. Koletsou⁵, A.A. Komar^{98,*}, Y. Komori¹⁵⁷, T. Kondo⁶⁹, N. Kondrashova^{36c},
K. Köneke⁵¹, A.C. König¹⁰⁸, T. Kono^{69,ae}, R. Konoplich^{112,af}, N. Konstantinidis⁸¹, R. Kopeliansky⁶⁴,
S. Koperny^{41a}, A.K. Kopp⁵¹, K. Korcyl⁴², K. Kordas¹⁵⁶, A. Korn⁸¹, A.A. Korol^{111,c}, I. Korolkov¹³,
E.V. Korolkova¹⁴¹, O. Kortner¹⁰³, S. Kortner¹⁰³, T. Kosek¹³¹, V.V. Kostyukhin²³, A. Kotwal⁴⁸,
A. Koulouris¹⁰, A. Kourkouveli-Charalampidi^{123a,123b}, C. Kourkouvelis⁹, E. Kourlitis¹⁴¹,
V. Kouskoura²⁷, A.B. Kowalewska⁴², R. Kowalewski¹⁷², T.Z. Kowalski^{41a}, C. Kozakai¹⁵⁷,
W. Kozanecki¹³⁸, A.S. Kozhin¹³², V.A. Kramarenko¹⁰¹, G. Kramberger⁷⁸, D. Krasnopevtsev¹⁰⁰,
M.W. Krasny⁸³, A. Krasznahorkay³², D. Krauss¹⁰³, J.A. Kremer^{41a}, J. Kretzschmar⁷⁷, K. Kreutzfeldt⁵⁵,
P. Krieger¹⁶¹, K. Krizka³³, K. Kroeninger⁴⁶, H. Kroha¹⁰³, J. Kroll¹²⁹, J. Kroll¹²⁴, J. Kroseberg²³,
J. Krstic¹⁴, U. Kruchonak⁶⁸, H. Krüger²³, N. Krumnack⁶⁷, M.C. Kruse⁴⁸, T. Kubota⁹¹, H. Kucuk⁸¹,
S. Kuday^{4b}, J.T. Kuechler¹⁷⁸, S. Kuehn³², A. Kugel^{60a}, F. Kuger¹⁷⁷, T. Kuhl⁴⁵, V. Kukhtin⁶⁸, R. Kukla⁸⁸,
Y. Kulchitsky⁹⁵, S. Kuleshov^{34b}, Y.P. Kulinich¹⁶⁹, M. Kuna^{134a,134b}, T. Kunigo⁷¹, A. Kupco¹²⁹,
T. Kupfer⁴⁶, O. Kuprash¹⁵⁵, H. Kurashige⁷⁰, L.L. Kurchaninov^{163a}, Y.A. Kurochkin⁹⁵, M.G. Kurth^{35a},
V. Kus¹²⁹, E.S. Kuwertz¹⁷², M. Kuze¹⁵⁹, J. Kvita¹¹⁷, T. Kwan¹⁷², D. Kyriazopoulos¹⁴¹, A. La Rosa¹⁰³,
J.L. La Rosa Navarro^{26d}, L. La Rotonda^{40a,40b}, F. La Ruffa^{40a,40b}, C. Lacasta¹⁷⁰, F. Lacava^{134a,134b},
J. Lacey⁴⁵, H. Lacker¹⁷, D. Lacour⁸³, E. Ladygin⁶⁸, R. Lafaye⁵, B. Laforge⁸³, T. Lagouri¹⁷⁹, S. Lai⁵⁷,
S. Lammers⁶⁴, W. Lamp⁷, E. Lançon²⁷, U. Landgraf⁵¹, M.P.J. Landon⁷⁹, M.C. Lanfermann⁵²,
V.S. Lang^{60a}, J.C. Lange¹³, R.J. Langenberg³², A.J. Lankford¹⁶⁶, F. Lanni²⁷, K. Lantzschtz²³,

A. Lanza^{123a}, A. Lapertosa^{53a,53b}, S. Laplace⁸³, J.F. Laporte¹³⁸, T. Lari^{94a}, F. Lasagni Manghi^{22a,22b},
 M. Lassnig³², P. Laurelli⁵⁰, W. Lavrijsen¹⁶, A.T. Law¹³⁹, P. Laycock⁷⁷, T. Lazovich⁵⁹,
 M. Lazzaroni^{94a,94b}, B. Le⁹¹, O. Le Dortz⁸³, E. Le Guirriec⁸⁸, E.P. Le Quilleuc¹³⁸, M. LeBlanc¹⁷²,
 T. LeCompte⁶, F. Ledroit-Guillon⁵⁸, C.A. Lee²⁷, G.R. Lee^{133,ag}, S.C. Lee¹⁵³, L. Lee⁵⁹, B. Lefebvre⁹⁰,
 G. Lefebvre⁸³, M. Lefebvre¹⁷², F. Legger¹⁰², C. Leggett¹⁶, G. Lehmann Miotto³², X. Lei⁷,
 W.A. Leight⁴⁵, M.A.L. Leite^{26d}, R. Leitner¹³¹, D. Lellouch¹⁷⁵, B. Lemmer⁵⁷, K.J.C. Leney⁸¹, T. Lenz²³,
 B. Lenzi³², R. Leone⁷, S. Leone^{126a,126b}, C. Leonidopoulos⁴⁹, G. Lerner¹⁵¹, C. Leroy⁹⁷,
 A.A.J. Lesage¹³⁸, C.G. Lester³⁰, M. Levchenko¹²⁵, J. Levêque⁵, D. Levin⁹², L.J. Levinson¹⁷⁵,
 M. Levy¹⁹, D. Lewis⁷⁹, B. Li^{36a,w}, Changqiao Li^{36a}, H. Li¹⁵⁰, L. Li^{36c}, Q. Li^{35a}, S. Li⁴⁸, X. Li^{36c},
 Y. Li¹⁴³, Z. Liang^{35a}, B. Liberti^{135a}, A. Liblong¹⁶¹, K. Lie^{62c}, J. Liebal²³, W. Liebig¹⁵, A. Limosani¹⁵²,
 S.C. Lin¹⁸², T.H. Lin⁸⁶, R.A. Linck⁶⁴, B.E. Lindquist¹⁵⁰, A.E. Lioni⁵², E. Lipeles¹²⁴, A. Lipniacka¹⁵,
 M. Lisovyi^{60b}, T.M. Liss^{169,ah}, A. Lister¹⁷¹, A.M. Litke¹³⁹, B. Liu^{153,ai}, H. Liu⁹², H. Liu²⁷,
 J.K.K. Liu¹²², J. Liu^{36b}, J.B. Liu^{36a}, K. Liu⁸⁸, L. Liu¹⁶⁹, M. Liu^{36a}, Y.L. Liu^{36a}, Y. Liu^{36a},
 M. Livan^{123a,123b}, A. Lleres⁵⁸, J. Llorente Merino^{35a}, S.L. Lloyd⁷⁹, C.Y. Lo^{62b}, F. Lo Sterzo¹⁵³,
 E.M. Lobodzinska⁴⁵, P. Loch⁷, F.K. Loebinger⁸⁷, A. Loesle⁵¹, K.M. Loew²⁵, A. Loginov^{179,*},
 T. Lohse¹⁷, K. Lohwasser¹⁴¹, M. Lokajicek¹²⁹, B.A. Long²⁴, J.D. Long¹⁶⁹, R.E. Long⁷⁵, L. Longo^{76a,76b},
 K.A. Looper¹¹³, J.A. Lopez^{34b}, D. Lopez Mateos⁵⁹, I. Lopez Paz¹³, A. Lopez Solis⁸³, J. Lorenz¹⁰²,
 N. Lorenzo Martinez⁵, M. Losada²¹, P.J. Lösel¹⁰², X. Lou^{35a}, A. Lounis¹¹⁹, J. Love⁶, P.A. Love⁷⁵,
 H. Lu^{62a}, N. Lu⁹², Y.J. Lu⁶³, H.J. Lubatti¹⁴⁰, C. Luci^{134a,134b}, A. Lucotte⁵⁸, C. Luedtke⁵¹, F. Luehring⁶⁴,
 W. Lukas⁶⁵, L. Luminari^{134a}, O. Lundberg^{148a,148b}, B. Lund-Jensen¹⁴⁹, M.S. Lutz⁸⁹, P.M. Luzi⁸³,
 D. Lynn²⁷, R. Lysak¹²⁹, E. Lytken⁸⁴, F. Lyu^{35a}, V. Lyubushkin⁶⁸, H. Ma²⁷, L.L. Ma^{36b}, Y. Ma^{36b},
 G. Maccarrone⁵⁰, A. Macchiolo¹⁰³, C.M. Macdonald¹⁴¹, B. Maček⁷⁸, J. Machado Miguens^{124,128b},
 D. Madaffari¹⁷⁰, R. Madar³⁷, W.F. Mader⁴⁷, A. Madsen⁴⁵, J. Maeda⁷⁰, S. Maeland¹⁵, T. Maeno²⁷,
 A.S. Maevskiy¹⁰¹, V. Magerl⁵¹, J. Mahlstedt¹⁰⁹, C. Maiani¹¹⁹, C. Maidantchik^{26a}, A.A. Maier¹⁰³,
 T. Maier¹⁰², A. Maio^{128a,128b,128d}, O. Majersky^{146a}, S. Majewski¹¹⁸, Y. Makida⁶⁹, N. Makovec¹¹⁹,
 B. Malaescu⁸³, Pa. Malecki⁴², V.P. Maleev¹²⁵, F. Malek⁵⁸, U. Mallik⁶⁶, D. Malon⁶, C. Malone³⁰,
 S. Maltezos¹⁰, S. Malyukov³², J. Mamuzic¹⁷⁰, G. Mancini⁵⁰, I. Mandić⁷⁸, J. Maneira^{128a,128b},
 L. Manhaes de Andrade Filho^{26b}, J. Manjarres Ramos⁴⁷, K.H. Mankinen⁸⁴, A. Mann¹⁰², A. Manousos³²,
 B. Mansoulie¹³⁸, J.D. Mansour^{35a}, R. Mantifel⁹⁰, M. Mantoani⁵⁷, S. Manzoni^{94a,94b}, L. Mapelli³²,
 G. Marceca²⁹, L. March⁵², L. Marchese¹²², G. Marchiori⁸³, M. Marcisovsky¹²⁹, M. Marjanovic³⁷,
 D.E. Marley⁹², F. Marroquim^{26a}, S.P. Marsden⁸⁷, Z. Marshall¹⁶, M.U.F. Martensson¹⁶⁸,
 S. Marti-Garcia¹⁷⁰, C.B. Martin¹¹³, T.A. Martin¹⁷³, V.J. Martin⁴⁹, B. Martin dit Latour¹⁵,
 M. Martinez^{13,v}, V.I. Martinez Outschoorn¹⁶⁹, S. Martin-Haugh¹³³, V.S. Martoiu^{28b}, A.C. Martyniuk⁸¹,
 A. Marzin³², L. Masetti⁸⁶, T. Mashimo¹⁵⁷, R. Mashinistov⁹⁸, J. Masik⁸⁷, A.L. Maslennikov^{111,c},
 L. Massa^{135a,135b}, P. Mastrandrea⁵, A. Mastroberardino^{40a,40b}, T. Masubuchi¹⁵⁷, P. Mättig¹⁷⁸,
 J. Maurer^{28b}, S.J. Maxfield⁷⁷, D.A. Maximov^{111,c}, R. Mazini¹⁵³, I. Maznas¹⁵⁶, S.M. Mazza^{94a,94b},
 N.C. Mc Fadden¹⁰⁷, G. Mc Goldrick¹⁶¹, S.P. Mc Kee⁹², A. McCarn⁹², R.L. McCarthy¹⁵⁰,
 T.G. McCarthy¹⁰³, L.I. McClymont⁸¹, E.F. McDonald⁹¹, J.A. Mcfayden⁸¹, G. Mchedlidze⁵⁷,
 S.J. McMahon¹³³, P.C. McNamara⁹¹, R.A. McPherson^{172,o}, S. Meehan¹⁴⁰, T.J. Megy⁵¹, S. Mehlhase¹⁰²,
 A. Mehta⁷⁷, T. Meideck⁵⁸, K. Meier^{60a}, B. Meirose⁴⁴, D. Melini^{170,aj}, B.R. Mellado Garcia^{147c},
 J.D. Mellenthin⁵⁷, M. Melo^{146a}, F. Meloni¹⁸, A. Melzer²³, S.B. Menary⁸⁷, L. Meng⁷⁷, X.T. Meng⁹²,
 A. Mengarelli^{22a,22b}, S. Menke¹⁰³, E. Meoni^{40a,40b}, S. Mergelmeyer¹⁷, P. Mermod⁵², L. Merola^{106a,106b},
 C. Meroni^{94a}, F.S. Merritt³³, A. Messina^{134a,134b}, J. Metcalfe⁶, A.S. Mete¹⁶⁶, C. Meyer¹²⁴, J-P. Meyer¹³⁸,
 J. Meyer¹⁰⁹, H. Meyer Zu Theenhausen^{60a}, F. Miano¹⁵¹, R.P. Middleton¹³³, S. Miglioranza^{53a,53b},
 L. Mijović⁴⁹, G. Mikenberg¹⁷⁵, M. Mikesikova¹²⁹, M. Mikuž⁷⁸, M. Milesi⁹¹, A. Milic¹⁶¹, D.W. Miller³³,
 C. Mills⁴⁹, A. Milov¹⁷⁵, D.A. Milstead^{148a,148b}, A.A. Minaenko¹³², Y. Minami¹⁵⁷, I.A. Minashvili^{54b},
 A.I. Mincer¹¹², B. Mindur^{41a}, M. Mineev⁶⁸, Y. Minegishi¹⁵⁷, Y. Ming¹⁷⁶, L.M. Mir¹³, K.P. Mistry¹²⁴,

T. Mitani¹⁷⁴, J. Mitrevski¹⁰², V.A. Mitsou¹⁷⁰, A. Miucci¹⁸, P.S. Miyagawa¹⁴¹, A. Mizukami⁶⁹, J.U. Mjörnmark⁸⁴, T. Mkrtchyan¹⁸⁰, M. Mlynarikova¹³¹, T. Moa^{148a,148b}, K. Mochizuki⁹⁷, P. Mogg⁵¹, S. Mohapatra³⁸, S. Molander^{148a,148b}, R. Moles-Valls²³, R. Monden⁷¹, M.C. Mondragon⁹³, K. Mönig⁴⁵, J. Monk³⁹, E. Monnier⁸⁸, A. Montalbano¹⁵⁰, J. Montejo Berlingen³², F. Monticelli⁷⁴, S. Monzani^{94a,94b}, R.W. Moore³, N. Morange¹¹⁹, D. Moreno²¹, M. Moreno Llácer³², P. Morettini^{53a}, S. Morgenstern³², D. Mori¹⁴⁴, T. Mori¹⁵⁷, M. Morii⁵⁹, M. Morinaga¹⁵⁷, V. Morisbak¹²¹, A.K. Morley³², G. Mornacchi³², J.D. Morris⁷⁹, L. Morvaj¹⁵⁰, P. Moschovakos¹⁰, M. Mosidze^{54b}, H.J. Moss¹⁴¹, J. Moss^{145,ak}, K. Motohashi¹⁵⁹, R. Mount¹⁴⁵, E. Mountricha²⁷, E.J.W. Moyse⁸⁹, S. Muanza⁸⁸, F. Mueller¹⁰³, J. Mueller¹²⁷, R.S.P. Mueller¹⁰², D. Muenstermann⁷⁵, P. Mullen⁵⁶, G.A. Mullier¹⁸, F.J. Munoz Sanchez⁸⁷, W.J. Murray^{173,133}, H. Musheghyan³², M. Muškinja⁷⁸, A.G. Myagkov^{132,al}, M. Myska¹³⁰, B.P. Nachman¹⁶, O. Nackenhorst⁵², K. Nagai¹²², R. Nagai^{69,ae}, K. Nagano⁶⁹, Y. Nagasaka⁶¹, K. Nagata¹⁶⁴, M. Nagel⁵¹, E. Nagy⁸⁸, A.M. Nairz³², Y. Nakahama¹⁰⁵, K. Nakamura⁶⁹, T. Nakamura¹⁵⁷, I. Nakano¹¹⁴, R.F. Naranjo Garcia⁴⁵, R. Narayan¹¹, D.I. Narrias Villai^{60a}, I. Naryshkin¹²⁵, T. Naumann⁴⁵, G. Navarro²¹, R. Nayyar⁷, H.A. Neal⁹², P.Yu. Nechaeva⁹⁸, T.J. Neep¹³⁸, A. Negri^{123a,123b}, M. Negrini^{22a}, S. Nektarijevic¹⁰⁸, C. Nellist¹¹⁹, A. Nelson¹⁶⁶, M.E. Nelson¹²², S. Nemecek¹²⁹, P. Nemethy¹¹², M. Nessi^{32,am}, M.S. Neubauer¹⁶⁹, M. Neumann¹⁷⁸, P.R. Newman¹⁹, T.Y. Ng^{62c}, T. Nguyen Manh⁹⁷, R.B. Nickerson¹²², R. Nicolaidou¹³⁸, J. Nielsen¹³⁹, V. Nikolaenko^{132,al}, I. Nikolic-Audit⁸³, K. Nikolopoulos¹⁹, J.K. Nilsen¹²¹, P. Nilsson²⁷, Y. Ninomiya¹⁵⁷, A. Nisati^{134a}, N. Nishu^{35c}, R. Nisius¹⁰³, I. Nitsche⁴⁶, T. Nitta¹⁷⁴, T. Nobe¹⁵⁷, Y. Noguchi⁷¹, M. Nomachi¹²⁰, I. Nomidis³¹, M.A. Nomura²⁷, T. Nooney⁷⁹, M. Nordberg³², N. Norjoharuddeen¹²², O. Novgorodova⁴⁷, M. Nozaki⁶⁹, L. Nozka¹¹⁷, K. Ntekas¹⁶⁶, E. Nurse⁸¹, F. Nuti⁹¹, K. O'connor²⁵, D.C. O'Neil¹⁴⁴, A.A. O'Rourke⁴⁵, V. O'Shea⁵⁶, F.G. Oakham^{31,d}, H. Oberlack¹⁰³, T. Obermann²³, J. Ocariz⁸³, A. Ochi⁷⁰, I. Ochoa³⁸, J.P. Ochoa-Ricoux^{34a}, S. Oda⁷³, S. Odaka⁶⁹, A. Oh⁸⁷, S.H. Oh⁴⁸, C.C. Ohm¹⁶, H. Ohman¹⁶⁸, H. Oide^{53a,53b}, H. Okawa¹⁶⁴, Y. Okumura¹⁵⁷, T. Okuyama⁶⁹, A. Olariu^{28b}, L.F. Oleiro Seabra^{128a}, S.A. Olivares Pino⁴⁹, D. Oliveira Damazio²⁷, A. Olszewski⁴², J. Olszowska⁴², A. Onofre^{128a,128e}, K. Onogi¹⁰⁵, P.U.E. Onyisi^{11,aa}, H. Oppen¹²¹, M.J. Oreglia³³, Y. Oren¹⁵⁵, D. Orestano^{136a,136b}, N. Orlando^{62b}, R.S. Orr¹⁶¹, B. Osculati^{53a,53b,*}, R. Ospanov^{36a}, G. Otero y Garzon²⁹, H. Otono⁷³, M. Ouchrif^{137d}, F. Ould-Saada¹²¹, A. Ouraou¹³⁸, K.P. Oussoren¹⁰⁹, Q. Ouyang^{35a}, M. Owen⁵⁶, R.E. Owen¹⁹, V.E. Ozcan^{20a}, N. Ozturk⁸, K. Pachal¹⁴⁴, A. Pacheco Pages¹³, L. Pacheco Rodriguez¹³⁸, C. Padilla Aranda¹³, S. Pagan Griso¹⁶, M. Paganini¹⁷⁹, F. Paige²⁷, G. Palacino⁶⁴, S. Palazzo^{40a,40b}, S. Palestini³², M. Palka^{41b}, D. Pallin³⁷, E.St. Panagiotopoulou¹⁰, I. Panagoulas¹⁰, C.E. Pandini⁸³, J.G. Panduro Vazquez⁸⁰, P. Pani³², S. Panitkin²⁷, D. Pantea^{28b}, L. Paolozzi⁵², Th.D. Papadopoulou¹⁰, K. Papageorgiou^{9,s}, A. Paramonov⁶, D. Paredes Hernandez¹⁷⁹, A.J. Parker⁷⁵, M.A. Parker³⁰, K.A. Parker⁴⁵, F. Parodi^{53a,53b}, J.A. Parsons³⁸, U. Parzefall⁵¹, V.R. Pascuzzi¹⁶¹, J.M. Pasner¹³⁹, E. Pasqualucci^{134a}, S. Passaggio^{53a}, Fr. Pastore⁸⁰, S. Patariaia⁸⁶, J.R. Pater⁸⁷, T. Pauly³², B. Pearson¹⁰³, S. Pedraza Lopez¹⁷⁰, R. Pedro^{128a,128b}, S.V. Peleganchuk^{111,c}, O. Penc¹²⁹, C. Peng^{35a}, H. Peng^{36a}, J. Penwell⁶⁴, B.S. Peralva^{26b}, M.M. Perego¹³⁸, D.V. Perepelitsa²⁷, F. Peri¹⁷, L. Perini^{94a,94b}, H. Pernegger³², S. Perrella^{106a,106b}, R. Peschke⁴⁵, V.D. Peshekhonov^{68,*}, K. Peters⁴⁵, R.F.Y. Peters⁸⁷, B.A. Petersen³², T.C. Petersen³⁹, E. Petit⁵⁸, A. Petridis¹, C. Petridou¹⁵⁶, P. Petroff¹¹⁹, E. Petrolo^{134a}, M. Petrov¹²², F. Petrucci^{136a,136b}, N.E. Pettersson⁸⁹, A. Peyaud¹³⁸, R. Pezoa^{34b}, F.H. Phillips⁹³, P.W. Phillips¹³³, G. Piacquadio¹⁵⁰, E. Pianori¹⁷³, A. Picazio⁸⁹, E. Piccaro⁷⁹, M.A. Pickering¹²², R. Piegaia²⁹, J.E. Pilcher³³, A.D. Pilkington⁸⁷, A.W.J. Pin⁸⁷, M. Pinamonti^{135a,135b}, J.L. Pinfold³, H. Pirumov⁴⁵, M. Pitt¹⁷⁵, L. Plazak^{146a}, M.-A. Pleier²⁷, V. Pleskot⁸⁶, E. Plotnikova⁶⁸, D. Pluth⁶⁷, P. Podberezko¹¹¹, R. Poettgen^{148a,148b}, R. Poggi^{123a,123b}, L. Poggioli¹¹⁹, D. Pohl²³, G. Polesello^{123a}, A. Poley⁴⁵, A. Policicchio^{40a,40b}, R. Polifka³², A. Polini^{22a}, C.S. Pollard⁵⁶, V. Polychronakos²⁷, K. Pommès³², D. Ponomarenko¹⁰⁰, L. Pontecorvo^{134a}, G.A. Popeneciu^{28d}, A. Poppleton³², S. Pospisil¹³⁰, K. Potamianos¹⁶, I.N. Potrap⁶⁸, C.J. Potter³⁰, G. Poulard³², T. Poulsen⁸⁴,

J. Poveda³², M.E. Pozo Astigarraga³², P. Pralavorio⁸⁸, A. Pranko¹⁶, S. Prell⁶⁷, D. Price⁸⁷,
M. Primavera^{76a}, S. Prince⁹⁰, N. Proklova¹⁰⁰, K. Prokofiev^{62c}, F. Prokoshin^{34b}, S. Protopopescu²⁷,
J. Proudfoot⁶, M. Przybycien^{41a}, A. Puri¹⁶⁹, P. Puzo¹¹⁹, J. Qian⁹², G. Qin⁵⁶, Y. Qin⁸⁷, A. Quadt⁵⁷,
M. Queitsch-Maitland⁴⁵, D. Quilty⁵⁶, S. Raddum¹²¹, V. Radeka²⁷, V. Radescu¹²²,
S.K. Radhakrishnan¹⁵⁰, P. Radloff¹¹⁸, P. Rados⁹¹, F. Ragusa^{94a,94b}, G. Rahal¹⁸¹, J.A. Raine⁸⁷,
S. Rajagopalan²⁷, C. Rangel-Smith¹⁶⁸, T. Rashid¹¹⁹, S. Raspopov⁵, M.G. Ratti^{94a,94b}, D.M. Rauch⁴⁵,
F. Rauscher¹⁰², S. Rave⁸⁶, I. Ravinovich¹⁷⁵, J.H. Rawling⁸⁷, M. Raymond³², A.L. Read¹²¹,
N.P. Readioff⁵⁸, M. Reale^{76a,76b}, D.M. Rebuzzi^{123a,123b}, A. Redelbach¹⁷⁷, G. Redlinger²⁷, R. Reece¹³⁹,
R.G. Reed^{147c}, K. Reeves⁴⁴, L. Rehnisch¹⁷, J. Reichert¹²⁴, A. Reiss⁸⁶, C. Rembser³², H. Ren^{35a},
M. Rescigno^{134a}, S. Resconi^{94a}, E.D. Resseguie¹²⁴, S. Rettie¹⁷¹, E. Reynolds¹⁹, O.L. Rezanova^{111,c},
P. Reznicek¹³¹, R. Rezvani⁹⁷, R. Richter¹⁰³, S. Richter⁸¹, E. Richter-Was^{41b}, O. Ricken²³, M. Ridel⁸³,
P. Rieck¹⁰³, C.J. Riegel¹⁷⁸, J. Rieger⁵⁷, O. Rifki¹¹⁵, M. Rijssenbeek¹⁵⁰, A. Rimoldi^{123a,123b},
M. Rimoldi¹⁸, L. Rinaldi^{22a}, G. Ripellino¹⁴⁹, B. Ristic³², E. Ritsch³², I. Riu¹³, F. Rizatdinova¹¹⁶,
E. Rizvi⁷⁹, C. Rizzi¹³, R.T. Roberts⁸⁷, S.H. Robertson^{90,o}, A. Robichaud-Veronneau⁹⁰, D. Robinson³⁰,
J.E.M. Robinson⁴⁵, A. Robson⁵⁶, E. Rocco⁸⁶, C. Roda^{126a,126b}, Y. Rodina^{88,an}, S. Rodriguez Bosca¹⁷⁰,
A. Rodriguez Perez¹³, D. Rodriguez Rodriguez¹⁷⁰, S. Roe³², C.S. Rogan⁵⁹, O. Röhne¹²¹, J. Roloff⁵⁹,
A. Romaniouk¹⁰⁰, M. Romano^{22a,22b}, S.M. Romano Saez³⁷, E. Romero Adam¹⁷⁰, N. Rompotis⁷⁷,
M. Ronzani⁵¹, L. Roos⁸³, S. Rosati^{134a}, K. Rosbach⁵¹, P. Rose¹³⁹, N.-A. Rosien⁵⁷, E. Rossi^{106a,106b},
L.P. Rossi^{53a}, J.H.N. Rosten³⁰, R. Rosten¹⁴⁰, M. Rotaru^{28b}, J. Rothberg¹⁴⁰, D. Rousseau¹¹⁹,
A. Rozanov⁸⁸, Y. Rozen¹⁵⁴, X. Ruan^{147c}, F. Rubbo¹⁴⁵, F. Rühr⁵¹, A. Ruiz-Martinez³¹, Z. Rurikova⁵¹,
N.A. Rusakovich⁶⁸, H.L. Russell⁹⁰, J.P. Rutherford¹⁷, N. Ruthmann³², Y.F. Ryabov¹²⁵, M. Rybar¹⁶⁹,
G. Rybkin¹¹⁹, S. Ryu⁶, A. Ryzhov¹³², G.F. Rzehorz⁵⁷, A.F. Saavedra¹⁵², G. Sabato¹⁰⁹, S. Sacerdoti²⁹,
H.F.W. Sadrozinski¹³⁹, R. Sadykov⁶⁸, F. Safai Tehrani^{134a}, P. Saha¹¹⁰, M. Sahinsoy^{60a}, M. Saimpert⁴⁵,
M. Saito¹⁵⁷, T. Saito¹⁵⁷, H. Sakamoto¹⁵⁷, Y. Sakurai¹⁷⁴, G. Salamanna^{136a,136b}, J.E. Salazar Loyola^{34b},
D. Salek¹⁰⁹, P.H. Sales De Bruin¹⁶⁸, D. Salihagic¹⁰³, A. Salnikov¹⁴⁵, J. Salt¹⁷⁰, D. Salvatore^{40a,40b},
F. Salvatore¹⁵¹, A. Salvucci^{62a,62b,62c}, A. Salzburger³², D. Sammel⁵¹, D. Sampsonidis¹⁵⁶,
D. Sampsonidou¹⁵⁶, J. Sánchez¹⁷⁰, V. Sanchez Martinez¹⁷⁰, A. Sanchez Pineda^{167a,167c}, H. Sandaker¹²¹,
R.L. Sandbach⁷⁹, C.O. Sander⁴⁵, M. Sandhoff¹⁷⁸, C. Sandoval²¹, D.P.C. Sankey¹³³, M. Sannino^{53a,53b},
Y. Sano¹⁰⁵, A. Sansoni⁵⁰, C. Santoni³⁷, H. Santos^{128a}, I. Santoyo Castillo¹⁵¹, A. Saprionov⁶⁸,
J.G. Saraiva^{128a,128d}, B. Sarrazin²³, O. Sasaki⁶⁹, K. Sato¹⁶⁴, E. Sauvan⁵, G. Savage⁸⁰, P. Savard^{161,d},
N. Savic¹⁰³, C. Sawyer¹³³, L. Sawyer^{82,u}, J. Saxon³³, C. Sbarra^{22a}, A. Sbrizzi^{22a,22b}, T. Scanlon⁸¹,
D.A. Scannicchio¹⁶⁶, M. Scarcella¹⁵², J. Schaarschmidt¹⁴⁰, P. Schacht¹⁰³, B.M. Schachtner¹⁰²,
D. Schaefer³², L. Schaefer¹²⁴, R. Schaefer⁴⁵, J. Schaeffer⁸⁶, S. Schaepe²³, S. Schaezel^{60b}, U. Schäfer⁸⁶,
A.C. Schaffer¹¹⁹, D. Schaile¹⁰², R.D. Schamberger¹⁵⁰, V.A. Schegelsky¹²⁵, D. Scheirich¹³¹,
M. Schernau¹⁶⁶, C. Schiavi^{53a,53b}, S. Schier¹³⁹, L.K. Schildgen²³, C. Schillo⁵¹, M. Schioppa^{40a,40b},
S. Schlenker³², K.R. Schmidt-Sommerfeld¹⁰³, K. Schmieden³², C. Schmitt⁸⁶, S. Schmitt⁴⁵, S. Schmitz⁸⁶,
U. Schnoor⁵¹, L. Schoeffel¹³⁸, A. Schoening^{60b}, B.D. Schoenrock⁹³, E. Schopf²³, M. Schott⁸⁶,
J.F.P. Schouwenberg¹⁰⁸, J. Schovancova³², S. Schramm⁵², N. Schuh⁸⁶, A. Schulte⁸⁶, M.J. Schultens²³,
H.-C. Schultz-Coulon^{60a}, H. Schulz¹⁷, M. Schumacher⁵¹, B.A. Schumm¹³⁹, Ph. Schune¹³⁸,
A. Schwartzman¹⁴⁵, T.A. Schwarz⁹², H. Schweiger⁸⁷, Ph. Schwemling¹³⁸, R. Schvienhorst⁹³,
J. Schwindling¹³⁸, A. Sciandra²³, G. Sciolla²⁵, M. Scornajenghi^{40a,40b}, F. Scuri^{126a,126b}, F. Scutti⁹¹,
J. Searcy⁹², P. Seema²³, S.C. Seidel¹⁰⁷, A. Seiden¹³⁹, J.M. Seixas^{26a}, G. Sekhniaidze^{106a}, K. Sekhon⁹²,
S.J. Sekula⁴³, N. Semprini-Cesari^{22a,22b}, S. Senkin³⁷, C. Serfon¹²¹, L. Serin¹¹⁹, L. Serkin^{167a,167b},
M. Sessa^{136a,136b}, R. Seuster¹⁷², H. Severini¹¹⁵, T. Sfiligoj⁷⁸, F. Sforza³², A. Sfyrta⁵², E. Shabalina⁵⁷,
N.W. Shaikh^{148a,148b}, L.Y. Shan^{35a}, R. Shang¹⁶⁹, J.T. Shank²⁴, M. Shapiro¹⁶, P.B. Shatalov⁹⁹,
K. Shaw^{167a,167b}, S.M. Shaw⁸⁷, A. Shcherbakova^{148a,148b}, C.Y. Shehu¹⁵¹, Y. Shen¹¹⁵, N. Sherafati³¹,
P. Sherwood⁸¹, L. Shi^{153,ao}, S. Shimizu⁷⁰, C.O. Shimmin¹⁷⁹, M. Shimojima¹⁰⁴, I.P.J. Shipsey¹²²,

S. Shirabe⁷³, M. Shiyakova^{68,ap}, J. Shlomi¹⁷⁵, A. Shmeleva⁹⁸, D. Shoaleh Saadi⁹⁷, M.J. Shochet³³, S. Shojaii^{94a}, D.R. Shope¹¹⁵, S. Shrestha¹¹³, E. Shulga¹⁰⁰, M.A. Shupe⁷, P. Sicho¹²⁹, A.M. Sickles¹⁶⁹, P.E. Sidebo¹⁴⁹, E. Sideras Haddad^{147c}, O. Sidiropoulou¹⁷⁷, A. Sidoti^{22a,22b}, F. Siegert⁴⁷, Dj. Sijacki¹⁴, J. Silva^{128a,128d}, S.B. Silverstein^{148a}, V. Simak¹³⁰, L. Simic¹⁴, S. Simion¹¹⁹, E. Simioni⁸⁶, B. Simmons⁸¹, M. Simon⁸⁶, P. Sinervo¹⁶¹, N.B. Sinev¹¹⁸, M. Sioli^{22a,22b}, G. Siragusa¹⁷⁷, I. Siral⁹², S.Yu. Sivoklov¹⁰¹, J. Sjölin^{148a,148b}, M.B. Skinner⁷⁵, P. Skubic¹¹⁵, M. Slater¹⁹, T. Slavicek¹³⁰, M. Slawinska⁴², K. Sliwa¹⁶⁵, R. Slovak¹³¹, V. Smakhtin¹⁷⁵, B.H. Smart⁵, J. Smiesko^{146a}, N. Smirnov¹⁰⁰, S.Yu. Smirnov¹⁰⁰, Y. Smirnov¹⁰⁰, L.N. Smirnova^{101,aq}, O. Smirnova⁸⁴, J.W. Smith⁵⁷, M.N.K. Smith³⁸, R.W. Smith³⁸, M. Smizanska⁷⁵, K. Smolek¹³⁰, A.A. Snesarev⁹⁸, I.M. Snyder¹¹⁸, S. Snyder²⁷, R. Sobie^{172,o}, F. Socher⁴⁷, A. Soffer¹⁵⁵, A. Søggaard⁴⁹, D.A. Soh¹⁵³, G. Sokhrannyi⁷⁸, C.A. Solans Sanchez³², M. Solar¹³⁰, E.Yu. Soldatov¹⁰⁰, U. Soldevila¹⁷⁰, A.A. Solodkov¹³², A. Soloshenko⁶⁸, O.V. Solovyanov¹³², V. Solovyev¹²⁵, P. Sommer⁵¹, H. Son¹⁶⁵, A. Sopczak¹³⁰, D. Sosa^{60b}, C.L. Sotiropoulou^{126a,126b}, R. Soualah^{167a,167c}, A.M. Soukharev^{111,c}, D. South⁴⁵, B.C. Sowden⁸⁰, S. Spagnolo^{76a,76b}, M. Spalla^{126a,126b}, M. Spangenberg¹⁷³, F. Spanò⁸⁰, D. Sperlich¹⁷, F. Spettel¹⁰³, T.M. Spieker^{60a}, R. Spighi^{22a}, G. Spigo³², L.A. Spiller⁹¹, M. Spousta¹³¹, R.D. St. Denis^{56,*}, A. Stabile^{94a}, R. Stamen^{60a}, S. Stamm¹⁷, E. Stanecka⁴², R.W. Stanek⁶, C. Stanescu^{136a}, M.M. Stanitzki⁴⁵, B.S. Stapf¹⁰⁹, S. Stapnes¹²¹, E.A. Starchenko¹³², G.H. Stark³³, J. Stark⁵⁸, S.H. Stark³⁹, P. Staroba¹²⁹, P. Starovoitov^{60a}, S. Stärz³², R. Staszewski⁴², P. Steinberg²⁷, B. Stelzer¹⁴⁴, H.J. Stelzer³², O. Stelzer-Chilton^{163a}, H. Stenzel⁵⁵, G.A. Stewart⁵⁶, M.C. Stockton¹¹⁸, M. Stoebe⁹⁰, G. Stoicea^{28b}, P. Stolte⁵⁷, S. Stonjek¹⁰³, A.R. Stradling⁸, A. Straessner⁴⁷, M.E. Stramaglia¹⁸, J. Strandberg¹⁴⁹, S. Strandberg^{148a,148b}, M. Strauss¹¹⁵, P. Strizenec^{146b}, R. Ströhmer¹⁷⁷, D.M. Strom¹¹⁸, R. Stroynowski⁴³, A. Strubig⁴⁹, S.A. Stucci²⁷, B. Stugu¹⁵, N.A. Styles⁴⁵, D. Su¹⁴⁵, J. Su¹²⁷, S. Suchek^{60a}, Y. Sugaya¹²⁰, M. Suk¹³⁰, V.V. Sulin⁹⁸, DMS Sultan^{162a,162b}, S. Sultansoy^{4c}, T. Sumida⁷¹, S. Sun⁵⁹, X. Sun³, K. Suruliz¹⁵¹, C.J.E. Suster¹⁵², M.R. Sutton¹⁵¹, S. Suzuki⁶⁹, M. Svatos¹²⁹, M. Swiatlowski³³, S.P. Swift², I. Sykora^{146a}, T. Sykora¹³¹, D. Ta⁵¹, K. Tackmann⁴⁵, J. Taenzer¹⁵⁵, A. Taffard¹⁶⁶, R. Tafirout^{163a}, N. Taiblum¹⁵⁵, H. Takai²⁷, R. Takashima⁷², E.H. Takasugi¹⁰³, T. Takeshita¹⁴², Y. Takubo⁶⁹, M. Talby⁸⁸, A.A. Talyshev^{111,c}, J. Tanaka¹⁵⁷, M. Tanaka¹⁵⁹, R. Tanaka¹¹⁹, S. Tanaka⁶⁹, R. Tanioka⁷⁰, B.B. Tannenwald¹¹³, S. Tapia Araya^{34b}, S. Tapprogge⁸⁶, S. Tarem¹⁵⁴, G.F. Tartarelli^{94a}, P. Tas¹³¹, M. Tasevsky¹²⁹, T. Tashiro⁷¹, E. Tassi^{40a,40b}, A. Tavares Delgado^{128a,128b}, Y. Tayalati^{137e}, A.C. Taylor¹⁰⁷, G.N. Taylor⁹¹, P.T.E. Taylor⁹¹, W. Taylor^{163b}, P. Teixeira-Dias⁸⁰, D. Temple¹⁴⁴, H. Ten Kate³², P.K. Teng¹⁵³, J.J. Teoh¹²⁰, F. Tepel¹⁷⁸, S. Terada⁶⁹, K. Terashi¹⁵⁷, J. Terron⁸⁵, S. Terzo¹³, M. Testa⁵⁰, R.J. Teuscher^{161,o}, T. Thevenaux-Pelzer⁸⁸, F. Thiele³⁹, J.P. Thomas¹⁹, J. Thomas-Wilsker⁸⁰, P.D. Thompson¹⁹, A.S. Thompson⁵⁶, L.A. Thomsen¹⁷⁹, E. Thomson¹²⁴, M.J. Tibbetts¹⁶, R.E. Ticse Torres⁸⁸, V.O. Tikhomirov^{98,ar}, Yu.A. Tikhonov^{111,c}, S. Timoshenko¹⁰⁰, P. Tipton¹⁷⁹, S. Tisserant⁸⁸, K. Todome¹⁵⁹, S. Todorova-Nova⁵, S. Todt⁴⁷, J. Tojo⁷³, S. Tokár^{146a}, K. Tokushuku⁶⁹, E. Tolley⁵⁹, L. Tomlinson⁸⁷, M. Tomoto¹⁰⁵, L. Tompkins^{145,as}, K. Toms¹⁰⁷, B. Tong⁵⁹, P. Tornambe⁵¹, E. Torrence¹¹⁸, H. Torres¹⁴⁴, E. Torró Pastor¹⁴⁰, J. Toth^{88,at}, F. Touchard⁸⁸, D.R. Tovey¹⁴¹, C.J. Treado¹¹², T. Trefzger¹⁷⁷, F. Tresoldi¹⁵¹, A. Tricoli²⁷, I.M. Trigger^{163a}, S. Trincas-Duvoid⁸³, M.F. Tripijana¹³, W. Trischuk¹⁶¹, B. Trocmé⁵⁸, A. Trofymov⁴⁵, C. Troncon^{94a}, M. Trotter-McDonald¹⁶, M. Trovatelli¹⁷², L. Truong^{147b}, M. Trzebinski⁴², A. Trzupek⁴², K.W. Tsang^{62a}, J.C.-L. Tseng¹²², P.V. Tsiarashka⁹⁵, G. Tsipolitis¹⁰, N. Tsirintanis⁹, S. Tsiskaridze¹³, V. Tsiskaridze⁵¹, E.G. Tskhadadze^{54a}, K.M. Tsui^{62a}, I.I. Tsukerman⁹⁹, V. Tsulaia¹⁶, S. Tsuno⁶⁹, D. Tsybychev¹⁵⁰, Y. Tu^{62b}, A. Tudorache^{28b}, V. Tudorache^{28b}, T.T. Tulbure^{28a}, A.N. Tuna⁵⁹, S.A. Tuppiti^{22a,22b}, S. Turchikhin⁶⁸, D. Turgeman¹⁷⁵, I. Turk Cakir^{4b,au}, R. Turra^{94a}, P.M. Tuts³⁸, G. Ucchielli^{22a,22b}, I. Ueda⁶⁹, M. Ughetto^{148a,148b}, F. Ukegawa¹⁶⁴, G. Unal³², A. Undrus²⁷, G. Unel¹⁶⁶, F.C. Ungaro⁹¹, Y. Unno⁶⁹, C. Unverdorben¹⁰², J. Urban^{146b}, P. Urquijo⁹¹, P. Urrejola⁸⁶, G. Usai⁸, J. Usui⁶⁹, L. Vacavant⁸⁸, V. Vacek¹³⁰, B. Vachon⁹⁰, K.O.H. Vadla¹²¹, A. Vaidya⁸¹, C. Valderanis¹⁰², E. Valdes Santurio^{148a,148b}, S. Valentinetti^{22a,22b},

A. Valero¹⁷⁰, L. Valéry¹³, S. Valkar¹³¹, A. Vallier⁵, J.A. Valls Ferrer¹⁷⁰, W. Van Den Wollenberg¹⁰⁹, H. van der Graaf¹⁰⁹, P. van Gemmeren⁶, J. Van Nieuwkoop¹⁴⁴, I. van Vulpen¹⁰⁹, M.C. van Woerden¹⁰⁹, M. Vanadia^{135a,135b}, W. Vandelli³², A. Vaniachine¹⁶⁰, P. Vankov¹⁰⁹, G. Vardanyan¹⁸⁰, R. Vari^{134a}, E.W. Varnes⁷, C. Varni^{53a,53b}, T. Varol⁴³, D. Varouchas¹¹⁹, A. Vartapetian⁸, K.E. Varvell¹⁵², J.G. Vasquez¹⁷⁹, G.A. Vasquez^{34b}, F. Vazeille³⁷, T. Vazquez Schroeder⁹⁰, J. Veatch⁵⁷, V. Veeraraghavan⁷, L.M. Veloce¹⁶¹, F. Veloso^{128a,128c}, S. Veneziano^{134a}, A. Ventura^{76a,76b}, M. Venturi¹⁷², N. Venturi³², A. Venturini²⁵, V. Vercesi^{123a}, M. Verducci^{136a,136b}, W. Verkerke¹⁰⁹, A.T. Vermeulen¹⁰⁹, J.C. Vermeulen¹⁰⁹, M.C. Vetterli^{144,d}, N. Viaux Maira^{34b}, O. Viazlo⁸⁴, I. Vichou^{169,*}, T. Vickey¹⁴¹, O.E. Vickey Boeriu¹⁴¹, G.H.A. Viehhauser¹²², S. Viel¹⁶, L. Vigani¹²², M. Villa^{22a,22b}, M. Villaplana Perez^{94a,94b}, E. Vilucchi⁵⁰, M.G. Vinciter³¹, V.B. Vinogradov⁶⁸, A. Vishwakarma⁴⁵, C. Vittori^{22a,22b}, I. Vivarelli¹⁵¹, S. Vlachos¹⁰, M. Vogel¹⁷⁸, P. Vokac¹³⁰, G. Volpi^{126a,126b}, H. von der Schmitt¹⁰³, E. von Toerne²³, V. Vorobel¹³¹, K. Vorobev¹⁰⁰, M. Vos¹⁷⁰, R. Voss³², J.H. Vossebeld⁷⁷, N. Vranjes¹⁴, M. Vranjes Milosavljevic¹⁴, V. Vrba¹³⁰, M. Vreeswijk¹⁰⁹, R. Vuillermet³², I. Vukotic³³, P. Wagner²³, W. Wagner¹⁷⁸, J. Wagner-Kuhr¹⁰², H. Wahlberg⁷⁴, S. Wahrmond⁴⁷, J. Wakabayashi¹⁰⁵, J. Walder⁷⁵, R. Walker¹⁰², W. Walkowiak¹⁴³, V. Wallangen^{148a,148b}, C. Wang^{35b}, C. Wang^{36b,av}, F. Wang¹⁷⁶, H. Wang¹⁶, H. Wang³, J. Wang⁴⁵, J. Wang¹⁵², Q. Wang¹¹⁵, R. Wang⁶, S.M. Wang¹⁵³, T. Wang³⁸, W. Wang^{153,aw}, W. Wang^{36a,ax}, Z. Wang^{36c}, C. Wanotayaroj¹¹⁸, A. Warburton⁹⁰, C.P. Ward³⁰, D.R. Wardrope⁸¹, A. Washbrook⁴⁹, P.M. Watkins¹⁹, A.T. Watson¹⁹, M.F. Watson¹⁹, G. Watts¹⁴⁰, S. Watts⁸⁷, B.M. Waugh⁸¹, A.F. Webb¹¹, S. Webb⁸⁶, M.S. Weber¹⁸, S.W. Weber¹⁷⁷, S.A. Weber³¹, J.S. Webster⁶, A.R. Weidberg¹²², B. Weinert⁶⁴, J. Weingarten⁵⁷, M. Weirich⁸⁶, C. Weiser⁵¹, H. Weits¹⁰⁹, P.S. Wells³², T. Wenaus²⁷, T. Wengler³², S. Wenig³², N. Worme²³, M.D. Werner⁶⁷, P. Werner³², M. Wessels^{60a}, K. Whalen¹¹⁸, N.L. Whallon¹⁴⁰, A.M. Wharton⁷⁵, A.S. White⁹², A. White⁸, M.J. White¹, R. White^{34b}, D. Whiteson¹⁶⁶, B.W. Whitmore⁷⁵, F.J. Wickens¹³³, W. Wiedenmann¹⁷⁶, M. Wielers¹³³, C. Wiglesworth³⁹, L.A.M. Wiik-Fuchs⁵¹, A. Wildauer¹⁰³, F. Wilk⁸⁷, H.G. Wilkens³², H.H. Williams¹²⁴, S. Williams¹⁰⁹, C. Willis⁹³, S. Willocq⁸⁹, J.A. Wilson¹⁹, I. Wingerter-Seez⁵, E. Winkels¹⁵¹, F. Winklmeier¹¹⁸, O.J. Winston¹⁵¹, B.T. Winter²³, M. Wittgen¹⁴⁵, M. Wobisch^{82,u}, T.M.H. Wolf¹⁰⁹, R. Wolff⁸⁸, M.W. Wolter⁴², H. Wolters^{128a,128c}, V.W.S. Wong¹⁷¹, S.D. Worm¹⁹, B.K. Wosiek⁴², J. Wotschack³², K.W. Wozniak⁴², M. Wu³³, S.L. Wu¹⁷⁶, X. Wu⁵², Y. Wu⁹², T.R. Wyatt⁸⁷, B.M. Wynne⁴⁹, S. Xella³⁹, Z. Xi⁹², L. Xia^{35c}, D. Xu^{35a}, L. Xu²⁷, T. Xu¹³⁸, B. Yabsley¹⁵², S. Yacoub^{147a}, D. Yamaguchi¹⁵⁹, Y. Yamaguchi¹²⁰, A. Yamamoto⁶⁹, S. Yamamoto¹⁵⁷, T. Yamanaka¹⁵⁷, M. Yamatani¹⁵⁷, K. Yamauchi¹⁰⁵, Y. Yamazaki⁷⁰, Z. Yan²⁴, H. Yang^{36c}, H. Yang¹⁶, Y. Yang¹⁵³, Z. Yang¹⁵, W-M. Yao¹⁶, Y.C. Yap⁸³, Y. Yasu⁶⁹, E. Yatsenko⁵, K.H. Yau Wong²³, J. Ye⁴³, S. Ye²⁷, I. Yeletsikh⁶⁸, E. Yigitbasi²⁴, E. Yildirim⁸⁶, K. Yorita¹⁷⁴, K. Yoshihara¹²⁴, C. Young¹⁴⁵, C.J.S. Young³², J. Yu⁸, J. Yu⁶⁷, S.P.Y. Yuen²³, I. Yusuff^{30,ay}, B. Zabinski⁴², G. Zacharis¹⁰, R. Zaidan¹³, A.M. Zaitsev^{132,al}, N. Zakharchuk⁴⁵, J. Zalieckas¹⁵, A. Zaman¹⁵⁰, S. Zambito⁵⁹, D. Zanzi⁹¹, C. Zeitnitz¹⁷⁸, G. Zemaityte¹²², A. Zemla^{41a}, J.C. Zeng¹⁶⁹, Q. Zeng¹⁴⁵, O. Zenin¹³², T. Ženiš^{146a}, D. Zerwas¹¹⁹, D. Zhang⁹², F. Zhang¹⁷⁶, G. Zhang^{36a,ax}, H. Zhang^{35b}, J. Zhang⁶, L. Zhang⁵¹, L. Zhang^{36a}, M. Zhang¹⁶⁹, P. Zhang^{35b}, R. Zhang²³, R. Zhang^{36a,av}, X. Zhang^{36b}, Y. Zhang^{35a}, Z. Zhang¹¹⁹, X. Zhao⁴³, Y. Zhao^{36b,az}, Z. Zhao^{36a}, A. Zhemchugov⁶⁸, B. Zhou⁹², C. Zhou¹⁷⁶, L. Zhou⁴³, M. Zhou^{35a}, M. Zhou¹⁵⁰, N. Zhou^{35c}, C.G. Zhu^{36b}, H. Zhu^{35a}, J. Zhu⁹², Y. Zhu^{36a}, X. Zhuang^{35a}, K. Zhukov⁹⁸, A. Zibell¹⁷⁷, D. Zieminska⁶⁴, N.I. Zimine⁶⁸, C. Zimmermann⁸⁶, S. Zimmermann⁵¹, Z. Zinonos¹⁰³, M. Zinser⁸⁶, M. Ziolkowski¹⁴³, L. Živković¹⁴, G. Zobernig¹⁷⁶, A. Zoccoli^{22a,22b}, R. Zou³³, M. zur Nedden¹⁷, L. Zwalinski³².

¹ Department of Physics, University of Adelaide, Adelaide, Australia

² Physics Department, SUNY Albany, Albany NY, United States of America

³ Department of Physics, University of Alberta, Edmonton AB, Canada

- ⁴ ^(a) Department of Physics, Ankara University, Ankara; ^(b) Istanbul Aydin University, Istanbul; ^(c) Division of Physics, TOBB University of Economics and Technology, Ankara, Turkey
- ⁵ LAPP, CNRS/IN2P3 and Université Savoie Mont Blanc, Annecy-le-Vieux, France
- ⁶ High Energy Physics Division, Argonne National Laboratory, Argonne IL, United States of America
- ⁷ Department of Physics, University of Arizona, Tucson AZ, United States of America
- ⁸ Department of Physics, The University of Texas at Arlington, Arlington TX, United States of America
- ⁹ Physics Department, National and Kapodistrian University of Athens, Athens, Greece
- ¹⁰ Physics Department, National Technical University of Athens, Zografou, Greece
- ¹¹ Department of Physics, The University of Texas at Austin, Austin TX, United States of America
- ¹² Institute of Physics, Azerbaijan Academy of Sciences, Baku, Azerbaijan
- ¹³ Institut de Física d'Altes Energies (IFAE), The Barcelona Institute of Science and Technology, Barcelona, Spain
- ¹⁴ Institute of Physics, University of Belgrade, Belgrade, Serbia
- ¹⁵ Department for Physics and Technology, University of Bergen, Bergen, Norway
- ¹⁶ Physics Division, Lawrence Berkeley National Laboratory and University of California, Berkeley CA, United States of America
- ¹⁷ Department of Physics, Humboldt University, Berlin, Germany
- ¹⁸ Albert Einstein Center for Fundamental Physics and Laboratory for High Energy Physics, University of Bern, Bern, Switzerland
- ¹⁹ School of Physics and Astronomy, University of Birmingham, Birmingham, United Kingdom
- ²⁰ ^(a) Department of Physics, Bogazici University, Istanbul; ^(b) Department of Physics Engineering, Gaziantep University, Gaziantep; ^(d) Istanbul Bilgi University, Faculty of Engineering and Natural Sciences, Istanbul; ^(e) Bahcesehir University, Faculty of Engineering and Natural Sciences, Istanbul, Turkey
- ²¹ Centro de Investigaciones, Universidad Antonio Narino, Bogota, Colombia
- ²² ^(a) INFN Sezione di Bologna; ^(b) Dipartimento di Fisica e Astronomia, Università di Bologna, Bologna, Italy
- ²³ Physikalisches Institut, University of Bonn, Bonn, Germany
- ²⁴ Department of Physics, Boston University, Boston MA, United States of America
- ²⁵ Department of Physics, Brandeis University, Waltham MA, United States of America
- ²⁶ ^(a) Universidade Federal do Rio De Janeiro COPPE/EE/IF, Rio de Janeiro; ^(b) Electrical Circuits Department, Federal University of Juiz de Fora (UFJF), Juiz de Fora; ^(c) Federal University of Sao Joao del Rei (UFSJ), Sao Joao del Rei; ^(d) Instituto de Fisica, Universidade de Sao Paulo, Sao Paulo, Brazil
- ²⁷ Physics Department, Brookhaven National Laboratory, Upton NY, United States of America
- ²⁸ ^(a) Transilvania University of Brasov, Brasov; ^(b) Horia Hulubei National Institute of Physics and Nuclear Engineering, Bucharest; ^(c) Department of Physics, Alexandru Ioan Cuza University of Iasi, Iasi; ^(d) National Institute for Research and Development of Isotopic and Molecular Technologies, Physics Department, Cluj Napoca; ^(e) University Politehnica Bucharest, Bucharest; ^(f) West University in Timisoara, Timisoara, Romania
- ²⁹ Departamento de Física, Universidad de Buenos Aires, Buenos Aires, Argentina
- ³⁰ Cavendish Laboratory, University of Cambridge, Cambridge, United Kingdom
- ³¹ Department of Physics, Carleton University, Ottawa ON, Canada
- ³² CERN, Geneva, Switzerland
- ³³ Enrico Fermi Institute, University of Chicago, Chicago IL, United States of America
- ³⁴ ^(a) Departamento de Física, Pontificia Universidad Católica de Chile, Santiago; ^(b) Departamento de Física, Universidad Técnica Federico Santa María, Valparaíso, Chile
- ³⁵ ^(a) Institute of High Energy Physics, Chinese Academy of Sciences, Beijing; ^(b) Department of Physics,

- Nanjing University, Jiangsu; ^(c) Physics Department, Tsinghua University, Beijing 100084, China
- ³⁶ ^(a) Department of Modern Physics and State Key Laboratory of Particle Detection and Electronics, University of Science and Technology of China, Anhui; ^(b) School of Physics, Shandong University, Shandong; ^(c) Department of Physics and Astronomy, Key Laboratory for Particle Physics, Astrophysics and Cosmology, Ministry of Education; Shanghai Key Laboratory for Particle Physics and Cosmology, Shanghai Jiao Tong University, Shanghai(also at PKU-CHEP), China
- ³⁷ Université Clermont Auvergne, CNRS/IN2P3, LPC, Clermont-Ferrand, France
- ³⁸ Nevis Laboratory, Columbia University, Irvington NY, United States of America
- ³⁹ Niels Bohr Institute, University of Copenhagen, Kobenhavn, Denmark
- ⁴⁰ ^(a) INFN Gruppo Collegato di Cosenza, Laboratori Nazionali di Frascati; ^(b) Dipartimento di Fisica, Università della Calabria, Rende, Italy
- ⁴¹ ^(a) AGH University of Science and Technology, Faculty of Physics and Applied Computer Science, Krakow; ^(b) Marian Smoluchowski Institute of Physics, Jagiellonian University, Krakow, Poland
- ⁴² Institute of Nuclear Physics Polish Academy of Sciences, Krakow, Poland
- ⁴³ Physics Department, Southern Methodist University, Dallas TX, United States of America
- ⁴⁴ Physics Department, University of Texas at Dallas, Richardson TX, United States of America
- ⁴⁵ DESY, Hamburg and Zeuthen, Germany
- ⁴⁶ Lehrstuhl für Experimentelle Physik IV, Technische Universität Dortmund, Dortmund, Germany
- ⁴⁷ Institut für Kern- und Teilchenphysik, Technische Universität Dresden, Dresden, Germany
- ⁴⁸ Department of Physics, Duke University, Durham NC, United States of America
- ⁴⁹ SUPA - School of Physics and Astronomy, University of Edinburgh, Edinburgh, United Kingdom
- ⁵⁰ INFN e Laboratori Nazionali di Frascati, Frascati, Italy
- ⁵¹ Fakultät für Mathematik und Physik, Albert-Ludwigs-Universität, Freiburg, Germany
- ⁵² Departement de Physique Nucleaire et Corpusculaire, Université de Genève, Geneva, Switzerland
- ⁵³ ^(a) INFN Sezione di Genova; ^(b) Dipartimento di Fisica, Università di Genova, Genova, Italy
- ⁵⁴ ^(a) E. Andronikashvili Institute of Physics, Iv. Javakhishvili Tbilisi State University, Tbilisi; ^(b) High Energy Physics Institute, Tbilisi State University, Tbilisi, Georgia
- ⁵⁵ II Physikalisches Institut, Justus-Liebig-Universität Giessen, Giessen, Germany
- ⁵⁶ SUPA - School of Physics and Astronomy, University of Glasgow, Glasgow, United Kingdom
- ⁵⁷ II Physikalisches Institut, Georg-August-Universität, Göttingen, Germany
- ⁵⁸ Laboratoire de Physique Subatomique et de Cosmologie, Université Grenoble-Alpes, CNRS/IN2P3, Grenoble, France
- ⁵⁹ Laboratory for Particle Physics and Cosmology, Harvard University, Cambridge MA, United States of America
- ⁶⁰ ^(a) Kirchhoff-Institut für Physik, Ruprecht-Karls-Universität Heidelberg, Heidelberg; ^(b) Physikalisches Institut, Ruprecht-Karls-Universität Heidelberg, Heidelberg, Germany
- ⁶¹ Faculty of Applied Information Science, Hiroshima Institute of Technology, Hiroshima, Japan
- ⁶² ^(a) Department of Physics, The Chinese University of Hong Kong, Shatin, N.T., Hong Kong; ^(b) Department of Physics, The University of Hong Kong, Hong Kong; ^(c) Department of Physics and Institute for Advanced Study, The Hong Kong University of Science and Technology, Clear Water Bay, Kowloon, Hong Kong, China
- ⁶³ Department of Physics, National Tsing Hua University, Taiwan, Taiwan
- ⁶⁴ Department of Physics, Indiana University, Bloomington IN, United States of America
- ⁶⁵ Institut für Astro- und Teilchenphysik, Leopold-Franzens-Universität, Innsbruck, Austria
- ⁶⁶ University of Iowa, Iowa City IA, United States of America
- ⁶⁷ Department of Physics and Astronomy, Iowa State University, Ames IA, United States of America
- ⁶⁸ Joint Institute for Nuclear Research, JINR Dubna, Dubna, Russia

- ⁶⁹ KEK, High Energy Accelerator Research Organization, Tsukuba, Japan
- ⁷⁰ Graduate School of Science, Kobe University, Kobe, Japan
- ⁷¹ Faculty of Science, Kyoto University, Kyoto, Japan
- ⁷² Kyoto University of Education, Kyoto, Japan
- ⁷³ Research Center for Advanced Particle Physics and Department of Physics, Kyushu University, Fukuoka, Japan
- ⁷⁴ Instituto de Física La Plata, Universidad Nacional de La Plata and CONICET, La Plata, Argentina
- ⁷⁵ Physics Department, Lancaster University, Lancaster, United Kingdom
- ⁷⁶ ^(a) INFN Sezione di Lecce; ^(b) Dipartimento di Matematica e Fisica, Università del Salento, Lecce, Italy
- ⁷⁷ Oliver Lodge Laboratory, University of Liverpool, Liverpool, United Kingdom
- ⁷⁸ Department of Experimental Particle Physics, Jožef Stefan Institute and Department of Physics, University of Ljubljana, Ljubljana, Slovenia
- ⁷⁹ School of Physics and Astronomy, Queen Mary University of London, London, United Kingdom
- ⁸⁰ Department of Physics, Royal Holloway University of London, Surrey, United Kingdom
- ⁸¹ Department of Physics and Astronomy, University College London, London, United Kingdom
- ⁸² Louisiana Tech University, Ruston LA, United States of America
- ⁸³ Laboratoire de Physique Nucléaire et de Hautes Energies, UPMC and Université Paris-Diderot and CNRS/IN2P3, Paris, France
- ⁸⁴ Fysiska institutionen, Lunds universitet, Lund, Sweden
- ⁸⁵ Departamento de Física Teórica C-15, Universidad Autónoma de Madrid, Madrid, Spain
- ⁸⁶ Institut für Physik, Universität Mainz, Mainz, Germany
- ⁸⁷ School of Physics and Astronomy, University of Manchester, Manchester, United Kingdom
- ⁸⁸ CPPM, Aix-Marseille Université and CNRS/IN2P3, Marseille, France
- ⁸⁹ Department of Physics, University of Massachusetts, Amherst MA, United States of America
- ⁹⁰ Department of Physics, McGill University, Montreal QC, Canada
- ⁹¹ School of Physics, University of Melbourne, Victoria, Australia
- ⁹² Department of Physics, The University of Michigan, Ann Arbor MI, United States of America
- ⁹³ Department of Physics and Astronomy, Michigan State University, East Lansing MI, United States of America
- ⁹⁴ ^(a) INFN Sezione di Milano; ^(b) Dipartimento di Fisica, Università di Milano, Milano, Italy
- ⁹⁵ B.I. Stepanov Institute of Physics, National Academy of Sciences of Belarus, Minsk, Republic of Belarus
- ⁹⁶ Research Institute for Nuclear Problems of Byelorussian State University, Minsk, Republic of Belarus
- ⁹⁷ Group of Particle Physics, University of Montreal, Montreal QC, Canada
- ⁹⁸ P.N. Lebedev Physical Institute of the Russian Academy of Sciences, Moscow, Russia
- ⁹⁹ Institute for Theoretical and Experimental Physics (ITEP), Moscow, Russia
- ¹⁰⁰ National Research Nuclear University MEPhI, Moscow, Russia
- ¹⁰¹ D.V. Skobeltsyn Institute of Nuclear Physics, M.V. Lomonosov Moscow State University, Moscow, Russia
- ¹⁰² Fakultät für Physik, Ludwig-Maximilians-Universität München, München, Germany
- ¹⁰³ Max-Planck-Institut für Physik (Werner-Heisenberg-Institut), München, Germany
- ¹⁰⁴ Nagasaki Institute of Applied Science, Nagasaki, Japan
- ¹⁰⁵ Graduate School of Science and Kobayashi-Maskawa Institute, Nagoya University, Nagoya, Japan
- ¹⁰⁶ ^(a) INFN Sezione di Napoli; ^(b) Dipartimento di Fisica, Università di Napoli, Napoli, Italy
- ¹⁰⁷ Department of Physics and Astronomy, University of New Mexico, Albuquerque NM, United States of America

- ¹⁰⁸ Institute for Mathematics, Astrophysics and Particle Physics, Radboud University Nijmegen/Nikhef, Nijmegen, Netherlands
- ¹⁰⁹ Nikhef National Institute for Subatomic Physics and University of Amsterdam, Amsterdam, Netherlands
- ¹¹⁰ Department of Physics, Northern Illinois University, DeKalb IL, United States of America
- ¹¹¹ Budker Institute of Nuclear Physics, SB RAS, Novosibirsk, Russia
- ¹¹² Department of Physics, New York University, New York NY, United States of America
- ¹¹³ Ohio State University, Columbus OH, United States of America
- ¹¹⁴ Faculty of Science, Okayama University, Okayama, Japan
- ¹¹⁵ Homer L. Dodge Department of Physics and Astronomy, University of Oklahoma, Norman OK, United States of America
- ¹¹⁶ Department of Physics, Oklahoma State University, Stillwater OK, United States of America
- ¹¹⁷ Palacký University, RCPTM, Olomouc, Czech Republic
- ¹¹⁸ Center for High Energy Physics, University of Oregon, Eugene OR, United States of America
- ¹¹⁹ LAL, Univ. Paris-Sud, CNRS/IN2P3, Université Paris-Saclay, Orsay, France
- ¹²⁰ Graduate School of Science, Osaka University, Osaka, Japan
- ¹²¹ Department of Physics, University of Oslo, Oslo, Norway
- ¹²² Department of Physics, Oxford University, Oxford, United Kingdom
- ¹²³ (a) INFN Sezione di Pavia; (b) Dipartimento di Fisica, Università di Pavia, Pavia, Italy
- ¹²⁴ Department of Physics, University of Pennsylvania, Philadelphia PA, United States of America
- ¹²⁵ National Research Centre "Kurchatov Institute" B.P.Konstantinov Petersburg Nuclear Physics Institute, St. Petersburg, Russia
- ¹²⁶ (a) INFN Sezione di Pisa; (b) Dipartimento di Fisica E. Fermi, Università di Pisa, Pisa, Italy
- ¹²⁷ Department of Physics and Astronomy, University of Pittsburgh, Pittsburgh PA, United States of America
- ¹²⁸ (a) Laboratório de Instrumentação e Física Experimental de Partículas - LIP, Lisboa; (b) Faculdade de Ciências, Universidade de Lisboa, Lisboa; (c) Department of Physics, University of Coimbra, Coimbra; (d) Centro de Física Nuclear da Universidade de Lisboa, Lisboa; (e) Departamento de Física, Universidade do Minho, Braga; (f) Departamento de Física Teórica y del Cosmos, Universidad de Granada, Granada; (g) Dep Física and CEFITEC of Faculdade de Ciências e Tecnologia, Universidade Nova de Lisboa, Caparica, Portugal
- ¹²⁹ Institute of Physics, Academy of Sciences of the Czech Republic, Praha, Czech Republic
- ¹³⁰ Czech Technical University in Prague, Praha, Czech Republic
- ¹³¹ Charles University, Faculty of Mathematics and Physics, Prague, Czech Republic
- ¹³² State Research Center Institute for High Energy Physics (Protvino), NRC KI, Russia
- ¹³³ Particle Physics Department, Rutherford Appleton Laboratory, Didcot, United Kingdom
- ¹³⁴ (a) INFN Sezione di Roma; (b) Dipartimento di Fisica, Sapienza Università di Roma, Roma, Italy
- ¹³⁵ (a) INFN Sezione di Roma Tor Vergata; (b) Dipartimento di Fisica, Università di Roma Tor Vergata, Roma, Italy
- ¹³⁶ (a) INFN Sezione di Roma Tre; (b) Dipartimento di Matematica e Fisica, Università Roma Tre, Roma, Italy
- ¹³⁷ (a) Faculté des Sciences Ain Chock, Réseau Universitaire de Physique des Hautes Energies - Université Hassan II, Casablanca; (b) Centre National de l'Energie des Sciences Techniques Nucleaires, Rabat; (c) Faculté des Sciences Semlalia, Université Cadi Ayyad, LPHEA-Marrakech; (d) Faculté des Sciences, Université Mohamed Premier and LPTPM, Oujda; (e) Faculté des sciences, Université Mohammed V, Rabat, Morocco
- ¹³⁸ DSM/IRFU (Institut de Recherches sur les Lois Fondamentales de l'Univers), CEA Saclay

- (Commissariat à l’Energie Atomique et aux Energies Alternatives), Gif-sur-Yvette, France
- ¹³⁹ Santa Cruz Institute for Particle Physics, University of California Santa Cruz, Santa Cruz CA, United States of America
- ¹⁴⁰ Department of Physics, University of Washington, Seattle WA, United States of America
- ¹⁴¹ Department of Physics and Astronomy, University of Sheffield, Sheffield, United Kingdom
- ¹⁴² Department of Physics, Shinshu University, Nagano, Japan
- ¹⁴³ Department Physik, Universität Siegen, Siegen, Germany
- ¹⁴⁴ Department of Physics, Simon Fraser University, Burnaby BC, Canada
- ¹⁴⁵ SLAC National Accelerator Laboratory, Stanford CA, United States of America
- ¹⁴⁶ ^(a) Faculty of Mathematics, Physics & Informatics, Comenius University, Bratislava; ^(b) Department of Subnuclear Physics, Institute of Experimental Physics of the Slovak Academy of Sciences, Kosice, Slovak Republic
- ¹⁴⁷ ^(a) Department of Physics, University of Cape Town, Cape Town; ^(b) Department of Physics, University of Johannesburg, Johannesburg; ^(c) School of Physics, University of the Witwatersrand, Johannesburg, South Africa
- ¹⁴⁸ ^(a) Department of Physics, Stockholm University; ^(b) The Oskar Klein Centre, Stockholm, Sweden
- ¹⁴⁹ Physics Department, Royal Institute of Technology, Stockholm, Sweden
- ¹⁵⁰ Departments of Physics & Astronomy and Chemistry, Stony Brook University, Stony Brook NY, United States of America
- ¹⁵¹ Department of Physics and Astronomy, University of Sussex, Brighton, United Kingdom
- ¹⁵² School of Physics, University of Sydney, Sydney, Australia
- ¹⁵³ Institute of Physics, Academia Sinica, Taipei, Taiwan
- ¹⁵⁴ Department of Physics, Technion: Israel Institute of Technology, Haifa, Israel
- ¹⁵⁵ Raymond and Beverly Sackler School of Physics and Astronomy, Tel Aviv University, Tel Aviv, Israel
- ¹⁵⁶ Department of Physics, Aristotle University of Thessaloniki, Thessaloniki, Greece
- ¹⁵⁷ International Center for Elementary Particle Physics and Department of Physics, The University of Tokyo, Tokyo, Japan
- ¹⁵⁸ Graduate School of Science and Technology, Tokyo Metropolitan University, Tokyo, Japan
- ¹⁵⁹ Department of Physics, Tokyo Institute of Technology, Tokyo, Japan
- ¹⁶⁰ Tomsk State University, Tomsk, Russia
- ¹⁶¹ Department of Physics, University of Toronto, Toronto ON, Canada
- ¹⁶² ^(a) INFN-TIFPA; ^(b) University of Trento, Trento, Italy
- ¹⁶³ ^(a) TRIUMF, Vancouver BC; ^(b) Department of Physics and Astronomy, York University, Toronto ON, Canada
- ¹⁶⁴ Faculty of Pure and Applied Sciences, and Center for Integrated Research in Fundamental Science and Engineering, University of Tsukuba, Tsukuba, Japan
- ¹⁶⁵ Department of Physics and Astronomy, Tufts University, Medford MA, United States of America
- ¹⁶⁶ Department of Physics and Astronomy, University of California Irvine, Irvine CA, United States of America
- ¹⁶⁷ ^(a) INFN Gruppo Collegato di Udine, Sezione di Trieste, Udine; ^(b) ICTP, Trieste; ^(c) Dipartimento di Chimica, Fisica e Ambiente, Università di Udine, Udine, Italy
- ¹⁶⁸ Department of Physics and Astronomy, University of Uppsala, Uppsala, Sweden
- ¹⁶⁹ Department of Physics, University of Illinois, Urbana IL, United States of America
- ¹⁷⁰ Instituto de Física Corpuscular (IFIC), Centro Mixto Universidad de Valencia - CSIC, Spain
- ¹⁷¹ Department of Physics, University of British Columbia, Vancouver BC, Canada
- ¹⁷² Department of Physics and Astronomy, University of Victoria, Victoria BC, Canada
- ¹⁷³ Department of Physics, University of Warwick, Coventry, United Kingdom

- ¹⁷⁴ Waseda University, Tokyo, Japan
- ¹⁷⁵ Department of Particle Physics, The Weizmann Institute of Science, Rehovot, Israel
- ¹⁷⁶ Department of Physics, University of Wisconsin, Madison WI, United States of America
- ¹⁷⁷ Fakultät für Physik und Astronomie, Julius-Maximilians-Universität, Würzburg, Germany
- ¹⁷⁸ Fakultät für Mathematik und Naturwissenschaften, Fachgruppe Physik, Bergische Universität Wuppertal, Wuppertal, Germany
- ¹⁷⁹ Department of Physics, Yale University, New Haven CT, United States of America
- ¹⁸⁰ Yerevan Physics Institute, Yerevan, Armenia
- ¹⁸¹ Centre de Calcul de l'Institut National de Physique Nucléaire et de Physique des Particules (IN2P3), Villeurbanne, France
- ¹⁸² Academia Sinica Grid Computing, Institute of Physics, Academia Sinica, Taipei, Taiwan
- ^a Also at Department of Physics, King's College London, London, United Kingdom
- ^b Also at Institute of Physics, Azerbaijan Academy of Sciences, Baku, Azerbaijan
- ^c Also at Novosibirsk State University, Novosibirsk, Russia
- ^d Also at TRIUMF, Vancouver BC, Canada
- ^e Also at Department of Physics & Astronomy, University of Louisville, Louisville, KY, United States of America
- ^f Also at Physics Department, An-Najah National University, Nablus, Palestine
- ^g Also at Department of Physics, California State University, Fresno CA, United States of America
- ^h Also at Department of Physics, University of Fribourg, Fribourg, Switzerland
- ⁱ Also at II Physikalisches Institut, Georg-August-Universität, Göttingen, Germany
- ^j Also at Departament de Física de la Universitat Autònoma de Barcelona, Barcelona, Spain
- ^k Also at Departamento de Física e Astronomia, Faculdade de Ciências, Universidade do Porto, Portugal
- ^l Also at Tomsk State University, Tomsk, and Moscow Institute of Physics and Technology State University, Dolgoprudny, Russia
- ^m Also at The Collaborative Innovation Center of Quantum Matter (CICQM), Beijing, China
- ⁿ Also at Università di Napoli Parthenope, Napoli, Italy
- ^o Also at Institute of Particle Physics (IPP), Canada
- ^p Also at Horia Hulubei National Institute of Physics and Nuclear Engineering, Bucharest, Romania
- ^q Also at Department of Physics, St. Petersburg State Polytechnical University, St. Petersburg, Russia
- ^r Also at Borough of Manhattan Community College, City University of New York, New York City, United States of America
- ^s Also at Department of Financial and Management Engineering, University of the Aegean, Chios, Greece
- ^t Also at Centre for High Performance Computing, CSIR Campus, Rosebank, Cape Town, South Africa
- ^u Also at Louisiana Tech University, Ruston LA, United States of America
- ^v Also at Institutio Catalana de Recerca i Estudis Avancats, ICREA, Barcelona, Spain
- ^w Also at Department of Physics, The University of Michigan, Ann Arbor MI, United States of America
- ^x Also at Graduate School of Science, Osaka University, Osaka, Japan
- ^y Also at Fakultät für Mathematik und Physik, Albert-Ludwigs-Universität, Freiburg, Germany
- ^z Also at Institute for Mathematics, Astrophysics and Particle Physics, Radboud University Nijmegen/Nikhef, Nijmegen, Netherlands
- ^{aa} Also at Department of Physics, The University of Texas at Austin, Austin TX, United States of America
- ^{ab} Also at Institute of Theoretical Physics, Ilia State University, Tbilisi, Georgia
- ^{ac} Also at CERN, Geneva, Switzerland
- ^{ad} Also at Georgian Technical University (GTU), Tbilisi, Georgia

- ae* Also at Ochadai Academic Production, Ochanomizu University, Tokyo, Japan
- af* Also at Manhattan College, New York NY, United States of America
- ag* Also at Departamento de Física, Pontificia Universidad Católica de Chile, Santiago, Chile
- ah* Also at The City College of New York, New York NY, United States of America
- ai* Also at School of Physics, Shandong University, Shandong, China
- aj* Also at Departamento de Física Teórica y del Cosmos, Universidad de Granada, Granada, Portugal
- ak* Also at Department of Physics, California State University, Sacramento CA, United States of America
- al* Also at Moscow Institute of Physics and Technology State University, Dolgoprudny, Russia
- am* Also at Departement de Physique Nucleaire et Corpusculaire, Université de Genève, Geneva, Switzerland
- an* Also at Institut de Física d'Altes Energies (IFAE), The Barcelona Institute of Science and Technology, Barcelona, Spain
- ao* Also at School of Physics, Sun Yat-sen University, Guangzhou, China
- ap* Also at Institute for Nuclear Research and Nuclear Energy (INRNE) of the Bulgarian Academy of Sciences, Sofia, Bulgaria
- aq* Also at Faculty of Physics, M.V.Lomonosov Moscow State University, Moscow, Russia
- ar* Also at National Research Nuclear University MEPhI, Moscow, Russia
- as* Also at Department of Physics, Stanford University, Stanford CA, United States of America
- at* Also at Institute for Particle and Nuclear Physics, Wigner Research Centre for Physics, Budapest, Hungary
- au* Also at Giresun University, Faculty of Engineering, Turkey
- av* Also at CPPM, Aix-Marseille Université and CNRS/IN2P3, Marseille, France
- aw* Also at Department of Physics, Nanjing University, Jiangsu, China
- ax* Also at Institute of Physics, Academia Sinica, Taipei, Taiwan
- ay* Also at University of Malaya, Department of Physics, Kuala Lumpur, Malaysia
- az* Also at LAL, Univ. Paris-Sud, CNRS/IN2P3, Université Paris-Saclay, Orsay, France
- * Deceased